Novel screens to identify genes regulating global chromatin structure during female meiotic prophase

Benjamin Loh Jia Hui

Presented for the Degree of

Doctor of Philosophy

The University of Edinburgh

January 2010

Declaration

I declare that I alone have composed this thesis and that the work presented is my own, except where otherwise stated.

Benjamin Loh Jia Hui

January 2010

Acknowledgements

Firstly, I would like to thank Christiane Nusslein-Volhard for kindly providing the mutant collection used in my screen.

Big thanks to Hiro for his patient instruction and guidance during my PhD and especially in the writing of this thesis. These last three years have been some of the most productive, interesting and enjoyable times of my life and this is due in no small part to his influence. I have learned so much from him and I could not have asked for a better supervisor for my PhD.

I would also like to thank the members of the Ohkura lab both past and present for all their help and encouragement. Especially Fiona Cullen, Sara Clohise and Heather Syred for proofreading this thesis, Nathalie Colombie for her help in making the figures and Ana Sousa for her advice on thesis layout.

My deepest gratitude to my parents, without whom, in a very real sense, this thesis would not have been possible. Thank you so much for your constant guidance and encouragement, Mom and Pap. Every success that I have, you guys made possible for me.

Though the work was my own, the impetus was given to me by so many others. Praise God for the providence of these last three years and for all who helped me on the way.

Abstract

During female meiotic prophase in many organisms, a specialized chromatin structure is formed in the oocyte nucleus. This structure is known as the karyosome, and has been proposed to be important for the formation of the female meiotic bipolar spindle. However, how the karyosome is formed and maintained is not very well understood.

To identify proteins involved in the formation and maintenance of the karyosome, I carried out a cytological screen on a collection of 220 mutant fly lines for mutants that were defective in karyosome morphology. The screen identified 46 mutants on the X and 2nd chromosome with abnormal karyosomes. Genetic analysis of these 46 mutants, followed by molecular analysis of one mutant, identified SRPK (SR Protein Kinase) as a protein that is important for the proper formation of the karyosome.

NHK-1 (Nucleosomal Histone Kinase 1) was previously identified as a protein that is essential for the formation of the karyosome via its phosphorylation of BAF (Barrier-to-Autointegration Factor). NHK-1 phosphorylation of BAF leads to the release of chromatin from the nuclear membrane, an essential step for the formation of the karyosome, however, the regulation of this process is unclear.

In order to identify genes that interact with *NHK-1*, I carried out a genetic modifier screen using a semi-lethal allele of *NHK-1, NHK-1^{trip}*. After screening a collection of 44 deficiencies located on the 2nd chromosome, I identified a genetic region (44B8-44D1) containing a gene that interacts with *NHK-1* and, when gene dosage is halved, enhanced the semi-lethal phenotype of *NHK-1^{trip}*.

Contents

Figures

Abbreviations

2L	Left arm of the second chromosome in *Drosophila melanogaster*
2R	Right arm of the second chromosome in *Drosophila melanogaster*
A	Adenine
A2	Second alpha helix domain in CenH3
APC/C	Anaphase-Promoting Complex / Cyclosome
BAF	Barrier-to-Autointegration Factor
bp	Base pair
C	Cytosine
CATD	Cenp-A Targeting Domain
CID	Centromere Identifier
CPC	Chromosome Passenger Complex
DAPI	4',6-diamidino-2-phenylindole
DNA	Deoxyribonucleic acid
dNTPs	Deoxyribonucleotides
DSBs	Double Stranded Breaks
D-TACC	Drosophila Transforming Acidic Coiled-Coil protein
Dup	Double Parked
EDTA	Ethylenediaminetetraacetic acid
EGTA	Ethylene Glycol Tetraacetic Acid
EMS	Ethyl MethaneSulfonate
FISH	Fluorescence In Situ Hybridization
FLP-DFS	Flippase – Dominant Female Sterile
FRT	Flippase Recognition Target
G	Guanine
GAP	GTPase-Activating Protein

GEF	Guanine nucleotide exchange factors
GLC	Germline Clone
GTP	Guanosine-5'-triphosphate
HP1	Heterochromatin Protein 1
hs-hid	Heat shock - head involution defective
INCENP	INner CENtromere Protein
kbs	Kilobases
KMN	Knl-1, Mis12 and Ndc80
L1	First loop domain in CenH3
Lap2	Lamina Associated Polypeptide 2
LBR	Lamin B Receptor
LEM	LAP2, Emirin, MAN1
MCAK	Mitotic Centromere-Associated Kinesin
MRC	Meiotic Recombination Checkpoint
mRNA	Messenger ribonucleic acid
Msps	Mini-Spindles
Ncd	Non-claret disjunctional
NHK-1	Nucleosomal Histone Kinase-1
NLS	Nuclear Localization Signal
NSN	Non-Surrounded Nucleolus
PBS	Phosphate Buffered Saline
PCR	Polymerase Chain Reaction
Phl	Pole hole
PP1	Protein Phosphatase 1
RCA	Regulator of Chromosome Architecture
RCC1	Regulator of Chromosome Condensation 1
RNA	Ribonucleic Acid

RNAi	RNA interference
RTK	Receptor Tyrosine Kinase
S/MARS	Scaffold/Matrix Attachment Region
SN	Surrounded Nucleolus
SpnB	Spindle-B
SRPK	SR Protein Kinase
T	Thymine
TAE	Tris-acetate
TE	Tris / EDTA buffer
TIFF	Tagged Image File Format
TPX2	Targeting Protein for Xklp2
UV	Ultraviolet
Xklp2	Xenopus Kinesin-Like Protein 2

Chapter 1:

Introduction

Chapter 1: Introduction

DNA (Deoxyribonucleic acid) is a biological polymer formed from four nitrogenous bases, adenine, cytosine, guanine and thymine, arranged on a sugar and phosphate backbone. Our current understanding of biology has, as a centrepiece, a model whereby DNA is used as a template for transcribing RNA (a related Ribonucleic acid), which is then translated into the vast array of proteins that make up virtually all cellular structures.

Over the course of the cell cycle, DNA is replicated and packaged into discrete structures known as chromosomes. During cell division, the chromosomes, are separated and segregated to the two resulting daughter cells during a process known as mitosis. Due to the central role of DNA in directing the activities of the cell, its proper replication and transfer during cell division is of the utmost importance, and failure to properly segregate the chromosomes during mitosis can lead to cell death or cancer.

Of arguably even greater importance than mitosis is meiosis, which is responsible for generating the haploid germ cells that fuse during fertilization to give rise to a new organism. Errors in chromosome segregation during meiosis can lead to offspring with an abnormal chromosome number, a condition known as aneuploidy. In humans 35% of spontaneous abortions are caused by aneuploidy arising during meiosis. Even chromosomal aneuploidy that is compatible with live birth, specifically those on chromosome X, 18 and 21 can cause defects in development and mental retardation in the resulting offspring (Hassold and Hunt, 2001). By studying the karyotype of both aneuploid foetuses and live born offspring, a trend has been identified whereby a majority of aneuploidies originate during female meiosis, i.e. the process that gives rise to the oocytes. This disparity

between aneuploidies of male and female parental origin is thought to be caused by the differences between male and female meiosis in humans (Hassold et al., 2007).

In human males, the germline precursor cells are mitotically proliferative throughout the entire lifetime of the organism. Meiosis in human males initiates upon sexual maturity and all steps of meiosis occur sequentially. In human females however, the germline precursor cells are only proliferative for a brief period during foetal development. Following the brief window of proliferation, meiosis is then initiated, with the oocytes arresting early during meiotic prophase after having completed meiotic recombination. This arrest is called the extended dictyate stage and in human females can last for decades (from the initial prophase in the foetus until the final oocyte is ovulated and the onset of menopause) before the eggs re-enter and complete meiosis (Hassold and Hunt, 2001). Thus, as opposed to the human male's constantly renewing pool of germ cells that undergo a sequential meiosis, female germ cells are both limited and experience a meiotic arrest that can last up to several decades. Both of these factors are thought to contribute to the comparatively higher rates of foetal aneuploidy arising from the female parent, and highlights the importance of research into the processes involved in female meiosis.

Due to the limited amount of human oocytes available for study (mostly originating from in vitro fertilization), it is useful to study female meiosis in model organisms. *Drosophila melanogaster* is a suitable substitute in this regard, not only because of the numerous points of congruency between female meiosis in both organisms, but also because of its powerful genetics and comparatively manageable genome.

In *Drosophila* females the two ovaries are made up of an assembly line of eggs of increasing maturity known as the ovariole. Each ovary has numerous ovarioles, resembling nothing so much as a tightly grouped bunch of bananas. At the tip of each ovariole is the oval structure known as the germarium, which is

designated as the 1st stage of *Drosophila* oogenesis (i.e. stage 1). The germarium is further subdivided into three regions (1, 2 and 3). In region 1 of the germarium reside a population of germline stem cells. To initiate oogenesis, these germline stem cells undergo 4 rounds of incomplete mitotic division to generate a 16 cell cyst (King, 1970). As mitotic closure is incomplete, the cells of the cyst are connected by ring canals, through which cytoplasm can flow. These ring canals are filled with a spectrin rich cytoplasmic matrix known as the fusome which has been proposed to be responsible for the specification of cell identity within the 16 cell cyst (de Cuevas and Spradling, 1998; Lin and Spradling, 1995).

Only two cells within the 16 cell cyst have 4 ring canals and one of these two cells will eventually mature into the oocyte proper. The remaining 15 cells will undergo multiple rounds of genome endoreplication and eventually become the polyploid nurse cells that are responsible for transcribing the RNA complement that will be used in the developing oocyte (King, 1970).

In region 2 of the germarium, meiotic recombination is initiated in all 16 cells, with the synaptonemal complex forming between the paired homologues, however only the oocyte will complete meiotic recombination as the synaptonemal complex will be disassembled early on in the remaining 15 cells within the developing cyst (Page and Hawley, 2001). Once the synaptonemal complex has been assembled between the paired homologues within the oocyte nucleus, double stranded breaks are generated on the chromosomes. These double stranded breaks serve to initiate strand invasion and repair, and are eventually repaired, by region 3, as chiasmata holding the two paired homologues together (McKim et al., 2002). Once meiotic recombination is complete, the synaptonemal complex will start to disassemble and will be completely removed from the chromatin by stage 6-7 (Oscar Lancaster, personal communication).

In region 2, the 16 cell cyst is surrounded by the mesoderm derived follicle cells that are responsible for eventually secreting the egg shell, also known as the chorion (King, 1970). The assemblage of the 16 cell cyst and the follicle cells is now recognizable as an immature *Drosophila* egg chamber and begins to bud off from the germarium, eventually graduating to stage 2 of development. From stage 2 onwards, the *Drosophila* egg chamber will undergo continual growth as the oocyte within the 16 cell cyst continues to increase in cytoplasmic volume, driven by the transcriptional and translational activity of the nurse cells (King, 1970).

By stage 3, the chromatin within the oocyte nucleus (also known as the germinal vesicle) has attained a compact morphology. This compact configuration of the chromatin within the oocyte nucleus is known as the karyosome. In contrast to the oocyte nucleus, which will expand in tandem with the growth of the oocyte, the karyosome will continually occupy the same volume within the nucleus (Liu et al., 2006). The karyosome persists throughout all remaining steps of *Drosophila* oocyte development, eventually playing a role in assembling the meiotic spindle which is necessary for segregating the chromosomes (Doubilet and McKim, 2007).

In *Drosophila*, the karyosome stage corresponds to the extended dictyate period during female meiosis in humans. In humans, the long dictyate period (lasting anywhere from one to five decades) is thought to be a contributing factor to the high incidence of aneuploidy with maternal meiotic origin (Eichenlaub-Ritter, 1996). Thus, by studying the formation and maintenance of an analogous structure in *Drosophila*, the karyosome, insight might be gained into the factors that contribute to chromosome mis-segregation in human female meiosis.

From stage 8 onwards, the growth of the oocyte is at the expense of the nurse cells which start to shrink and atrophy (King, 1970). During stage 9, the oocyte nucleus migrates to a dorsal-anterior position within the oocyte and a cap of the axis patterning directing protein, Gurken, forms around the oocyte nucleus to

influence the dorsal patterning of the follicle cells (Neuman-Silberberg and Schupbach, 1993). In the *spindle* class of mutants, this accumulation of the Gurken protein around the oocyte nucleus is disrupted, leading to improper dorsal development of the mature egg, most notably missing or fused dorsal appendages (Ghabrial et al., 1998). These Spindle mutants also cause defects in the morphology of the karyosome, and the link between karyosome morphology and dorsal patterning in *Drosophila* eggs is further explored in Chapter 1.7 (Ghabrial and Schupbach, 1999).

From stage 9-12, the oocyte continues its growth until it has reached 90,000 times its original volume (King, 1970). At the end of stage 13, the oocyte nuclear membrane breaks down and the chromatin (in the karyosome configuration) is released directly into the cytoplasm to form the meiosis I spindle (King, 1970). During stage 14, the formation of the meiotic spindle is proposed to be directed by a gradient of RanGTP around the chromatin and the chromosomes align themselves on the midzone of the spindle (Gruss and Vernos, 2004). As with human female meiosis, defects in meiotic recombination or the mutation of proteins involved in sister chromatid cohesion can lead to chromosome mis-segregation and subsequent aneuploidy.

Once the meiotic spindle is formed, the oocyte arrests in metaphase I of meiosis (unlike in humans where oocytes arrest in metaphase II to await fertilization). This metaphase I arrested oocyte is considered to be in stage 14, which denotes a fully mature, ready to be laid egg. Sperm stored in specialized organs known as spermatheca fertilize the mature egg as it progresses through the oviduct, and this activates the arrested oocyte and prompts it to complete metaphase I and II before receiving the male complement of DNA.

1.1: Interphase chromatin

During interphase, chromatin is located inside the nucleus. Due to its length, it is subject to multiple levels of packing. The first level is the nucleosome, where the DNA is wrapped around a histone octamer. This octamer consists of two heterodimers of H3 and H4 flanked by two heterodimers of H2A and H2B. 146 base pairs of DNA are wrapped 1.75 times around these histone octamers in a left handed superhelix giving rise to the characteristic “beads on a string” appearance of DNA associated with its histones (Kornberg and Lorch, 1999; Ramakrishnan, 1997).

These nucleosomes are separated by small stretches of non-nucleosome linker DNA. 20 bps of linker DNA is associated with histone H1, which sits atop the histone octamer that makes up the nucleosome and binds to the linker DNA as it enters and exits the nucleosome (Allan et al., 1980; Thomas, 1999). The entire assemblage of nucleosome, histone H1, and associated linker DNA is termed the chromatosome (Simpson, 1978). The histone H1 family is highly variable. In human cells, there are 11 different subtypes of histone H1, the expression of which are regulated according to cell type and stage of differentiation (Happel and Doenecke, 2009). There is evidence to suggest that histone H1 and linker DNA play a role in organizing the next level of chromatin compaction, the 30nm fibre (Hizume et al., 2005; Robinson and Rhodes, 2006), but due to the absence of a definitive model for the structure of the 30nm fibre, the exact function that it performs remains unclear.

The structure of the next level of compaction for chromatin, the 30nm fibre is still the subject of much debate. Initially identified via electron microscopy of nuclear sections, it has also been identified as one of the three products of nuclease digestion of chromatin (the nucleosome and the chromatosome being the other two) (Davies, 1968; Staynov, 2008; Staynov and Proykova, 1998). Two structural models for how the 30nm fibre forms have been suggested, the solenoid one start helix and

the zigzag two start helix (and its variants). In-vitro reconstitution studies seem to support the zigzag two start helix model, but conflicting data proposes that the solenoid one start helix might be possible depending on the presence of histone H1 (Osipova et al., 1990; Robinson et al., 2006; Rydberg et al., 1998; Tremethick, 2007). Controversially, recent imaging of prepared nuclei has shown no evidence of the 30nm fibre in-situ (Horowitz-Scherer and Woodcock, 2006), however this may be due to the limits of current imaging technology or the 30nm fibre might be compacted into even higher order chromatin structures (Kireeva et al., 2004).

All chromatin inside the nucleus can be divided into two categories, euchromatin and heterochromatin. Euchromatin refers to the gene rich, open, form of chromatin with the tails of its histones acetylated to provide access to the transcription machinery of the cell (Bassett et al., 2009). Conversely, heterochromatin is highly compacted, often gene poor and transcriptionally inactive. Heterochromatin is heavily methylated, and this recruits histone deacetylases that revert the chromatin to a more compact configuration, rendering it inaccessible to transcription factors. Methylation can also occur at the transcription start sites and directly inhibit the binding of transcription factors (Dillon and Festenstein, 2002).

Heterochromatin can be further divided into two subtypes, facultative heterochromatin and constitutive heterochromatin. Facultative heterochromatin contains sequences that are packaged as heterochromatin only in certain cells, and may be packaged as euchromatin in other cells. Examples of facultative heterochromatin are genes involved in differentiation or morphogenesis. Constitutive heterochromatin on the other hand, contains sequences that are packaged as heterochromatin regardless of the cell type. The centromeres and telomeres of chromosomes are packaged as heterochromatin in all cells and are thus examples of constitutive heterochromatin (Dillon, 2004).

In the nucleus, heterochromatin is associated with the nuclear periphery while euchromatin is more often located at the nuclear interior. This nuclear localization of heterochromatin is caused by Heterochromatin Protein 1 (HP1), a chromodomain containing family of proteins recruited by heterochromatin histone methylation. HP1 in turn interacts with proteins located at the nuclear periphery, specifically Lamin B receptor, leading to the peripheral localization of heterochromatin (Ye et al., 1997; Ye and Worman, 1996). This physical partition of heterochromatin and euchromatin is part of the cause of the next level of chromatin organization within the nucleus, chromosome territories.

The concept that each chromosome occupies a discrete territory within the nucleus is not a new one. Light microscopy of the nucleus in the early 1900s led to speculation that chromosomes occupy fixed domains within the nucleus (Foster and Bridger, 2005). Evidence for this theory was provided by experiments involving focal UV laser microbeam induced DNA damage in Chinese Hamster culture cells. Repair of this damage by H^3 thymidine revealed, in autoradiography assays, that the damage was limited to a small number of chromosomes, as would be the case if each chromosome occupied a discrete, largely non-overlapping region of the nucleus (Meaburn and Misteli, 2007). Of dispute however is the pattern by which the chromosomes are arranged within the nucleus. Currently, there are two, not mutually exclusive, models based on in-vivo studies of how the chromosomes are organized within the nucleus, gene density theory and position-size theory.

Gene density theory posits that chromosomes are organized within the nucleus based on how gene rich they are. Gene rich chromosomes localize more towards the nucleus interior while gene poor chromosomes are restricted to the periphery which is seen as the transcriptionally inert region of the nucleus (Cremer et al., 2003; Croft et al., 1999). This particular model synchs well with the observation that gene poor heterochromatin, is likewise localized to the nuclear

periphery. However, there is also evidence of transcriptionally active genes being localized to the nuclear pore complex on the nuclear periphery which appears to contradict this model of chromosome localization (Casolari et al., 2004).

The second model for how chromosomes are organized within the nucleus is the position-size theory, which as its name suggests, posits that chromosomes are arranged within the nucleus based on size. Specifically, small chromosomes are drawn towards the nuclear interior, while large chromosomes are localized to the nuclear periphery (Bolzer et al., 2005; Sun et al., 2000). Presently, it is not known how chromosomes come to have this organization, but two different models have been proposed as to how it might form. The first of these is the volume exclusion model, which states that the chromosomes are organized based on volume occupied within the nucleus, with smaller chromosomes localizing to the interior and larger chromosomes remaining at the periphery (Cremer et al., 2001). The second model is the mitotic pre-set model, where position is determined during the previous metaphase, with the arms of larger chromosomes being oriented more towards the periphery than the arms of smaller chromosomes (Sun et al., 2000).

As previously stated, the gene density and position size theory, are not necessarily mutually exclusive. In cells displaying chromosome organization in line with the gene density theory, the onset of quiescence can cause small chromosomes with formerly peripheral localization to localize to the nuclear interior, while large chromosomes remain attached to the nuclear periphery (Bridger et al., 2000).

In order to understand how chromosomes remain in their domains within the interphase nucleus, it is necessary to discuss a controversial structure, the nuclear matrix. The nuclear matrix is an underlying, partly proteinaceous, structure to which chromatin is attached during interphase. Though the exact composition of the nuclear matrix is not well understood, it is known that lamins and other intermediate

filament-like proteins comprise at least part of its structure (Barboro et al., 2002; Hozak et al., 1995; Neri et al., 1999). Furthermore, the stability of this structure, and indeed that of chromosome territories themselves, can be perturbed by a treatment involving RNase, implying that RNA has a role in the maintenance of the nuclear matrix (He et al., 1991; He et al., 1990; Ma et al., 1999). Chromatin is attached to the nuclear matrix via genetic sequences known as Scaffold/Matrix Attachment Regions (S/MARs), with the DNA between S/MARs looped out from the nuclear matrix (Heng et al., 2004). This model of chromatin attachment to the nuclear matrix with outwards extending loops is known as the radial loop model, and it has structural relevance during both mitotic and meiotic chromosome condensation.

Though there is now a general model of how chromatin is organized within the nucleus in interphase, it is fraught with uncertainty and conflicting evidence. More research and better tools are required to provide a clearer understanding of chromatin dynamics during interphase. (Fig. 1)

1.2: Mitotic chromatin condensation

During mitosis, chromatin within the nucleus condenses from the interphase space filling chromosome territories to that of fully mature mitotic chromosomes. How this condensation occurs is still not fully understood, however research has identified several proteins that might play a role in this process.

Experiments that stripped histones away from mature mitotic chromosomes revealed the presence of a central densely stained chromosome scaffold surrounded by a halo of outwardly expanding DNA. This DNA was attached to the scaffold in loops of around 30-90kbs (Paulson and Laemmli, 1977) similar to the radial loop structure of chromatin described in interphase. Two of the proteins

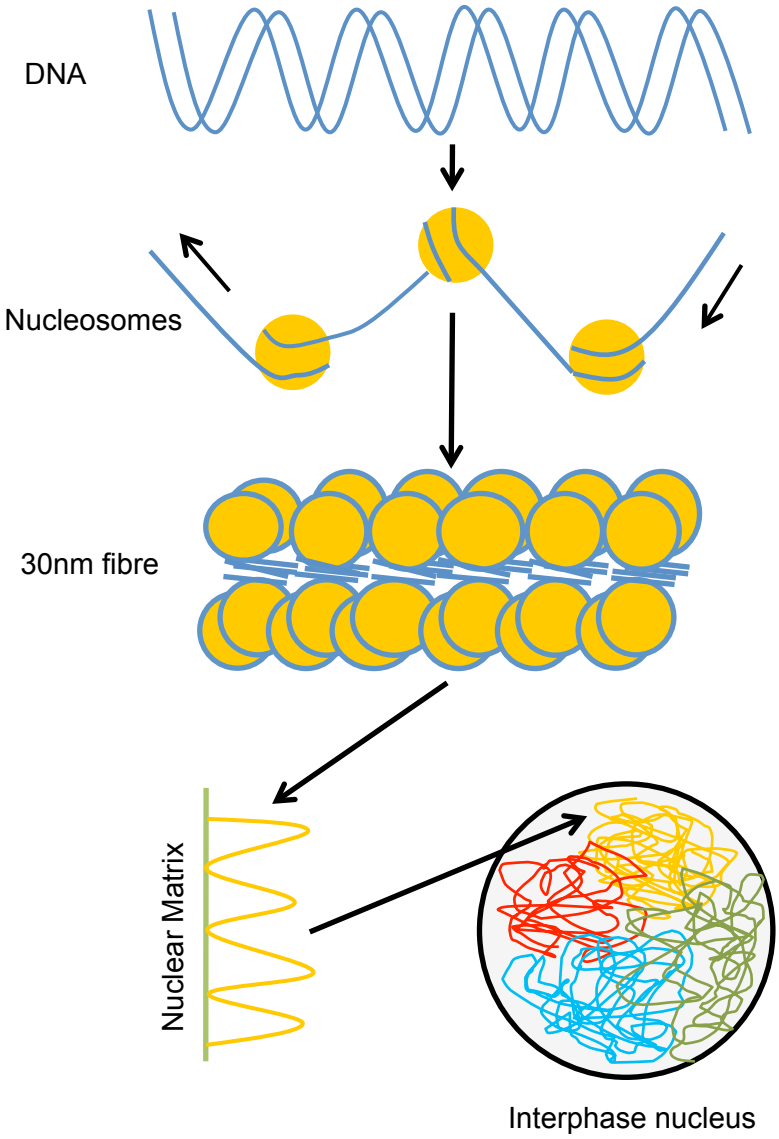

Figure 1. Interphase chromatin organization.
During interphase, double stranded DNA is wrapped around nucleosomes which are then folded into higher order structures such as the 30nm fibre. These higher order chromatin structures are attached to the nuclear matrix which has a role in organizing the chromosome territories within the interphase nucleus.

identified to form part of this scaffold were topoisomerase II (Earnshaw et al., 1985; Gasser et al., 1986) and SMC2, a member of the condensin complex (Saitoh et al., 1994; Strunnikov et al., 1995).

Drug inhibition of topoisomerase II inhibited chromosome condensation (Gorbsky, 1994), as did in vitro immunodepletion of condensin complex (Hirano et al., 1997). But while it might seem from these experiments that topoisomerase II and the condensin complex are the main proteins involved in chromosome condensation during mitosis, several studies have indicated that the story isn't quite so simple.

Experiments involving the in vitro extraction of topoisomerase II from already condensed chromosomes caused no appreciable change in the level of chromosome condensation (Hirano and Mitchison, 1993). Furthermore, the RNAi knockdown of topoisomerase II in both *Drosophila* (Chang et al., 2003) and mammalian cells (Sakaguchi and Kikuchi, 2004), revealed that while depletion of topoisomerase II does cause certain condensation related defects, chromosomes are still able to compact longitudinally in its absence (Belmont, 2006).

Likewise for condensin, when the *Drosophila* condensin subunit, CAP-D2 was knocked down via double stranded RNA mediated interference, chromosomes were still able to compact (Savvidou et al., 2005). However, topoisomerase II and condensin knockdown both led to defects in sister chromatid separation and chromosome segregation (Belmont, 2006).

To reconcile these conflicting views of the chromosome condensation activity of topoisomerase II and the condensin complex, two possibilities have been suggested. The first possibility is that while topoisomerase II and the condensin complex are important for chromosome condensation, in their absence a redundant pathway exists to fulfil that function (Belmont, 2006). The second is that the function of topoisomerase II and the condensin complex are to stabilize already condensed

chromosomes and that chromosome condensation is carried out by an alternate pathway (Hirota et al., 2004; Hudson et al., 2003).

Both of these suggestions posit that an alternate pathway is responsible for condensing the chromosomes, and recently there has been evidence to suggest that such a pathway actually exists. Experiments have shown that in conditional condensin knockout chicken DT 40 cells, chromosomes lost their compact architecture and prominent chromatin bridges were formed during anaphase. However these defects were rescued by exogenous expression of cyclin B3 or overexpression of a dominant negative mutant of Repo-Man. Both of these treatments preserve phosphorylation on the mitotic chromosomes, cyclin B3 by keeping cdk active, and the dominant negative Repo-Man by its inability to recruit protein phosphatase PP1 at the onset of anaphase (Vagnarelli et al., 2006).

Therefore, there exists some "activity" that allows for the condensation of mitotic chromosomes in the absence of condensin. This activity is proposed to be activated by cdk induced phosphorylation and turned off by dephosphorylation by phospatase PP1. Termed RCA (Regulator of Chromosome Architecture) (Vagnarelli et al., 2006), the identification of the protein/proteins responsible for this activity will be required for a full understanding of how the chromatin condenses during mitosis.

1.3: Segregation of the mitotic chromosomes

During mitotic chromosome segregation, the centromere, a specialized chromosomal region, organizes the formation of kinetochores, which act as the interface between chromosomes and microtubules within the mitotic spindle. The kinetochores themselves are complex proteinaceous structures that govern many aspects of chromosome segregation, including microtubule binding, tension sensing and the mitotic checkpoint. In order to grasp mitotic chromosomal dynamics, it is

necessary to understand how centromere identity is established, the role the centromere plays in kinetochore formation and how kinetochores mediate the myriad chromosome process during mitosis.

In eukaryotes, centromeres can be divided into two categories, holocentric and monocentric. Holocentric organisms, such as *Caenorhabditis elegans* have centromeres that are diffused along the entire length of the chromosome. Conversely monocentric organisms, a category which includes budding and fission yeast, *Drosophila*, plants and humans have centromeres that are restricted to a specific chromosome locus, though the size of this locus may vary (Torras-Llort et al., 2009).

In budding yeast, the centromere is organized by a 125 bp *CEN* sequence (Fitzgerald-Hayes et al., 1982b), that is sufficient to organize a functional centromere when inserted into a plasmid (Clarke and Carbon, 1980; Fitzgerald-Hayes et al., 1982a). However, in other organisms, the link between genetic sequence and centromere organization isn't as clear. In chromosomes with two centromere sequences (dicentric chromosomal rearrangements), one putative centromere is usually inactivated even though both centromeres have the associated genetic sequence (Agudo et al., 2000; Earnshaw and Migeon, 1985). Furthermore, ectopic centromeres (neocentromeres) have been shown to form on non-centromeric genetic sequences (Lo et al., 2001; Williams et al., 1998).

Instead, centromere identity seems to be established epigenetically via the presence of a centromere specific histone H3 variant known as Cenp-A in humans, and more widely as CenH3 (Palmer et al., 1987). CenH3 is different from canonical histone H3 in both its structure and how it is incorporated into the nucleosome. Structurally, the N-terminal tail of human CenH3 shows effectively no homology with human histone H3, and little sequence homology with CenH3 found in other eukaryotic lineages. Even the C-terminal histone fold domain, where human CenH3

shows considerable homology with histone H3, only has an average of 48% homology with the C-terminal histone fold domain of other eukaryotic species (Torras-Llort et al., 2009). This low homology between human Cenp-A, canonical human histone H3, and CenH3 found in other eukaryotic species is proposed to be due to the rapid evolution rate of CenH3, reflecting its association with the rapidly evolving centromere DNA (Malik and Henikoff, 2001; Talbert et al., 2004). Though there is low structural homology between the CenH3s of different eukaryotic species, a conserved insertion of 2-6 amino acids in the first loop (L1) region of the C-terminal histone fold domain hints at the importance of this region in the function and positioning of CenH3 (Black et al., 2004; Black et al., 2007b).

As mentioned in section 1.1, the nucleosome is the fundamental level of DNA packaging and consists of a strand of DNA coiled in a left handed superhelix around a histone octamer of the canonical histones (H3, H4, H2A and H2B). In vitro reconstitution experiments and affinity purification of CenH3 containing nucleosomes have indicated that CenH3 can incorporate into nucleosomes as well, taking the place of canonical histone H3 (Blower et al., 2002; Yoda et al., 2000). These CenH3 nucleosomes are more compact and conformationally rigid than canonical nucleosomes (Black et al., 2007a; Black et al., 2004), and these structural differences seem to be linked to the aforementioned L1 region and the adjoining second alpha-helix domain (A2).

There is evidence that CenH3 might be incorporated into non-canonical nucleosomes. For example, there is evidence of a CenH3/H4 hexamer nucleosome in budding yeast where the flanking H2A/H2B dimers are replaced by Scm3, a protein required to recruit CenH3 to the centromere (Camahort et al., 2007; Mizuguchi et al., 2007; Stoler et al., 2007). Even more bizarrely, in *Drosophila*, cross linking experiments and atomic force microscopy have indicated that CenH3 might be incorporated into half-nucleosomes, a tetramer of histones consisting of a single

copy of CenH3, H4, H2A and H2B (Dalal et al., 2007a; Dalal et al., 2007b). Though the purpose of these non-canonical nucleosomes is not clear, it has been proposed that they might play a role in the assembly/disassembly of the CenH3 nucleosome (Torras-Llort et al., 2009).

Intriguingly, the conserved L1/ A2 region, which is known to have an effect on nucleosome structure, is also known as the Cenp-A Targeting Domain (CATD) and is responsible and sufficient localizing human CenH3 to the centromere (Black et al., 2004). Domains with similar centromere targeting function have been identified in the histone fold domain of other organisms such as *Drosophila* (Vermaak et al., 2002) and budding yeast (Keith et al., 1999). Exactly how the CATD contributes to the targeting of CenH3 is still unknown, but from the evidence, two non-mutually exclusive possibilities present themselves.

The first possibility is that the CATD domain itself influences the binding of the CenH3 nucleosome to centromeric DNA. Experiments have revealed that swapping the CATD domain of *Drosophila melanogaster* into *Drosophila bipectinata* CenH3 is sufficient to allow localization of *D. bipectinata* CenH3 to the centromeres in *D. melanogaster* (Vermaak et al., 2002). And while CenH3 has been shown to be capable of localizing to multiple sites in the genome (Moreno-Moreno et al., 2006; Van Hooser et al., 2001), it remains tightly bound only at the centromere (Hemmerich et al., 2008) and is unstable and subject to proteolysis when bound elsewhere (Conde e Silva et al., 2007; Moreno-Moreno et al., 2006) possibly as a result of the more compact and structurally rigid configuration of the CenH3 nucleosome.

The second possibility is that the CenH3 CATD domain directly interacts with proteins that target it to the centromere. Several proteins have been shown to play a role in recruiting CenH3 to the centromere or in stabilizing its presence there. As previously mentioned, there is evidence in budding yeast that CenH3 forms a non-

canonical hexameric nucleosome with Scm3 taking the place of the H2A/H2B dimers. Scm3 itself interacts with the Mis16/Mis18 complex responsible for histone acetylation in the centromere (Hayashi et al., 2004). The Mis16/Mis18 complex recruits Scm3 to the centromere (Pidoux et al., 2009; Williams et al., 2009), and thus may play a role in recruiting CenH3 to the centromere as well. The protein HJURP (Holliday Junction Recognizing Protein) interacts directly with the CenH3 CATD (Foltz et al., 2009) and prevents the proteolysis of centromeric CenH3 (Dunleavy et al., 2009; Foltz et al., 2009). This activity of HJURP might explain why CenH3 is protected at the centromere while it is subject to proteolysis elsewhere in the genome.

The presence of CenH3 at the centromere not only establishes centromere identity, but it also recruits proteins involved in the assembly of the kinetochore, the protein complex responsible for regulating and effecting chromosome segregation (Santaguida and Musacchio, 2009). Structurally, the kinetochore is a tri-laminate structure with an inner plate that interacts with the centromeric chromatin, and an outer plate with a fibrous corona which interacts with microtubules (McEwen et al., 1998). To explain the function of each of the dozens of proteins that form the kinetochore is beyond the scope of this introduction. Instead, attention will be focused on the essential mitotic functions of the kinetochore, microtubule attachment, attachment error correction, chromosome segregation, and the proteins directly involved in each process.

On entry into mitosis, each centrosome nucleates a short, dynamic array of microtubules that probe the cytoplasm with their growing plus ends. The “search and capture” model proposes that when these dynamic microtubules encounter kinetochores, they are preferentially stabilized, and the build-up of these microtubules contributes to the formation of the spindle (Mitchison et al., 1986). Though the “search and capture” model does not account for all sources of

microtubule nucleation within the spindle, it does accurately predict microtubule capture by the kinetochores (Hayden et al., 1990).

This microtubule capture is facilitated by Cenp-E, a large kinesin like protein that is associated with the fibrous corona of the kinetochores (Cooke et al., 1997; Yao et al., 1997). Following the initial capture by the fibrous corona, microtubule binding protein complexes such as the KMN (Knl-1, Mis12 and Ndc80) complex (Cheeseman et al., 2006), the Dam1 complex in budding yeast (Miranda et al., 2005) and the Ska complex in metazoans (Gaitanos et al., 2009) anchor the microtubules to the kinetochores.

Correcting improper microtubule kinetochore attachments during prometaphase is the role of the chromosome passenger complex, which consists of the proteins Aurora B kinase, INCENP (INner CENtromere Protein), Survivin and Borealin (Vagnarelli and Earnshaw, 2004). The CPC accomplishes this by destabilizing improper microtubule-kinetochore attachments, such as when both kinetochores are attached to microtubules from the same spindle pole. Though the exact mechanisms of how this destabilization occurs are not clear, it has been shown that Aurora B can phosphorylate Ndc80, a protein that is part of the KMN microtubule binding complex (Cheeseman et al., 2002). This phosphorylation of Ndc80 leads to a reduction of microtubule affinity in vitro, and in vivo presumably results in the detachment of the mis-attached microtubule from the kinetochore (Cheeseman et al., 2006). Aurora B has also been shown to phosphorylate the Kin I kinesin MCAK (Mitotic Centromere-Associated Kinesin) that is responsible for depolymerising microtubules. By regulating the activity of this kinesin, Aurora B can induce the depolymerisation of improperly attached microtubules (Lan et al., 2004).

The current model for how the CPC detects improper chromosome attachment is based on tension (during proper bi-orientation) or lack thereof (when chromosomes are attached to the same spindle pole / unattached kinetochores)

(Tanaka et al., 2002). When chromosomes are properly bi-oriented, their kinetochores are under tension which stretches the kinetochores (Waters et al., 1996). When stretched, proteins on the kinetochores are spatially separated from proteins at the centromere. This separation prevents Aurora B, which is located on the centromere, from phosphorylating kinetochore proteins, such as Ndc80, leading to the stable capture of microtubules by the kinetochores. Conversely when the kinetochores are not under tension, Aurora B is able to phosphorylate kinetochore proteins, leading to microtubule detachment (Liu et al., 2009).

In parallel with the CPC, the Spindle Assembly Checkpoint (SAC) localizes to unattached kinetochores. Research is ongoing as to exactly how the SAC functions, but it is known is that the presence of the SAC at unattached kinetochores down regulates the activity of the Anaphase Promoting Complex, also known as the Cyclosome (APC/C). This prevents the APC/C from targeting cyclin B and Securin for degradation and precipitating the events of anaphase (Musacchio and Salmon, 2007). This down regulation of APC/C activity is a result of the SAC components Mad2 and BubR1 binding to and inhibiting the activity of the crucial APC/C co-factor Cdc20 (Davenport et al., 2006; Fang, 2002).

When microtubules bind to the kinetochores, they strip away the components of the SAC, such as Mad2 in a Dynein dependent manner and transport them to the spindle poles (Howell et al., 2001). The activity of BubR1 is also down-regulated upon Cenp-E capture of microtubules (Mao et al., 2005). With the SAC inactivated, the APC/C is activated by Cdc20 and chromosome segregation can begin.

During metaphase, sister chromatids are bound to each other at the pericentric heterochromatin by Cohesin (Nonaka et al., 2002), a ring shaped complex formed from the proteins Smc1, Smc 3 and Scc1 that encircles the sisters and maintains cohesion (Gruber et al., 2003). At the onset of anaphase, the APC/C releases Separase from its binding partner Securin by targeting Securin for

degradation (Zur and Brandeis, 2001). Separase then cleaves the Scc1 subunit of the Cohesin complex and releases the cohesion between the sister chromatids (Hauf et al., 2001; Waizenegger et al., 2002).

Upon initiation of anaphase, the microtubules that comprise the spindle undergo several changes in their dynamics. Depolymerisation of the kinetochore microtubules at their plus ends generates a force to pull the separated sister chromatids to the spindle poles (Cassimeris, 2006). Microtubule binding protein complexes at the kinetochore, such as the Dam1 complex, maintain binding to the depolymerizing microtubules by forming a ring behind the depolymerizing protofilaments (Westermann et al., 2006). By harnessing themselves via the kinetochores to depolymerizing microtubules, chromosomes are able to segregate to the spindle poles and thus complete mitosis.

1.4: Homologous pairing, the synaptonemal complex and meiotic recombination

During meiotic prophase, all sexually reproducing organisms undergo meiotic recombination. Meiotic recombination has two important functions within the context of meiosis, it generates genetic diversity among the resulting offspring, and it reconfigures the chromatin, preparing it for two consecutive rounds of chromosome segregation.

During meiotic recombination homologous chromosomes pair up and a proteinaceous structure known as the synaptonemal complex forms between them. It was thought that the synaptonemal complex was responsible for the pairing of the homologous chromosomes. However, the presence of homologous pairing in systems where the synaptonemal complex is absent, such as *Drosophila* males (von Wettstein, 1984) and mutants that abolish the synaptonemal complex, such as a null

allele of *zip1* in yeast (Nag et al., 1995) have shown that the story is not so straightforward.

Homologous pairing seems to be dependent on sequence homology between the pairing chromosomes. In Drosophila males with transpositions of chromosomal sequence from the 2nd chromosome to the Y chromosome, the Y chromosome was shown to pair with the 2nd chromosome at frequencies based on the size of the transposition (McKee et al., 1993). However, how a chromosome identifies homologous sequences on another chromosome is still not known (McKee, 2004).

Once homologous chromosomes are paired, the synaptonemal complex forms between them. Structurally, the synaptonemal complex resembles railroad tracks with the vertical lateral elements associated with the chromosomes connected by the horizontal transverse filaments between them (Page and Hawley, 2004). Formation of the synaptonemal complex can occur independently of meiotic recombination in some organisms, such as *Drosophila* females and *C. elegans* (MacQueen et al., 2002; McKim et al., 1998). Indeed, in the case of *Drosophila* females, formation of the synaptonemal complex is essential for the initiation of meiotic recombination (McKim et al., 2002). However in other organisms, like yeast, the initiation of meiotic recombination is required for synaptonemal complex formation (Page and Hawley, 2004). Functionally, the synaptonemal complex serves to convert recombination intermediates, formed during meiotic recombination to mature chiasmata (Page and Hawley, 2004).

The initiation of meiotic recombination occurs when Spo11, a protein with homology to type II Topoisomerases, introduces double stranded breaks (DSBs) in the DNA duplex. These DSBs are then processed to form single stranded 3' overhangs. One of these 3' overhangs invades a homologous duplex where it displaces its corresponding strand of homologous DNA in a D-loop, which anneals

to the remaining single stranded 3' overhang. Repair DNA synthesis then occurs to produce a structure known as a double Holliday Junction (Cromie and Smith, 2007). Cleavage of two of the strands in the double Holliday Junction results in the creation of either crossovers, where an entire arm of a chromosome is exchanged between two homologues, or non crossovers, where only certain sequences are exchanged (Sun et al., 1989; Szostak et al., 1983). The resolution of the double Holliday Junction results in chiasmata that connect the homologues, which are important for proper segregation of the homologues during meiosis, and persist even after the synaptonemal complex is disassembled (Page and Hawley, 2004).

1.5: Meiotic chromosome segregation

In many ways, the process of meiosis resembles that of mitosis. DNA duplication occurs, the spindle forms and chromosomes are captured and stabilized by microtubules nucleated from the centrosomes. However unlike mitosis, chromosomes in meiosis undergo two rounds of segregation, meiosis I and meiosis II, without any intervening DNA duplication.

Meiotic chromosomes are connected at two places so as to coordinate chromosome segregation such that the homologous chromosomes separate before the sister chromatids. As in mitosis, sister chromatids are joined at the centromere and held together by the cohesin complex as described in section 1.3. Additionally, the homologues are held together by chiasmata formed from the resolution of the double Holliday Junctions and the chiasmata themselves are reinforced by the presence of the cohesin complex on the chromosome arms (Watanabe, 2005).

At the onset of meiosis I, the two kinetochores of each homologue (each belonging to a sister chromatid) co-orient and begin to act as a single unit. In yeast, this requires the activity of the monopolin complex (Monje-Casas et al., 2007).

During metaphase I, paired homologues (known as a bivalent) then become bioriented at the spindle midzone, with the homologues within each bivalent facing opposite spindle poles. When anaphase I begins, cohesin is cleaved at the chromosome arms, but protected at the centromere by the protein Shugoshin (Watanabe and Kitajima, 2005). This releases the attachment of the homologous chromosomes, but not the sister chromatids, and the homologues are pulled towards opposite spindle poles. Homologue segregation is followed by telophase I and cytokinesis, which results in two daughter cells each containing half the homologues (and thus half the chromosome number) found in the original mother cell.

Meiosis II proceeds in a similar fashion to mitosis, with the chromosomes bi-oriented at the spindle midzone such that each sister chromatid faces an opposite spindle pole. When anaphase II occurs, the sister chromatids are drawn towards opposite poles. Following telophase II and cytokinesis, the four resulting daughter cells each have half the chromosome number of the original mother cell. Not until fertilization and fusion with its complementary gamete will the original chromosome number be reconstituted (Petronczki et al., 2003).

1.6: Chromatin mediated spindle formation during female meiosis

During female meiosis, the bipolar spindle is formed without the centrosomes. Research has indicated that several alternate microtubule nucleation pathways play a role in forming the female meiotic acentosomal spindle. Intriguingly, chromatin itself is an important determinant of female meiotic spindle formation and is able to nucleate the microtubules that form the spindle (Karsenti et al., 1984).

The main protein implicated in chromatin mediated microtubule nucleation is Ran, a small GTPase which can exist either in a GTP or a GDP bound state.

Though Ran has intrinsic GTPase activity, the conversion of RanGTP to RanGDP can be stimulated by the activity of RanGAP (Ran GTPase Activating Protein) (Bischoff et al., 1994). Conversely, RanGDP can be converted to RanGTP by the activity of the RanGEF (Guanine nucleotide Exchange Factor) RCC1 (Bischoff and Ponstingl, 1991). Since RCC1 is localized to the chromatin (Nemergut et al., 2001) and RanGAP is mostly cytoplasmic (Mattaj and Englmeier, 1998), a gradient of Ran is set up, with the GTP bound form predominating near the chromosomes and the GDP bound form becoming more prevalent further away (Li and Zheng, 2004).

Importins are a class of proteins that facilitate the nuclear transport of Nuclear Localization Signal (NLS) containing proteins (Gorlich et al., 1995). It has been shown that RanGTP can bind to Importins and cause them to release their cargo (Gorlich et al., 1996; Rexach and Blobel, 1995). Immunoprecipitation assays have indicated that one of the cargo molecules subject to Importin binding is TPX2 (Targeting Protein of Xklp2), a microtubule associated protein that is able to induce microtubule nucleation in Xenopus egg extracts (Gruss et al., 2001).

The current model for female meiosis starts with a high gradient of RanGTP around the chromatin causing the local release of Importin bound TPX2 following nuclear envelope break down (Gruss and Vernos, 2004). This local release of TPX2 initiates microtubule nucleation in the vicinity of the chromatin, with some of the microtubule fibres captured by the kinetochores as described in section 1.3. Other microtubules are organized by the spindle midzone, which is comprised of chromatin and other associated proteins such as Subito, into the interpolar microtubules which comprise the rest of the spindle (Jang et al., 2005).

Plus end directed microtubule motors such as the Eg5 kinesin are responsible for bundling the interpolar microtubules at the midzone (Sawin et al., 1992) and minus end directed motors such as Ncd (Non-claret disjunctional) focus the spindle poles (Hatsumi and Endow, 1992). In lieu of centrosomes, these focused

poles are stabilized by Msps (Mini-Spindles), a microtubule associated protein of the dis1/TOG family which is anchored by D-TACC (Drosophila Transforming Acidic Coiled Coil protein) at the spindle poles (Cullen and Ohkura, 2001). (Fig. 2)

Mutations in certain proteins, such as NHK-1 (Nucleosomal Histone Kinase 1), disrupt chromatin organization during female meiosis and also affect the proper formation of the female meiotic bipolar spindle (Cullen et al., 2005). In light of chromatin's importance in forming the female meiotic bipolar spindle, it is essential to understand the origins and maintenance of the unique configuration that chromatin assumes during female meiotic prophase: The Karyosome.

1.7: The Karyosome

During female meiosis in many species, a spherical structure is formed from all the chromatin within the developing oocyte nucleus (referenced in (Garagna et al., 2004; Parfenov et al., 1989)). The pathways involved in the formation of this structure, named alternatively the karyosome or the karyosphere, and the role that it plays in female meiosis are not well understood. However, its formation is proposed to be required for the oocyte to acquire full developmental competence (Zuccotti et al., 1998; Zuccotti et al., 2002).

The nucleolus is a nuclear structure that is intimately involved with the formation of the karyosome in many species, including mice (Garagna et al., 2004) and humans (Parfenov et al., 1989). During meiotic maturation in mice oocytes, the oocytes transition from a non-surrounded nucleolus (NSN) chromatin configuration to a surrounded nucleolus (SN) configuration (Mattson and Albertini, 1990). NSN oocytes are transcriptionally active (Debey et al., 1993), with homogenously diffused chromatin and heterochromatin localized preferentially to the nuclear periphery

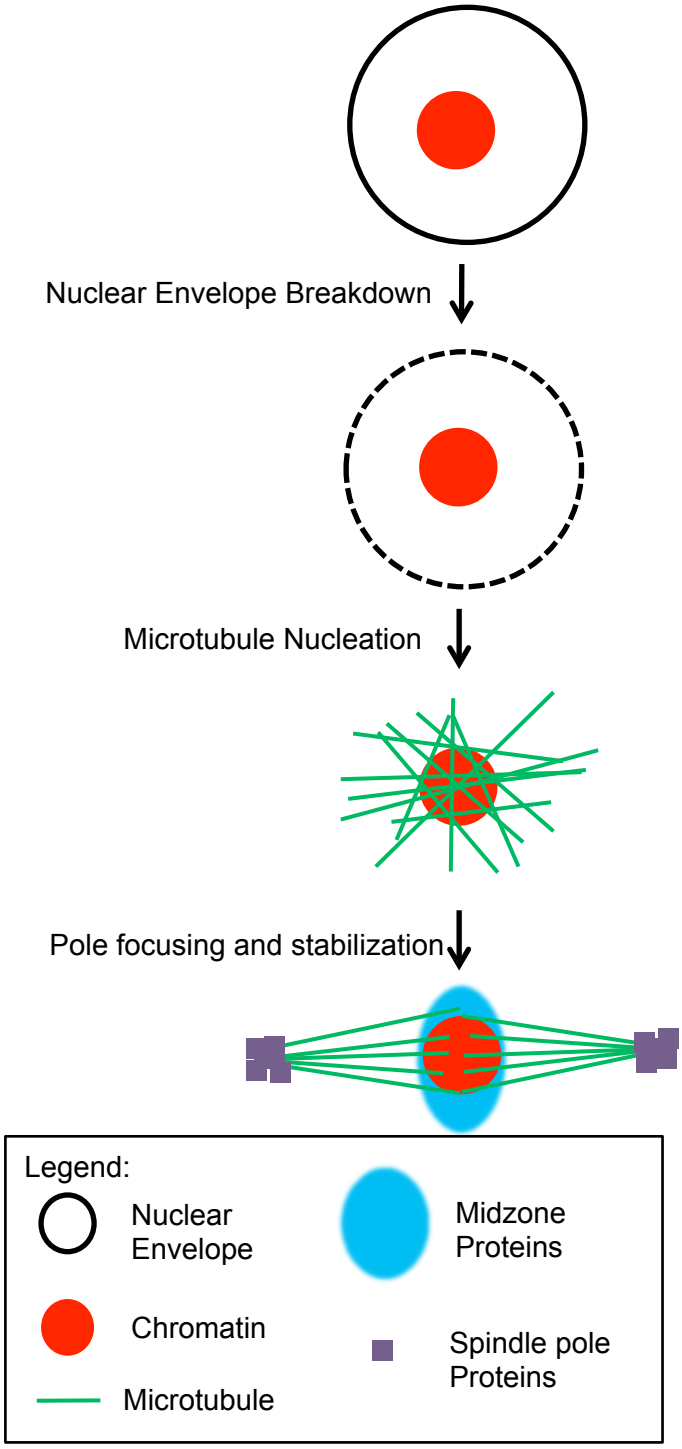

Figure 2. Formation of the acentrosomal bipolar spindle.
During female meiosis, the nuclear envelope breaks down and microtubules are nucleated around the chromatin. These microtubules are then organized into the bipolar spindle.

(Garagna et al., 2004). SN oocytes on the other hand are transcriptionally inactive (Debey et al., 1993; Longo et al., 2003) with chromatin taking on a more compact thread like morphology (Zuccotti et al., 1995) and heterochromatin forming a rim around the nucleolus (Longo et al., 2003).

Interestingly, antibodies specific for centromeric proteins in have revealed a progressive clustering of the centromeres around the nucleolus as the oocyte transitions to the SN configuration (Garagna et al., 2004). However it still remains to be seen whether centromeric clustering plays a role in the formation and maintenance of the karyosome.

In certain species such as *Drosophila melanogaster*, the nucleolus disappears early in oogenesis (Liu et al., 2006; Mahowald, 1972). How the karyosome forms in the absence of the nucleolus is not well understood, but experiments performed in *Drosophila* have revealed certain proteins that, either directly or indirectly, affect the formation of the karyosome.

During meiotic recombination in *Drosophila*, double stranded breaks (DSBs) are generated to facilitate strand invasion and crossover repair (McKim et al., 2002). To repair these DSBs *Drosophila* relies on two proteins, SpnB and Okra, the *Drosophila* homologues of the yeast DSB repair proteins Rad51 and Rad54 (Ghabrial et al., 1998). If these DSBs are not repaired, the meiotic recombination checkpoint is activated which causes egg dorsal/ventral patterning defects as well as karyosome morphology defects (Ghabrial et al., 1998; Gonzalez-Reyes et al., 1997).

Mutations in the translation initiation factor Vasa have been shown to cause similar phenotypes (Lasko and Ashburner, 1988; Styhler et al., 1998; Tomancak et al., 1998). Unlike SpnB or Okra, the defects caused by Vasa cannot be rescued by disabling the meiotic recombination checkpoint. Furthermore, when the meiotic recombination checkpoint is active, the mobility of the Vasa protein in an SDS-

PAGE gel is altered, indicating modification of the Vasa protein (Ghabrial and Schupbach, 1999). These results suggest that Vasa acts downstream of the meiotic recombination checkpoint and has two main functions when the meiotic recombination checkpoint is activated. It influences the dorsal/ventral patterning of oocytes by directly controlling the translation of the Gurken protein, and it affects karyosome morphology by an as yet unknown pathway (Ghabrial and Schupbach, 1999). (Fig. 3)

While these experiments have revealed that activation of the meiotic recombination checkpoint indirectly affects karyosome morphology, the actual proteins that directly play a role in karyosome formation have remained elusive. However, recent work has identified a protein, Nucleosomal Histone Kinase 1 (NHK-1) that directly effects the formation of the karyosome.

NHK-1 was originally identified as a kinase that phosphorylated nucleosomal Histone H2A (Aihara et al., 2004). A female sterile mutant of NHK-1 was subsequently found that affected the formation and maintenance of the karyosome (Cullen et al., 2005; Ivanovska et al., 2005). Experiments have shown that there are actually two separate pathways by which NHK-1 can affect the morphology of the karyosome.

In Drosophila female meiosis, the condensin complex is loaded onto the chromosomes following the disassembly of the synaptonemal complex. However, in NHK-1 mutants, the chromosomes do not disassemble the synaptonemal complex and the condensin complex is not loaded onto the chromosomes. The loss of phosphorylation on histone H2A is proposed to be the reason behind this failure to load condensin onto the chromosomes, and ultimately the root cause of the karyosome morphology defects (Ivanovska et al., 2005).

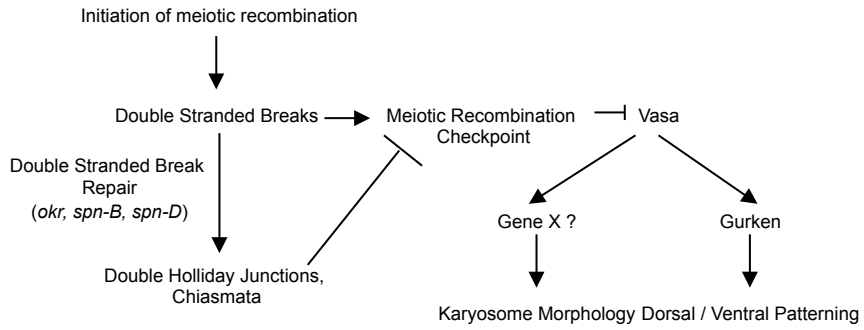

Figure 3. Activation of the meiotic recombination checkpoint leads to karyosome morphology defects.
The meiotic recombination checkpoint affects both dorsal patterning in the eggs as well as karyosome morphology via an as yet unidentified pathway.
Image adapted from (Ghabrial and Schupbach, 1999).

Histones are not the only proteins phosphorylated by NHK-1. An in-vitro kinase assay identified BAF (Barrier-to-Autointegration Factor) as a second phosphorylation target (Lancaster et al., 2007). The BAF protein binds to both chromatin and LEM (LAP2, Emirin, MAN1) domain containing nuclear membrane proteins, such as LAP2 and Emerin (Furukawa, 1999; Segura-Totten and Wilson, 2004). Phosphorylation of BAF has been shown in-vitro to reduce the affinity that BAF has for both chromatin and the LEM domain (Nichols et al., 2006). By binding to both chromatin and nuclear membrane proteins simultaneously, BAF is proposed to link chromatin to the inner nuclear envelope (Shumaker et al., 2001).

The current model is that phosphorylation by NHK-1 during female meiosis reduces the affinity that BAF has for both chromatin and LEM domain containing proteins. This releases the chromatin from its anchoring at the nuclear envelope and facilitates the formation of the karyosome (Lancaster et al., 2007). To test this hypothesis, a non-phosphorylatable form of BAF was created. This non-phosphorylatable BAF caused a karyosome morphology phenotype similar to that seen in NHK-1(Lancaster et al., 2007), indicating that the phosphorylation of BAF is an important step in the formation of the karyosome. (Fig. 4)

Even though *Drosophila* karyosomes do not organize around a nucleolus, as in mice and humans, there is still evidence of similarities between the two processes. Research has shown that in *Drosophila* karyosomes, the centromeres of non-homologous chromosomes are clustered (Dernburg et al., 1996). Whether this clustering of centromeres in *Drosophila* is analogous to centromere clustering around the nucleolus in mice still remains to be seen. However these similarities indicate that karyosome organization might proceed along similar lines even in disparate model systems.

Though current research is revealing proteins and pathways that are involved in the formation of the karyosome, it remains a little understood facet of

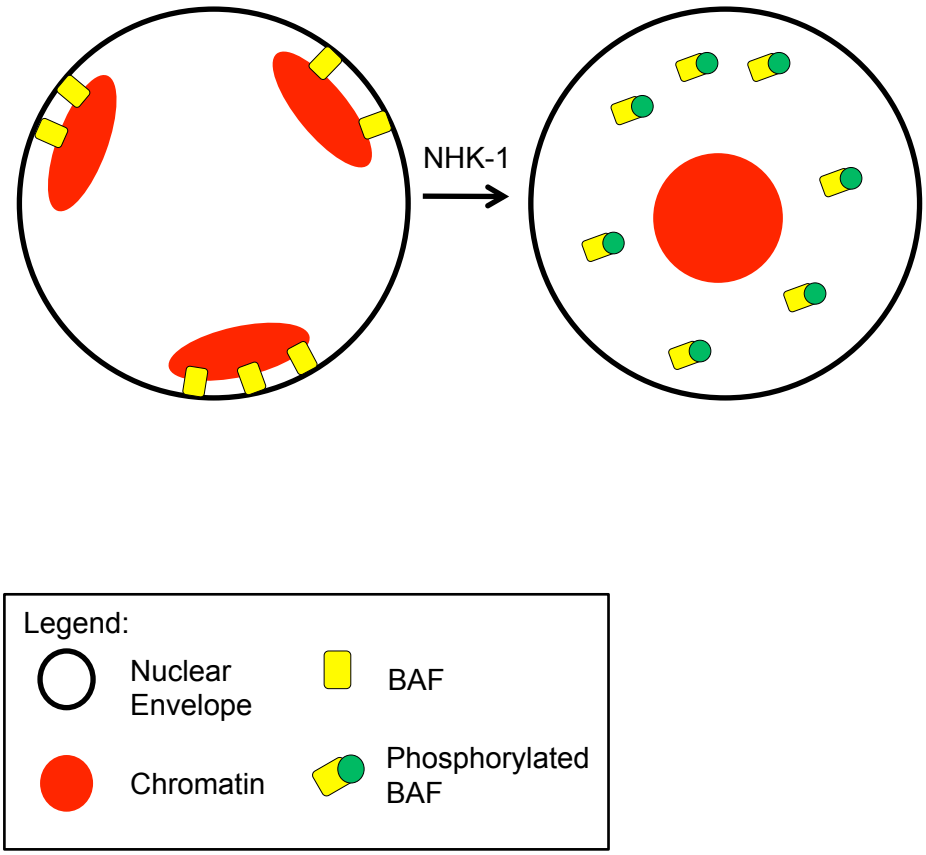

Figure 4. NHK-1 phosphorylation of BAF releases chromatin from the nuclear periphery.
Phosphorylation of BAF by NHK-1 reduces its affinity for both nuclear membrane proteins and chromatin. This release of chromatin is important in the formation of the karyosome.

female meiosis. More work is required to decipher the role and regulation, the formation and function of this enigmatic female meiotic specific structure.

1.8: Project aims

1.) To identify mutants defective in karyosome morphology

Recent research has proposed that the karyosome, a little studied chromatin structure that forms during female meiotic prophase, is important for both spindle formation and meiotic progression. However the proteins and pathways involved in the formation of this essential structure are mostly unknown.

The primary aim of my project will be to identify proteins that have a role in karyosome formation and maintenance. To identify these proteins, I will screen a collection of mutants, and identify those where karyosome morphology is affected. Subsequent genetic analysis of these particular mutants should identify the proteins that are directly involved in forming and maintaining the karyosome.

2.) To identify genetic modifier that interact with NHK-1, a protein essential for karyosome formation

NHK-1 directs proper karyosome formation by way of its phosphorylation target BAF. However the regulatory mechanisms governing this interaction and other potential phosphorylation targets of NHK-1 are not known. By screening deficiencies for modifiers of *NHK-1*^{trip}, a semi-lethal allele of *NHK-1* (using a viability assay), I hope to identify genes that interact with NHK-1 in either a synergistic or antagonistic manner

Chapter 2:

Materials and Methods

Chapter 2: Materials and Methods

2.1: Suppliers

All chemicals used in this study were supplied by Invitrogen, BDH or Sigma-Aldrich, and were of analytical grade. All oligonucleotides were purchased from MWG-Biotech. Suppliers of all other reagents, kits and equipment are stated in their respective sections. All fly stocks were obtained from the Bloomington stock centre unless stated otherwise.

2.2: Commonly used buffers

PBS

137mM Sodium chloride

2.7mM Potassium chloride

4.3mM Na_2HPO_4

1.4mM KH_2PO_4

Robbs Media (adjust to pH 7.4 with NaOH)

55mM Sodium Acetate

40mM Potassium Acetate

100mM Sucrose

10mM Glucose

1.2mM Magnesium chloride

1mM Calcium chloride

100mM Hepes

2x Fly fix buffer (adjust to pH 7.2 with acetic acid)

100mM Cacodylic acid

100mM Sucrose

40mM Potassium acetate

10mM Sodium acetate

10mM EGTA

Mounting Media

85% Glycol

2.5% Propyl gallate

10x DNA sample buffer

30% Glycerol

25mM EDTA

5% 6x Gel loading dye, blue (New England biolabs)

2.3: Fly stocks

2.3a: *ovo^{D}* stocks used to generate germline clones

Genotype	Origin
ovo^{D}, w^{+}, FRT9-2 [w^{+}] / Y	Nusslein-Volhard
y, w, FLP^{122} / Y ; FRT40A, ovo^{D} / CyO, [hs-hid]	Nusslein-Volhard
y, w, FLP^{122} / Y ; FRT42B, ovo^{D} / CyO, [hs-hid]	Ohkura lab

2.3b: Bloomington duplications used to rescue males from lethal X chromosome mutants for complementation testing

Name	Duplicated X segment
Dp(1;Y)y[2]67g19.1	1A1;2B17 -18 + 20A3;2Fh
Dp(1;f)R	1A3-4;3A1 - 2 + 20A1;20Fh
Dp(1;3)w[vco]	2B17 - C1;3C5 - 6
Dp(1;2;Y)w[+]	2D1 -2;3D3 - 4 + 1B1;1B2 + 20B;20F + 21A1;22E4
Dp(1;2)w-ec	3C1 - 2;3E7 - 8
Dp(1;2)4FRDup	3C2;3F + 3F;4E3 + 20Fh;20Fh + 4E3;5A1 - 2;26D7
Dp(1;Y)dx[+]5	4C11;6D8 + 1A1;1B4
Dp(1;3)sn[13a1]	6C;7C9 - D1
Dp(1;2)sn[+]72d	7A8 - 8A5
Dp(1;Y)619	7D;8B3 - D7 + 16A1;16A1 + 20B;20Fh
Dp(1;Y)FF1	8C - D;9B + 1A1;1B2
Dp(1;2)v[+]75d	9A2;10C2
Dp(1;Y)BSC1	1A1;1B1 - 2 + 10C1 - 2;11D3 - 8
Dp(1;Y)y[+]v[+]#3	9F4;10E3 - 4 + 1A1;1B2 + 20B;20Fh
Dp(1;f)y[+]	11D - 11F;12B7 + 1A1;1B2 - 12
Dp(1;f)LJ9	12A6 - 10;13A2 - 5 + 1A1;1B3 - 4
Dp(1;4)r[+]l	13F1 - 4;16A1 + probably X tip segment 1A1;1A
Dp(1;Y)W73	15B1-D;16F + 1A1;1B2 + 16A1;16A1 + 20A;20Fh + 20B;20Fh
Dp(1;Y)W39	16F1 - 4;18A5 - 7 + 1A1;1B2 + 19E5 - 7;20Fh
Dp(1;Y)y[+]mal[+]	18F1;20Fh + 1A1;1B2

2.3c: Stocks used in recombination mapping of X-339-19

Genotype	Origin
m	Bloomington stock center (#69)
FM0, B, f, m, sc, v, w, y / Y	Bloomington stock center (#1954)

2.3d: Bloomington deficiencies used to map lethal mutations in X-339-19

Name	Cytological region deleted
Df(1)A113	3D6 - 4F8
Df(1)BSC640	5E1 - 5E7
Df(1)BSC654	5B6 - 5D2
Df(1)BSC724	5C2 - 5D3
Df(1)C149	5A8 - 5C5
Df(1)dx81	5C3 - 6C12
Df(1)ED418	5C7 - 5E4
Df(1)Exel6238	5D3 - 5E4
Df(1)Exel6239	5F2 - 6B2
Df(1)Exel6240	6B2 - 6C4
Df(1)Exel6802	5A12 - 5D1
Df(1)Exel6829	5C7 - 5F3
Df(1)Exel6878	6C12 - 6D8
Df(1)G4e[L]H24i[R]	5E3 - 5E8;6B
Df(1)JC70	4C11 - 5A4
Df(1)JF5	5E5 - 5E8
Df(1)N-8	3C1 - 3D6
Df(1)N73	5C2 - 5D6
Df(1)RC40	4B1 - 4F1

2.3e: Bloomington deficiencies used to map sterile mutations in the single allele X chromosome mutants

Name	Cytological region deleted
Df(1)ED404	1D2 - 1E3
Df(1)ED447	17C1 - 17F1
Df(1)ED6443	1B14 - 1E1
Df(1)ED6521	1E3 - 1F4
Df(1)ED6565	2B14 - 2F5
Df(1)ED6574	2E1 - 3A2
Df(1)ED6630	3B1 - 3C5
Df(1)ED6712	3D3 - 3F1
Df(1)ED6716	3F2 - 4B3
Df(1)ED6720	4B3 - 4C7
Df(1)ED6727	4B6 - 4D5
Df(1)ED6802	5A12 - 5D1
Df(1)ED6829	5C7 - 5F3
Df(1)ED6906	7A3 - 7B2
Df(1)ED6957	8B6 - 8C13
Df(1)ED6991	8F9 - 9B4
Df(1)ED7005	9B1 - 9D3
Df(1)ED7010	9D3 - 9D4
Df(1)ED7067	10B8 - 10C10
Df(1)ED7147	10D6 - 11A1
Df(1)ED7153	11A1 - 11B1
Df(1)ED7170	11B15 - 11E8

Df(1)ED7217	12A9 - 12C6
Df(1)ED7225	12C4 - 12E8
Df(1)ED7229	12E5 - 12F2
Df(1)ED7294	13B1 - 13C3
Df(1)ED7331	13C3 - 13F1
Df(1)ED7344	13E1 - 13F17
Df(1)ED7364	14A8 - 14C6
Df(1)ED7374	15A1 - 15E3
Df(1)ED7424	17D1 - 18C1
Df(1)ED7620	18D10 - 19A2
Df(1)ED7635	19A2 - 19C1
Df(1)ED7664	19F1 - 19F6
Df(1)ED11354	2F6 - 3A4
Df(1)ED14021	20C3 - 20F1

2.3f: Stocks used in recombination mapping of 2R-242-29 and 2R-322-03

Genotype	Origin
eya / CyO	David Finnegan
al, dp, b, pr, Bl, c, px, sp / CyO	Bloomington stock center (#214)

2.3g: Bloomington deficiencies used to map sterile mutation in 2R-242-29

Name	Cytological region deleted
Df(2R)BSC132	45F6 - 46B4
Df(2R)BSC153	48C1 - 48D7

Df(2R)BSC199	48C5 - 48E4
Df(2R)BSC231	47F8 - 48B6
Df(2R)BSC259	48A3 - 48C4
Df(2R)BSC271	44F12 - 45A12
Df(2R)BSC274	50A7 - 50B4
Df(2R)BSC279	45A9 - 45E3
Df(2R)BSC281	46F1 - 47A9
Df(2R)BSC298	46B2 - 46C7
Df(2R)BSC303	46E1 - 46F3
Df(2R)BSC305	49A4 - 49A10
Df(2R)BSC307	50B6 - 50C18
Df(2R)BSC329	48A3 - 48D3
Df(2R)BSC361	50C3 - 50F1
Df(2R)BSC408	45D4 - 45F4
Df(2R)BSC595	47A3 - 47F1
Df(2R)BSC651	51C5 - 51E2
Df(2R)CB21	48E - 49A
Df(2R)ED2219	47D6 - 48B6
Df(2R)ED2222	47F13 - 48B6
Df(2R)ED2247	48A3 - 48D5
Df(2R)Exel6062	49E6 - 49F1
Df(2R)Exel8057	49F1 - 49F10
Df(2R)X3	46C1 - 46E2
Df(2R)01D09Y-M073	45F5 – 6 - 46C4 - 7

2.3h: Bloomington stocks used to map sterile mutation in 2R-129-09

Name	Cytological region deleted / comments
Df(2R)BSC398	52A13 - 52D2
Df(2R)BSC427	52A10 - 52D2
Df(2R)Exel6285	52A4 - 52B5
Df(2R)Exel9015	51F11 - 51F12
Df(2R)Exel9026	52A13 - 52A13
dup[a1]	Lethal allele of *Dup*
dup[a3]	Lethal allele of *Dup*
dup[k03308]	Lethal allele of *Dup*
dup[PA77]	Female sterile allele of *Dup*

2.3i: Stocks used for the *NHK-1* genetic modifier screen

Genotype	Origin
w ; cu, trip / TM6B	Ohkura lab
w / Dp(1;Y) y^+ ; CyO / nub, b, noc^{Sco}, lt, stw ; MKRS / TM6B, Tb	Bloomington stock center (#3703)

2.3j: Bloomington deficiencies used for genetic modifier screen and the mapping of single allele 2R mutants

The following deficiencies were used to identify genetic modifiers of *NHK1*. These deficiencies were also used to map the sterile and lethal mutations in the single

allele 2R mutants. *Df(2R)ED2426* and *Df(2R)ED2436* that mapped the sterility causing region of 2R-129-09 that contained *SRPK* are listed in bold.

Name	Cytological region deleted
Df(2L)ED19	21B3 - 21B7
Df(L)ED62	21D1 - 21E2
Df(2L)ED94	21E2 - 21E3
Df(2L)ED123	22B8 - 22D4
Df(2L)ED136	22F4 - 23A3
Df(2L)ED250	24F4 - 25A7
Df(2L)ED489	27E4 - 28B1
Df(2L)ED499	27F4 - 28C4
Df(2L)ED611	29B4 - 29C3
Df(2L)ED623	29C1 - 29E4
Df(2L)ED647	29E1 - 29F5
Df(2L)ED678	29F5 - 30B12
Df(2L)ED695	30C5 - 30E4
Df(2L)ED746	31F4 - 32A5
Df(2L)ED775	33B8 - 34A3
Df(2L)ED784	34A4 - 34B6
Df(2L)ED793	34E4 - 35B4
Df(2L)ED1050	35B8 - 35D4
Df(2L)ED1109	36A3 - 36A10
Df(2L)ED1231	37C5 - 37E3
Df(2L)ED1303	37E5 - 38C6
Df(2L)ED1315	38B4 - 38F5
Df(2L)ED1473	39B4 - 40A5
Df(2R)ED1618	42C3 - 43A1

Df(2R)ED1673	42E1 - 43D3
Df(2R)ED1715	43A4 - 43F1
Df(2R)ED1725	43E4 - 44B5
Df(2R)ED1735	43F8 - 44D4
Df(2R)ED1742	44B8 - 44E3
Df(2R)ED2155	47C6 - 47F8
Df(2R)ED2308	49C3 - 49E7
Df(2R)ED2354	50E6 - 51B1
Df(2R)ED2426	**51E2 - 52B1**
Df(2R)ED2436	**51F11 - 52D11**
Df(2R)ED2457	52D11 - 52E7
Df(2R)ED3610	54F1 - 55C8
Df(2R)ED3683	55C2 - 56C4
Df(2R)ED3728	56D10 - 56E2
Df(2R)ED3791	57B1 - 57D4
Df(2R)ED3923	57F6 - 57F10
Df(2R)ED3952	58B10 - 58E5
Df(2R)ED4065	60C8 - 60E8
Df(2L)ED5878	21B1 - 21B3
Df(2L)ED7007	27A1 - 27C7

2.3k: Bloomington deficiencies used to further map the interacting region in *Df(2R)ED1742*

Name	Cytological region deleted
Df(2R)BSC266	44A2 - 44D1
Df(2R)Exel6056	44A4 - 44C2

Df(2R)Exel6057	44B8 - 44C4
Df(2R)Exel6058	44C4 - 44D1
Df(2R)Exel7095	44B3 - 44C2
Df(2R)Exel7096	44C6 - 44D3
Df(2R)Exel8047	44D4 - 44D5

2.4: Fly handling

Standard techniques of fly manipulation were followed (Ashburner, 1989). Fly stocks were grown at 25^{o}C or 18^{o}C on standard cornmeal media. w^{1118} was used as the wild type in all experiments. All fly stocks listed in this chapter were obtained from Bloomington stock centre, and information concerning these stocks can be found on Flybase. The Nusslein-Volhard collection used in the screen was created in the lab of Christiane Nusslein-Volhard (Luschnig et al., 2004; Vogt et al., 2006).

2.5: Germline clone induction

To generate female flies with ovaries that were germline clones for the mutant chromosomes, the crossing scheme as laid out in (Fig. 5) was carried out. Mated females were allowed to lay eggs for two day. On the third day, the parents were tipped into a new bottle and stored at 18^{o}C. The bottles containing the larvae were then heat shocked at 37^{o}C in an agitating water bath (Grant) for 1 hr for the X chromosome mutants and 45 mins for the 2L (left arm of the second chromosome) and 2R (right arm of the second chromosome) mutants. After heat shocking, bottles containing the larvae were left overnight at 24^{o}C. On the 4th and 5th day, heat

X chromosome germline clone induction

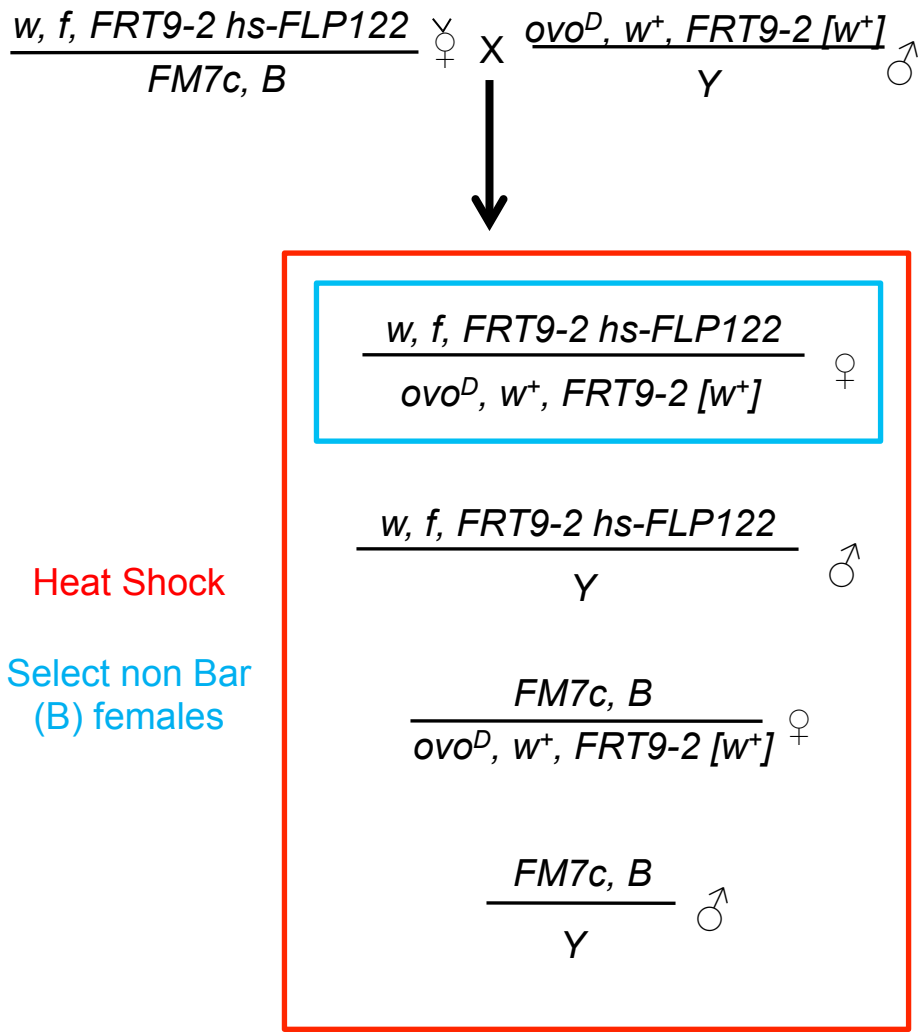

Figure 5. Crossing schemes for the generation of X chromosome germline clone females.
Crossing scheme to generate germline clone females of the X chromosome mutants. The X chromosome germline were chosen based on eye morphology (the germline clones have normal, non Barr, eyes).

2L chromosome germline clone induction

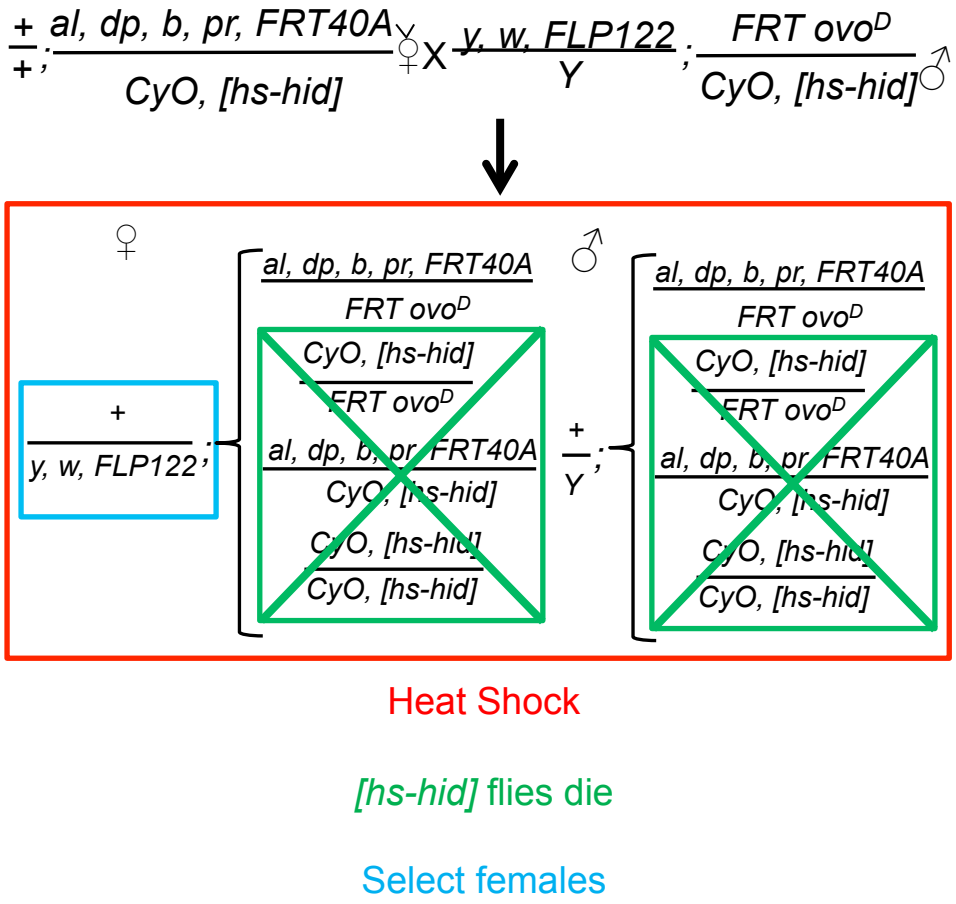

Figure 5 (cont). Crossing schemes for the generation of 2L chromosome germline clone females.
Crossing scheme to generate germline clone females of the 2L chromosome mutants. All flies with the *[hs-hid]* gene die upon heat shock. Remaining females have germline clone ovaries.

2R chromosome germline clone induction

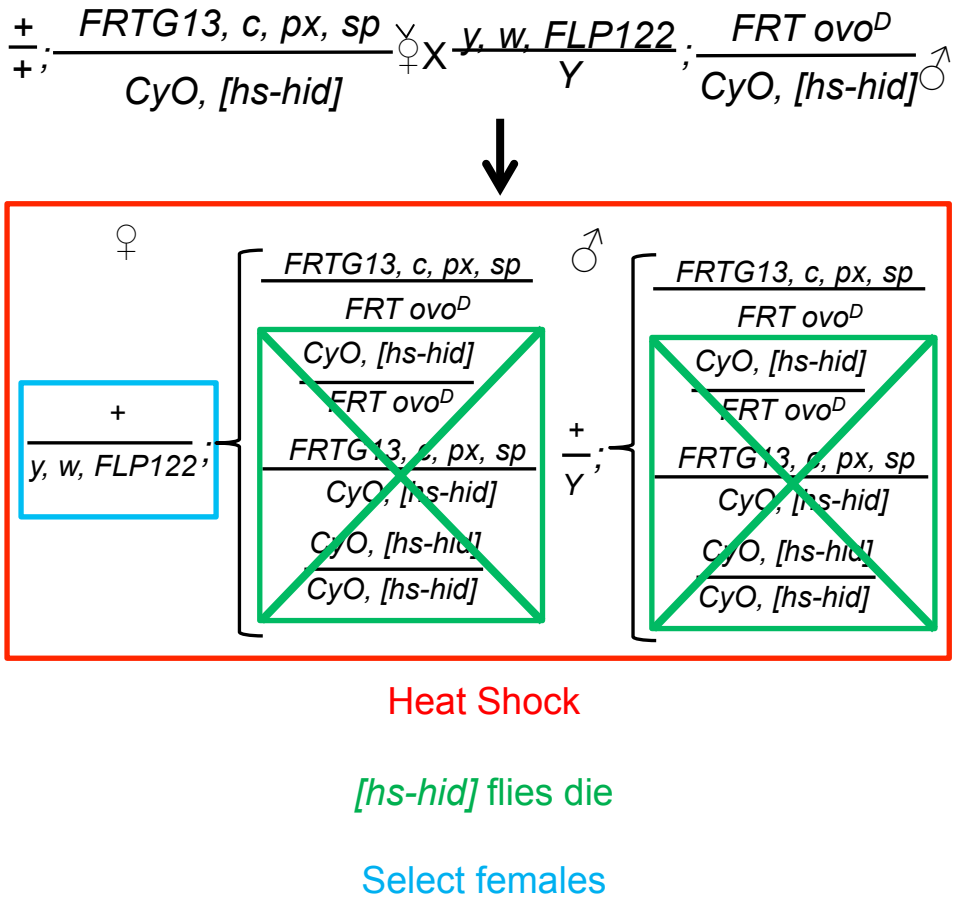

Figure 5 (cont). Crossing schemes for the generation of 2R chromosome germline clone females.
Crossing scheme to generate germline clone females of the 2R chromosome mutants. All flies with the *[hs-hid]* gene die upon heat shock. Remaining females have germline clone ovaries.

shocking was repeated as on the 3rd day and after heat shocking the bottles were stored at 24°C. After the third heat shock treatment on the 5th day, bottles were left at 24°C for five more days. On the 11th day after mating the parents, the heat shocked adult progeny of the cross were collected. For the X chromosome mutants, females with germline clone ovaries were selected on the basis of their eye phenotype (the females with germline clone ovaries have wild type eyes). For the 2nd chromosome mutants, because of presence of the *hid* gene (*head involution defective*) on the balancer chromosomes under control of a heat shock promoter [*hs-hid*], only the females with germline clone ovaries survive to adulthood. These females with germline clone ovaries were matured in yeasted bottles with half as many males as females for 3 days at 24°C or for 6 days at 18°C. After maturing, females with germline clone ovaries were dissected as described in section 2.6.

2.6: Fixing and staining of karyosomes

Females with germline clone ovaries were matured for dissection for 6 days at 18°C or for 3 days at 24°C. 4 or 5 mature females were put to sleep with carbon dioxide and decapitated. Decapitated females were dissected in Robbs medium under a light microscope at 15x magnification, and the ovaries were removed. Ovaries were slightly teased apart to allow entry of fixing and staining solutions and transferred to a 1.5ml tube. The ovaries were then fixed in 100µl of fly fix mixture containing 8% formaldehyde and 1x fly fix buffer for 10 mins. Following fixation, ovaries were washed in 0.1% Triton X-100 in PBS (henceforth known as PBST). After washing, ovaries were stained in 100µl staining mixture containing 0.2µg/ml propidium iodide, 0.4µg/ml DAPI, 0.4µg/µl RNase in PBST for 10 mins. Following staining, ovaries were washed twice in PBST. After washing, fixed and stained ovaries were placed on a coverslip containing 18µl of mounting medium. Under a light microscope at 15x

magnification, ovaries were completely teased apart and the fragments were pushed to the bottom of the mounting medium, adjacent to the coverslip. A glass slide was then lowered onto the ovaries in the mounting medium, and the coverslip was sealed with nail varnish.

2.7: Antibody staining

Females with germline clone ovaries were matured for dissection for 6 days at 18^{o}C or for 3 days at 24^{o}C. 4 or 5 mature females were put to sleep with carbon dioxide and decapitated. Decapitated females were dissected in Robbs medium under a light microscope at 15x magnification, and the ovaries were removed. Ovaries were slightly teased apart to allow entry of fixing and staining solutions and transferred to a 1.5ml tube. The ovaries were then fixed in 100µl of fly fix mixture containing 8% formaldehyde and 1x fly fix buffer for 10 mins. Following fixation, ovaries were washed in PBST. Ovaries were then blocked in 100µl of block solution containing 1% Triton X-100, 10% foetal calf serum in PBS for 2hrs. Ovaries were then washed in PBST. After washing, ovaries were stained in 50µl of 1/50 concentration of rabbit primary antibody against CID (Abcam) diluted in PBST overnight. After staining with the primary antibody, the ovaries were washed. After washing the ovaries were stained in 100µl of secondary antibody staining solution containing 1/250 concentration of 488 secondary antibody against the rabbit primary antibody (Alexa Fluor), 0.2µg/ml propidium iodide, 0.4µg/ml DAPI, 0.4µg/µl RNase diluted in PBST overnight. After staining with the secondary antibody, the ovaries were washed. After washing, the stained ovaries were placed on a coverslip containing 18µl of mounting medium. Under a light microscope at 15x magnification, ovaries were completely teased apart and the fragments were pushed to the bottom of the

mounting medium, adjacent to the coverslip. A glass slide was then lowered onto the ovaries in the mounting medium, and the coverslip was sealed with nail varnish.

2.8: Microscopy

All images were examined using the Axio Imager with an attached LSM5 exciter confocal microscope (Zeiss). Karyosomes were examined at 63x magnification, using the plan-apochromat 63x / 1.4 numerical aperture objective lens. Immersol 518F oil was applied to the coverslip to facilitate the oil immersion objective. Propidium iodide staining was visualized using the 543nm helium/neon laser and DAPI staining the 405nm diode laser. The secondary antibody used for CID staining was visualized with the 488nm argon laser. Normal karyosomes were imaged and a single, representative, Z section image was imaged. For morphologically abnormal karyosomes, 1μm thick Z sections that overlapped by 0.5μm were taken across the entire visible karyosome. Karyosomes stained with the anti-CID antibody were visualized in the same manner as morphologically abnormal karyosomes, using lasers for visualizing both propidium iodide and the secondary antibody to the primary CID antibody. Images used in the results were exported as Tagged Image File Format (TIFF) files. Some of the images shown in the results were a projection of 3-6 Z sections taken of a single karyosome that most clearly captured the relevant feature being depicted. Images were adjusted for contrast and brightness uniformly across the entire image and cropped to 250 pixels by 250 pixels in Photoshop.

2.9: Examining the dorsal patterning of eggs from germline clone ovaries

Females with germline clone ovaries were matured as described previously. A yeast paste was made by mixing yeast with water and stirring until homogenous. A small

amount of yeast paste was placed on grape juice plates 22.5g/l agar, 25g/l sucrose, 1.5g/l nipagin, 12.5% red wind concentrate. The grape juice plates with yeast were fitted to the bottom of truncated fly bottles and sealed in place with autoclave tape. The matured females were placed along with half as many males, in the bottles with the grape juice plates. These bottles containing the flies were sealed with cotton and placed at 24^{o}C for 2hrs. After 2hrs flies were tipped into a bottle containing a new grape juice plate with yeast and replaced at 24^{o}C and left overnight. The old grape juice plate with yeast was removed from the truncated bottle, covered with the plate cover, sealed with autoclave tape and labelled. These grape juice plates where the flies had laid their eggs were examined under a light microscope at 20x magnification. A maximum of 50 eggs for each mutant were examined and the dorsal patterning phenotype of these 50 eggs was recorded. Eggs were separated into the following 3 categories: Normal dorsal development, fused dorsal appendages and missing dorsal appendages. Normal dorsal appendages were well developed and completely separated from the base to the tips. If the dorsal appendages of an egg showed adhesion at the base then it was regarded as having fused dorsal appendages. If there were less than 50 eggs on the first grape juice plate, the second grape juice plate that had been left overnight was examined and the dorsal patterning of the eggs laid was recorded and the results combined with those of the first grape juice plate.

2.10: Oligonucleotides

To sequence Dup and SRPK, the following oligonucleotides were used:

Name	Sequence	Comments
oBL09	CTG GTT GTC AAG GTG CTT GTT	Forward PCR oligo for exon 3 of *Dup*
oBL10	ATC TAG CCT GAC CTT CCC TTT	Reverse PCR oligo for exon 3 of *Dup*
oBL11	ACA CTC CAC AGT CCG TGG TTT	Forward PCR oligo for exon 1, 2 of *Dup*
oBL12	AAC AGC TGA GTG GTT AGT GTT	Reverse PCR oligo for exon 1, 2 of *Dup*
oBL13	ATC GCT GTG GTC ACA CTG GAA	Forward PCR oligo for exon 1 of *SRPK*
oBL14	TGC TGT GCT TGT CTT TGG CAA	Reverse PCR oligo for exon 1 of *SRPK*
oBL15	ATC CCG TGA AAA CGC ACT CAA	Forward PCR oligo for exon 2, 3 of *SRPK*
oBL16	AAG AGT GCG GCC AGA ACT AAA	Reverse PCR oligo for exon 2,3 of *SRPK*
oBL17	AAC GAG AAG CGA AAG TTG CTT	Forward PCR oligo for exon 4 of *SRPK*
oBL18	CCT TTT AGT GCT GTT GCT CTT	Reverse PCR oligo for exon 4 of *SRPK*
oBL19	GGT TAG CCT AAT CCG GTT	Sequencing oligo for exon 3 of *Dup*
oBL20	CTC GAT CAG TGA TTT TGG	Sequencing oligo for exon 3 of *Dup*
oBL21	GAT CGA GCA GAA GGC TCT	Sequencing oligo for exon 3 of *Dup*
oBL22	GGA CTT GAA ACT ATA GGA	Sequencing oligo for exon 2 of *Dup*
oBL23	CCA GCT TAC TGG ACT GAG	Sequencing oligo for exon 1, 2 of *Dup*
oBL24	ATT TGC CAC ACA CAA CAG	Sequencing oligo for exon 1 of *SRPK*
oBL25	GAA TTC GCT GTC GTA TTT	Sequencing oligo for exon 2,3 of *SRPK*

oBL26	GGT GAC AAT CTG CTG AAA	Sequencing oligo for exon 3 of *SRPK*
oBL27	CCG ATG CTG ATG AAT ACT	Sequencing oligo for exon 3 of *SRPK*
oBL28	ACT TGC GCT TTC CTT TTT	Sequencing oligo for exon 4 of *SRPK*
oBL29	GAT CTG GGC AAC GCT TGT	Sequencing oligo for exon 4 of *SRPK*

2.11: PCR and sequencing

2.11a: DNA isolation

A male flies homozygous for the mutant to be sequenced and a control male fly were placed in two different 1.5ml tubes and frozen at -20^{o}C for 10 mins. A DNA isolation mixture was prepared containing 25mM NaCl, 0.2% Triton X-100 and 200µg/ml proteinase K in a pH8 TE solution (pH adjusted with HCL) (TE is a solution of 10mM Tris and 1mM EDTA). 40µl of DNA isolation mixture was added to each of the two separate tubes. The fly in each tube was homogenized in the DNA isolation mixture with an autoclaved plastic dounce. The homogenized fly mixtures were then incubated at 37^{o}C in a water bath for 30 mins. Following incubation, the homogenized fly mixtures were boiled in a heating block at 95^{o}C for 5mins to inactivate the proteinase K.

2.11b: PCR

To amplify sequences by PCR, a 30µl PCR reaction mixture was made, on ice, containing 1pmol/µl of each of the two PCR primers, 0.2mM of each of the 4 dNTPs, 1x concentration PCR buffer (Roche), 1µl of homogenized fly mixture mentioned

above, and 5 units of Taq DNA polymerase (Roche). The reaction mixtures containing the DNA from both the mutant fly and the wild type fly were run in PCR thermal cyclers (Thermo Hybaid) using the following program:

1: 95°C for 30 sec

2: 94°C for 20 sec
3: 55°C for 30 sec
4: 72°C for 1 min
} 30x

5: 72°C for 10 mins

Following the program, 5µl of PCR reaction mixture was run on a TAE (Tris-acetate) agarose gel as described in (Sambrook et al., 1989) to determine if the PCR was successful. Reaction mixtures were stored in freezers at -20°C.

2.11c: Sequencing

To sequence the PCR products, a mixture was made, on ice, containing 3µl of the PCR reaction mixture detailed above, 5 units of Exonuclease I (Usb) and 0.5 units of Shrimp Alkaline Phosphatase (Usb) In the PCR thermal cycler, the mixture was incubated at 37°C for 15 mins and then 80°C for 15 mins. After incubating the mixture was cooled down. After the mixture had cooled down, 4µl of the Big Dye sequencing mix (Applied Biosystems) and 2µl sequencing primer (at a concentration of 0.8pmol/µl) was added to the mixture for a final concentration of 0.16pmol/µl sequencing primer. This mixture was then run in the PCR thermal cycler using the following program:

1: 96°C for 30 sec
2: 50°C for 15 sec
3: 60°C for 4 mins
} 25x

After running, 10µl of H_2O was added and the entire sequencing mixture was sent off to Gene Pool (University of Edinburgh) for sequencing.

Chapter 3:

A screen to identify mutants disrupting karyosome formation and maintenance

Chapter 3: A screen to identify mutants disrupting karyosome formation and maintenance

In order to identify mutants that disrupt karyosome formation and maintenance, I carried out a screen for abnormal karyosomes on 220 lines of mutants derived from mutagenesis conducted in the Nusslein-Volhard lab (Luschnig et al., 2004; Vogt et al., 2006). These mutants may have meiotic defects as they lay eggs that don't develop, a phenotype shared among some meiotic mutants. From this screen, I hoped to identify the genes directly responsible for karyosome morphology and maintenance during meiosis.

3.1: The karyosome screen: Using germline clones and microscopy to identify mutants that disrupt the karyosome

The mutants used in this screen were generated in the Nusslein-Volhard lab in a separate screen for embryonic axis patterning mutants (Luschnig et al., 2004). The Nusslein-Volhard screen identified multiple classes of phenotypes, including mutants that laid eggs that didn't develop. Since their screen was primarily interested in studying embryonic axis patterning mutants, we were granted permission to use the class of mutants that laid eggs that didn't develop for our own screening purposes. The mutations generated in the Nusslein-Volhard lab were located on the X chromosome and the left and right arm of the 2nd chromosome, which in this thesis will be abbreviated as 2L and 2R respectively.

Due to the lethal nature of some of the mutations in the Nusslein-Volhard mutant stocks, the ovaries have to be examined in germline clones generated by the Flippase – Dominant Female Sterile (FLP-DFS) recombination system (Chou and

Perrimon, 1992). The FLP-DFS recombination system works by inducing mitotic recombination between homologous chromosomes at specific sites close to the centromere. The two homologous chromosomes undergoing mitotic recombination are the chromosome carrying the mutation of interest and a wild-type chromosome containing ovo^D, a dominant mutation that disrupts ovarian development. During mitosis these recombined chromosomes will be randomly segregated between the two daughter cells. The result is a mosaic fly with a proportion of cells that are homozygous for either the mutant or the wild type chromosome, with the remainder of the cells being heterozygous for both chromosomes. (Fig. 6)

In somatic cells, the daughter cells that are homozygous for the lethal chromosome will die. Viability is maintained by the cells that are heterozygous for both the mutant and wild type chromosomes and the cells that are homozygous for the wild type chromosome. Due to the presence of ovo^D on the viable chromosome in the female germ cells, only the cells that are homozygous for the mutant chromosome will propagate, leading to an ovary that is phenotypically representative of the mutant of interest.

Confocal microscopy was used to visualize the karyosomes. In preparation for this, the female flies were matured for a week with males at 18^{o}C and then dissected in a physiological buffer to preserve the ovaries. The ovaries were then teased apart, fixed and stained for DNA with DAPI and propidium iodide.

Both DAPI and propidium iodide were used to visualize the karyosome due to their unique staining patterns. DAPI stained only the chromatin and was useful for visualizing karyosomes with morphology defects. Propidium iodide stained chromatin and the cytoplasm to a lesser extent, making it useful for visualizing the nuclear outline.

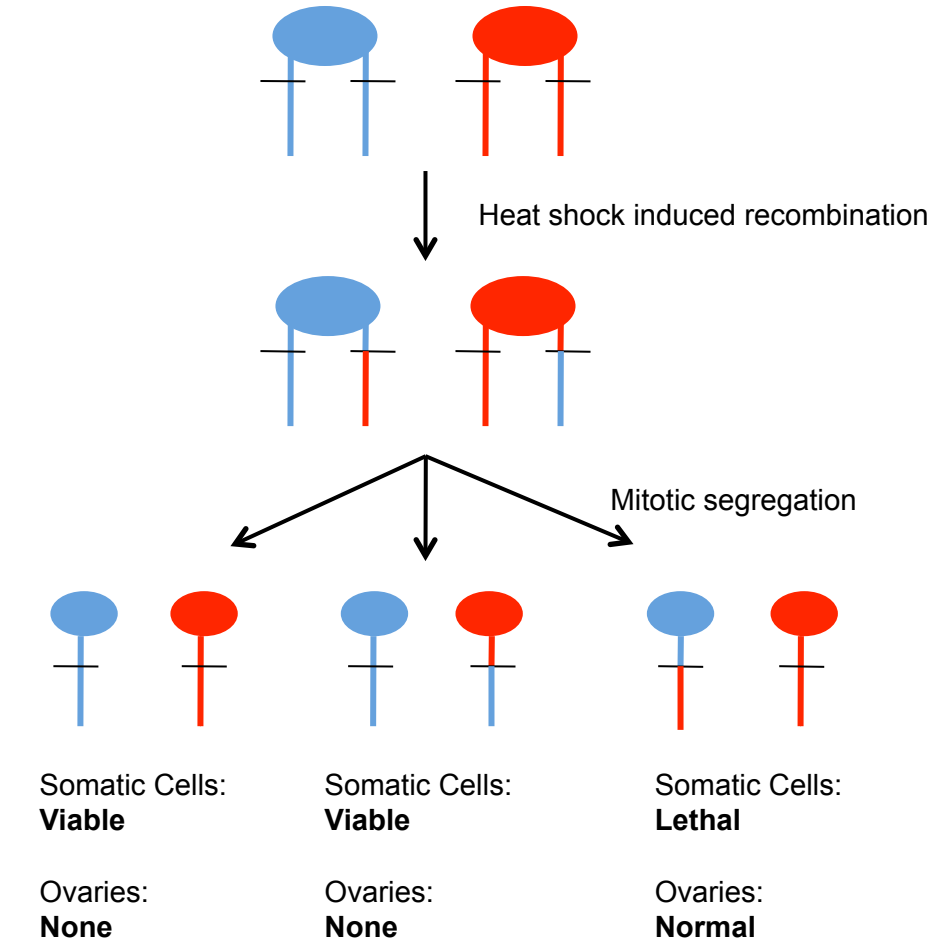

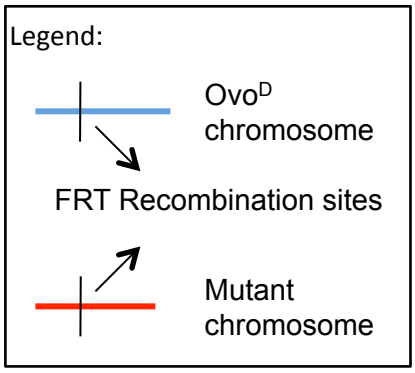

Figure 6. Generation of germline clones.
The mutant chromosome is assumed to have a mutation in a gene required for viability. The crossing scheme to generate the germline clones is detailed in section 2.5.

Though the FLP-DFS recombination system has been used to screen for other maternal specific mutations, (Bellotto et al., 2002; Fedorova et al., 2001; Luschnig et al., 2004; Page et al., 2007; Perrimon et al., 1989), this is the first time that mutants were screened for defects in karyosome formation and maintenance.

3.2: 26 karyosome affecting mutants were identified on the X and the 2L chromosomes

In the initial round of screening, I examined the morphology of 10 karyosomes in each mutant, in oocytes ranging from stages 3 – 8, for defects in order to gauge the penetrance of the phenotype. Only if half or more of the karyosomes examined were aberrant in their morphology, would they then be considered to have a possible defect in karyosome formation or maintenance.

The criteria used to judge the morphology of the mutant karyosomes were based on three characteristics of wild-type karyosomes. Wild-type karyosomes are spherical, compact, and completely detached from the walls of the oocyte nucleus. Only if the karyosomes in the mutant flies conformed to all three of these characteristics were they considered to be morphologically normal.

Based on their general morphology, karyosome defects were classified into the following three broad categories: misshapen, lobed and disassociated. (Fig. 7) In misshapen karyosomes, the chromatin often had protrusions or invaginations that affected the general spherical profile of the karyosome. However, the chromatin in misshapen karyosomes was still able to maintain an approximate centre of mass. This was not the case in lobed karyosomes where the chromatin was separated into multiple connected foci, usually numbering four or fewer (possibly corresponding to the four chromosomes found in *Drosophila*). Finally, in disassociated karyosomes the chromatin had come apart into multiple spatially separate foci. Rarer karyosome

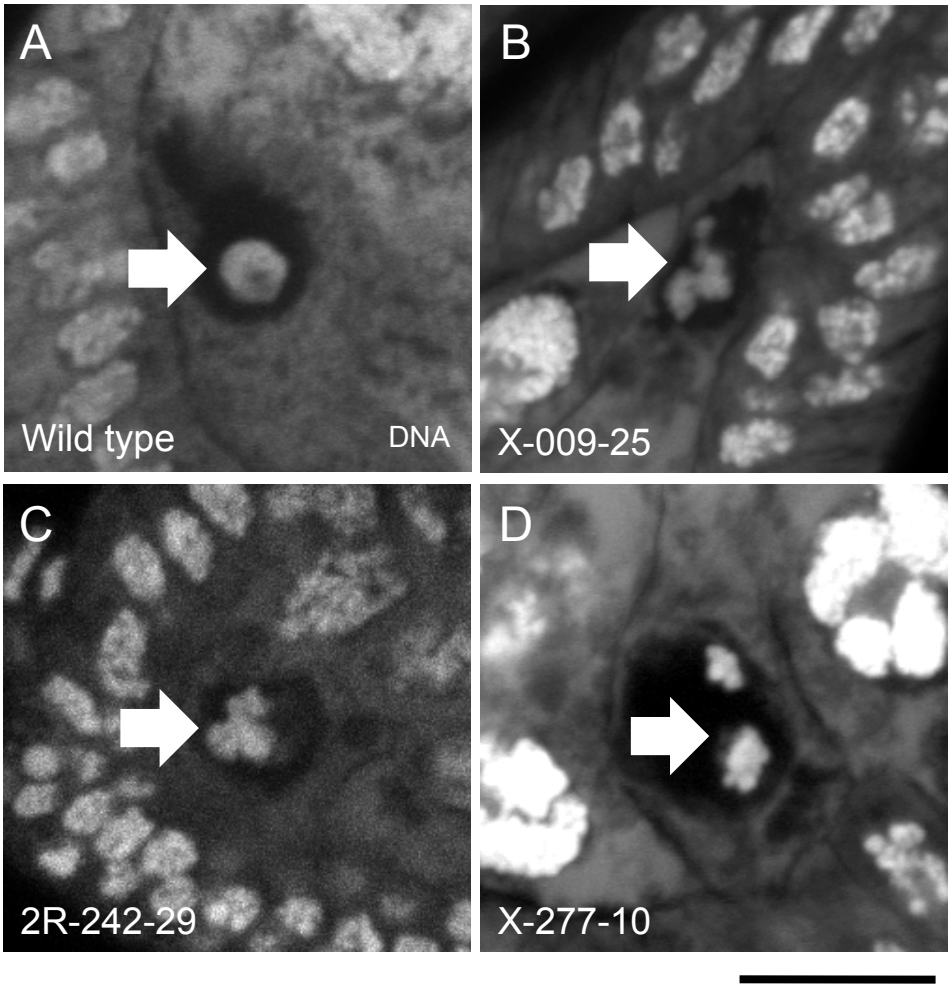

Figure 7. Karyosomes phenotypes seen in the screen.
The phenotype of (A) wild type karyosomes was used to judge the screened mutants. The most common abnormal karyosome phenotypes seen in the screen were the (B) misshapen, (C) lobed and (D) disassociated karyosomes. Karyosome indicated by white arrow. Scale bar represents 10μm.

defects, such as chromatin threads and chromatin adhesion to the nuclear wall were noted in addition to the categories outlined above.

During the course of the screen, I noticed that mutants with very underdeveloped ovaries consistently had greater than 50% karyosome defects when examined. Because this karyosome phenotype seems to arise due to the poor development of the ovary, rather than any specific cellular mechanism, I did not examine the karyosomes of the flies with very underdeveloped ovaries.

In total, 117 mutant lines were screened for karyosome defects on the X chromosome and the 2L chromosome. 26 mutants examined had abnormal karyosome morphology, 19 on the X chromosome and 7 on the 2L chromosome. (Fig. 8, 9)

3.3: 14 persistent karyosome mutants found on the X and 2L chromosomes

To gauge the persistence of the karyosome phenotype of the mutants isolated in the screen, I re-examined the karyosome morphology of each mutant. If a mutant showed morphology defects again in half or more of the karyosomes examined, then it was deemed a mutant with a persistent karyosome phenotype.

Out of the 26 mutants examined (19 on the X chromosome and 7 on the 2L chromosome), 14 had persistent karyosome phenotypes, 13 on the X chromosome and 1 on the 2L chromosome .

3.4: Identifying mutants that activated the meiotic recombination checkpoint on the X and 2L chromosomes

Activation of the meiotic recombination checkpoint by double stranded breaks causes an inhibition of the Vasa protein. The Vasa protein controls both axis

	Normal karyosome		Misshapen karyosome		Lobed karyosome		Disassociated karyosome		Other abnormality		CID staining	Dorsal Patterning defect	Persistant
X-002-27	5	8	5	1	0	0	0	1	0	0	Normal	Weak (5/44 Abnormal)	No
X-009-25	3	5	4	0	1	0	0	5	1	0	Abnormal	Strong (6/6 Abnormal)	Yes
X-023-02	5	4	4	2	0	1	0	2	1	1	Abnormal	Weak (7/40 Abnormal)	Yes
X-029-31	5	8	0	0	4	1	0	0	1	1	Normal	Weak (1/ 50 Abnormal)	No
X-040-13	3	4	0	2	0	2	0	2	4	0	Abnormal	Unknown (No eggs)	Yes
X-107-36	5	5	1	1	0	2	4	1	1	1	Normal	Strong (12/12 Abnormal)	Yes
X-107-39	3	10	0	0	0	0	1	0	2	0	Normal	Weak (2/50 Abnormal)	No
X-141-17	2	10	0	0	0	0	0	0	4	0	Normal	Weak (4/50 Abnormal)	No
X-176-32	5	5	1	0	0	1	2	4	2	0	Normal	Weak (1/9 Abnormal)	Yes
X-183-05	5	4	4	2	1	1	0	2	0	1	Normal	Weak (9/47 Abnormal)	Yes

Figure 8. X chromosome karyosome morphology affecting mutants.
For each phenotype, the numbers on the left represent results from the screen, the numbers on the right are from re-testing

	Normal karyosome		Misshapen karyosome		Lobed karyosome		Disassociated karyosome		Other abnormality		CID staining	Dorsal Patterning defect	Persistant
X-216-14	4	4	3	3	0	1	1	2	0	0	Normal	No (0/4 Abnormal)	Yes
X-250-01	1	3	4	2	1	3	4	2	0	0	Abnormal	Unknown (No eggs)	Yes
X-277-10	1	2	2	1	0	2	7	5	0	0	Normal	Unknown (No eggs)	Yes
X-283-06	4	4	6	4	0	1	0	0	0	1	Normal	Weak (11/50 Abnormal)	Yes
X-322-25	0	1	5	4	1	0	4	5	0	0	Abnormal	Unknown (No eggs)	Yes
X-326-35	1	6	2	1	3	1	4	2	0	0	Normal	Unknown (No eggs)	No
X-339-19	3	1	7	4	0	1	0	3	0	1	Normal	Unknown (No eggs)	Yes
X-370-17	0	4	8	3	1	1	1	2	0	0	Normal	Unknown (No eggs)	Yes
X-383-21	5	8	5	1	0	0	0	1	0	0	Normal	Strong (48/50 Abnormal)	No

Figure 8 (cont). X chromosome karyosome morphology affecting mutants.
For each pnenotype the numbers on the left represent results from the screen, the numbers on the right are from re-testing

	Normal karyosome		Misshapen karyosome		Lobed karyosome		Disassociated karyosome		Other abnormality		CID staining	Dorsal Patterning defect	Persistant
2L-142-21	4	6	0	0	1	2	1	1	2	1	Normal	Weak (2/29 Abnormal)	No
2L-213-17	3	6	4	2	0	3	1	0	2	1	Normal	No (0/50 Abnormal)	Yes
2L-244-20	4	6	4	0	0	0	0	0	2	0	Normal	No (0/50 Abnormal)	No
2L-246-13	4	8	2	2	0	0	3	0	0	0	Normal	No (0/11 Abnormal)	No
2L-295-21	3	7	2	2	3	1	0	0	2	0	Normal	No (0/50 Abnormal)	No
2L-301-05	3	5	3	0	2	0	1	1	1	0	Normal	Weak (1/50 Abnormal)	No
2L-336-03	4	6	2	0	2	0	0	0	2	0	Normal	Weak (47/50 Normal)	No

Figure 9. 2L chromosome karyosome morphology affecting mutants.
For each phenotype, the numbers on the left represent results from the screen, the numbers on the right are from re-testing

patterning of the oocyte by inducing the translation of the Gurken protein, and proper formation of the karyosome by an unknown mechanism (Ghabrial and Schupbach, 1999; Styhler et al., 1998; Tinker et al., 1998; Tomancak et al., 1998). In order to determine if the karyosome morphology defects were caused by an activation of the meiotic recombination checkpoint, I examined the axis patterning of oocytes.

In mutants that activate the meiotic recombination checkpoint, the egg dorsal appendages are often either fused or missing due to improper dorsal development caused by low levels of the Gurken protein (Ghabrial and Schupbach, 1999). By examining the dorsal appendages in eggs laid by germline clones of the karyosome morphology mutants, it will be possible to determine if the karyosome defects seen in the mutants are due, indirectly, to the activation of the meiotic recombination checkpoint.

I examined a maximum of 50 eggs from each of the mutants identified on the X and 2L chromosome. If a mutant had normal dorsal appendages in all eggs examined, then the meiotic recombination checkpoint had not been activated. If less than 30% of the oocytes examined had dorsal patterning defects, then they “weakly” activated the meiotic recombination checkpoint. And finally, if 30% or more of the oocytes examined had dorsal patterning defects, then they strongly activated the meiotic recombination checkpoint.

According to the above criteria, 5 of the mutants did not activate the meiotic recombination checkpoint (X-216-14, 2L-213-17, 2L-244-20, 2L-246-13 and 2L-295-21), 11 of the mutants weakly activated the checkpoint (X-002-27, X-023-02, X-029-31, X-107-39, X-141-17, X-176-32, X-183-05, X-283-06, 2L-142-21, 2L-301-05 and 2L-336-03) and finally, 3 of the mutants strongly activated the meiotic recombination checkpoint (X-009-25, X-107-36, and X-383-21). The remaining 7 mutants laid no eggs (X-040-13, X-250-01, X-277-10, X-322-25, X-326-35, X-339-19 and X-370-17)

making it impossible to determine whether the meiotic recombination checkpoint was being activated.

3.5: Centromere clustering studied in the X and 2L chromosome mutants

In wild-type karyosomes, all centromeres are localized to one or two punctate foci located at the periphery of the karyosome (Dernburg et al., 1996). This localization pattern must represent the clustering of the centromeres of non-homologous chromosomes. Mutations that affect this clustering of the centromeres might also be affecting the ability of the chromosomes to associate and form the karyosome.

In order to assess whether centromeres associate properly in the mutant karyosomes, the ovaries of mutants on the X and 2L chromosome were stained with an antibody against CID, the *Drosophila* homologue of CENP-A, a constitutive centromere protein (Blower and Karpen, 2001).

In most mutants identified during the screen, even when the chromatin had disassociated into multiple fragments, only one or two CID foci were observed as in wild-type karyosomes. However, in 5 out of the 14 mutants (namely X-040-13, X-023-02, X-009-25, X-322-25 and X-250-01) there were three or more CID foci in some of the karyosomes. (Fig. 10)

These results indicate that centromere clustering defects, while present in some karyosome morphology affecting mutants, do not seem to be the cause of most cases of karyosome morphology defects.

3.6: Identifying karyosome affecting mutants on the 2R chromosome

When I screened the X and 2L mutants, I noticed that karyosome morphological abnormalities tended to cluster in the same area on the slide, indicating that there

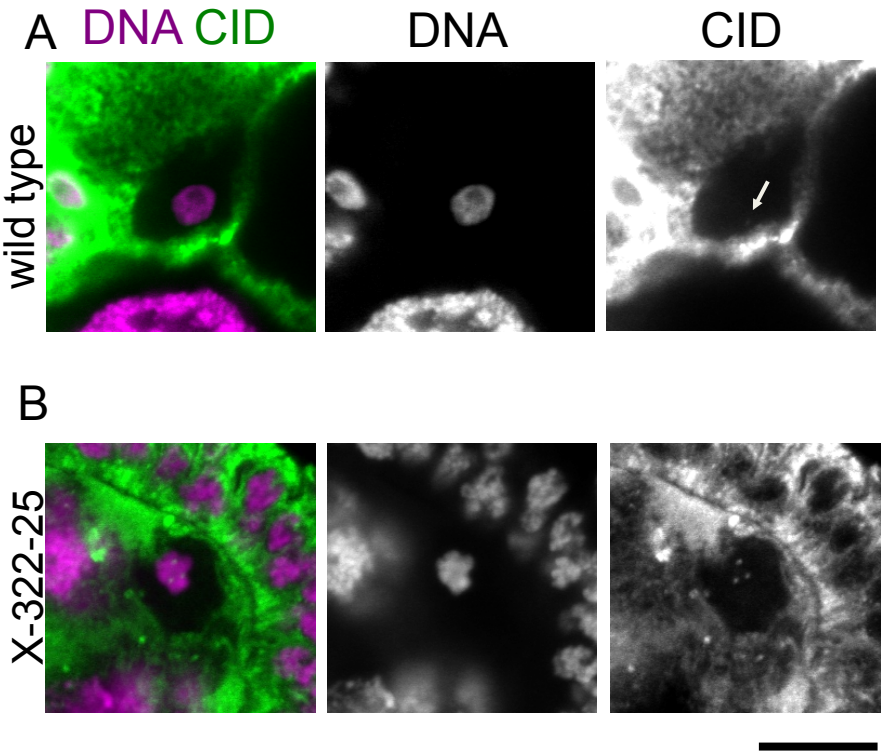

Figure 10. Wild-type and abnormal (more than 2 foci) CID staining.
(A) Confocal image of wild-type karyosome stained with propidium iodide (DNA) and anti-CID antibody (CID). CID foci indicated by white arrow.
(B) Confocal image of mutant (X-322-25) karyosome stained with propidium iodide (DNA) and anti-CID antibody (CID). Scale bar represents 10μm.

was an ovary specific bias for defects within the screen. In order to compensate for this, I altered my counting strategy for the 2R mutants.

For the 2R mutants, I started examining the karyosomes by microscope field as opposed to by single oocyte. All the karyosomes in a particular field of view were examined, and if there was a karyosome defect, it was noted before moving on to a different field of view. If conversely, all the karyosomes were normal, then one karyosome was imaged as representative of that particular field of view.

In hindsight, because this strategy concentrated on imaging abnormal karyosomes out of an entire microscope field, and did not take into account that the rest of the field might consist of normal karyosomes, it increased the likelihood that mutants with lower penetrance than the original desired cut-off, i.e. false positives, would be included in the results.

In total, 74 mutant lines were screened for karyosome defects on the right arm of the 2nd chromosome. 20 mutants out of the 74 examined had abnormal karyosome morphology. In order to correct for the false positives with lower than desired phenotype penetrance, all mutants identified in the 2R mutant screen will have to be examined again using the original counting strategy to eliminate the false positives in the results. (Fig. 11)

3.7: Discussion

In this screen, I used a forward genetics approach to identify *Drosophila melanogaster* mutants that affected the formation and maintenance of the karyosome, a chromatin structure that forms during the prophase of female meiosis. The mutants were examined using the FLP-DFS (Flipase-Dominant Female Sterile) Germline Clone (GLC) system pioneered by Chou and Perrimon (1992) to study the effect of mutations in genes required for viability on female germline development.

	Normal karyosome	Misshapen karyosome	Lobed karyosome	Disassociated karyosome	Other abnormality
2R-002-21	Karyosomes too large or oddly shaped				
2R-017-39	Karyosomes lobed				
2R-126-18	4	2	0	0	2
2R-129-09	5	3	2	0	1
2R-156-29	Karyosomes broken up				
2R-181-27	5	2	2	1	0
2R-184-34	Karyosomes disintegrated				
2R-194-34	4	6	0	0	0
2R-196-33	Karyosomes split up with intervening chromatin connections				
2R-205-08	2	1	1	4	1
2R-206-40	3	3	4	0	0
2R-217-15	2	7	0	0	1
2R-231-14	5	3	0	2	0
2R-242-29	4	3	1	1	0
2R-261-29	5	2	3	0	0
2R-322-03	0	5	0	0	5
2R-328-38	2	2	1	0	0
2R-330-21	3	7	0	0	0
2R-352-24	2	3	2	3	0
2R-361-19	3	5	0	0	1

Figure 11. 2R chromosome karyosome morphology affecting mutants.
Mutants listed in red were screened and described by Fiona Cullen (personal communication) prior to my arrival in the lab. Though I did not personally screen them, these mutants are included here for completeness.

With the exception of stage 1 and 2 *Drosophila* oocytes, the screen was deliberately unbiased with regard to oocyte stage, so as to identify mutants that affected the karyosome at various stages of oocyte development. (In stage 1 and 2 oocytes, the chromatin is contiguous with the oocyte nucleus and the karyosome cannot be distinguished as a discrete entity.) However, only the mutants with the most penetrant karyosome phenotypes were considered for further study. To select these mutants, an arbitrary cut off of at least 50% penetrance was used.

220 mutants on both the X and the 2nd chromosome were screened for karyosome defects and 46 mutants affected karyosome morphology in total, 19 on the X chromosome, 7 on the 2L chromosome and 20 on the 2R chromosome.

3.7a: Underdeveloped GLC ovaries

Early in the screening process, I noticed that following germline clone induction, 14% (30/220) of the mutants had underdeveloped, small ovaries resembling that of *ovo^{D}* expressing ovaries. *ovo^{D}* dominantly suppresses ovarian development, and in germline clone mosaics, this suppression allows the mutation carrying cells to predominate. I noticed two phenotypes common to these small, underdeveloped ovaries, (1) most of the oocytes did not develop past stage 2 and (2) those oocytes in which the karyosome was distinguishable had karyosome morphology defects.

These two phenotypes made it difficult to locate and image the karyosome, and when a mature karyosome was located, hard to determine whether the karyosome morphology defect was due to a mutation in a specific gene or the poor development of the ovary. It is possible that mutations in certain genes produce a phenotype similar to that seen in *ovo^{D}* ovaries, or that some mutations result in ovarian cell death, leaving the *ovo^{D}* expressing cells to predominate.

To determine if the small underdeveloped ovaries are showing an *ovo*^{D} phenotype, it will be necessary to compare the karyosome phenotype of *ovo*^{D} ovaries with karyosome phenotype of the mutants. Due to the predominance of karyosome defects in the few observable karyosomes in these mutants, I have excluded them from the main screen results so as not to bias the screen towards them.

3.7b: Dorsal patterning and Meiotic Recombination Checkpoint (MRC) activation

The 46 mutants identified in the screen were then further categorized according to the dorsal development of the eggs laid by the GLCs. Improper dorsal development (fused or missing dorsal appendages) can be indicative of incomplete meiotic recombination and activation of the MRC. Besides causing improper dorsal development, activation of the meiotic recombination checkpoint also leads to defects in karyosome morphology, though the mechanism for this is still unclear.

The mutants on the X and 2L chromosomes were grouped into three categories based on the percentage of eggs with improper dorsal development out of 50 eggs (or the total number of eggs if there were less than 50). The three categories were, no dorsal patterning defects, a weak dorsal patterning defect phenotype (30% or less eggs with improper dorsal development) and a strong dorsal patterning defect phenotype (more than 30% eggs with improper dorsal development). Perhaps not surprisingly, most of the mutants identified (11/26) fell into the weak dorsal patterning defect category as this category likely encompasses both mutants that actually activate the MRC weakly, and mutants where any eggs were misclassified as having dorsal development defects. In order to properly determine which mutants out of these 11 have actual egg dorsal patterning defects,

it will be necessary to repeat the GLC egg assay with sample sizes similar to those in screens for egg dorsal patterning mutants, i.e. >300 (Barbosa et al., 2007).

As a definitive assay of whether the MRC has been activated in these mutants, it will be useful to see whether these dorsal phenotypes persist in an MRC impaired background. Mei-41 is a kinase responsible for activating the checkpoint in response to unrepaired double stranded breaks (Lydall et al., 1996). By placing the mutants in a Mei-41 deficient background, mutants that activate the meiotic recombination checkpoint can be separated from those that merely affect the localization of dorsal patterning proteins.

3.7c: Centromere clustering in mutants with abnormal karyosome morphology

As stated in section 1.7, karyosomes form around the nucleolus in many species. Part of this transition from the non-surrounded nucleolus to surrounded nucleolus involves the progressive clustering of centromeres around the nucleolus, though the purpose for this clustering is not known. In *Drosophila*, where the nucleolus disappears early in female meiosis, female meiotic centromeric clustering has not been extensively studied. In a study by Dernburg et al. (1996), centromeres were imaged with Fluorescence In Situ Hybridization (FISH) using probes specific for the pericentromeric sequences of each chromosome. Though centric heterochromatin of several chromosomes clustered to one side of the karyosome, in many oocytes the pericentromeric heterochromatin of one chromosome was often at a marked distance from the others.

To examine whether centromeric clustering is preserved in mutants that had abnormal karyosome morphology, I stained the ovaries of the X and 2L chromosome mutants with an antibody against the *Drosophila* Cenp-A homologue, CID. Out of the 26 mutants that I had isolated on the X and 2L chromosomes, I

observed that 5 of them (X-040-13, X-023-02, X-009-25, X-322-25 and X-250-01) had more than 2 CID foci. These 5 mutants might represent a subset of mutants where defects in centromere clustering are leading to karyosome morphology abnormalities or vice versa. Conversely they might represent a previously undocumented natural centromere clustering configuration within the karyosome. Further work is required to determine which of these two hypotheses is correct.

3.7d: The Nusslein-Volhard collection

The 220 mutants that I used in my screen were part of a collection created in the Nusslein-Volhard lab via EMS (Ethyl MethaneSulfonate) mutagenesis in order to identify new genes involved in axis patterning in *Drosophila* embryos (Luschnig et al., 2004; Vogt et al., 2006). EMS reacts with guanine bases in-vivo and results in the replacement of G:C pairs with A:T pairs and the generation of multiple point mutations in the resulting progeny (Hoffmann, 1980). *Drosophila melanogaster* was chosen for the Nusslein-Volhard screen because the reduced functional redundancy of the *Drosophila* genome as compared to vertebrates makes it more likely that a mutation in a gene will produce a distinct phenotype.

The two criteria used in the Nusslein-Volhard lab to select for axis patterning mutants were (1) the inability of the mutant embryos to hatch and (2) a distinct phenotype recognizable in the embryonic cuticle. Our lab was granted use of mutants that fell into category (1), but not into category (2), i.e. mutants where embryos did not hatch but lacking a recognizable cuticle phenotype. Since some female meiotic mutants share this non-hatching embryo phenotype, this collection has theoretically already been enriched for female meiotic mutants, which are studied in our lab.

Chapter 4:

Genetic analysis of the mutants identified in the karyosome screen

Chapter 4: Genetic analysis of the mutants identified in the karyosome screen

Having identified 46 mutants that affected karyosome formation in a cytological screen of 220 mutant fly lines generated in the Nusslein-Volhard lab (Luschnig et al., 2004; Vogt et al., 2006), I carried out genetic analysis on the mutants identified. Furthermore, combined with molecular analysis, I identified one of the mutated genes causing the karyosome defects seen in the mutants.

4.1: Genetic analysis of the X chromosome mutants

As a first step in identifying the mutated genes that were causing the karyosome morphology defects, I performed genetic analysis on the 19 X chromosome mutants that I identified in the screen.

4.1a: Complementation testing identified 2 groups of non-complementing mutants on the X chromosome

Due to the large number of mutants that were generated by the Nusslein-Volhard lab, there was a possibility that some of the mutants shared mutations in the same gene. In order to determine whether any of the karyosome morphology mutants identified in the screen share mutations in the same gene, I carried out complementation testing.

Complementation testing works as follows: if you cross two mutants with mutations in different genes together, the healthy copy of one gene in one of the mutants will compensate for the mutated copy in the other mutant. However, if both

mutants have a mutation in the same gene, the resulting progeny will inherit a mutated copy of the gene from either parent and this will lead to the emergence of either lethality or sterility phenotypes. By this method it is possible to identify mutants with mutations in the same genes by observing whether their transheterozygote offspring are sterile or missing.

Many of the X chromosome mutants had lethal mutations on the X chromosome. In order to maintain X chromosome mutant stocks with lethal mutations, the flies were kept as heterozygotes. However, for complementation testing, males with the mutant X chromosome were required. This was problematic because males have only one X chromosome. Therefore duplications, chromosomal aberrations with large segments of the X chromosome duplicated on other chromosomes, were used to rescue the lethal mutation in these males.

I crossed a series of duplications located on the X chromosome overlapping with the lethal mutants that I had identified in the screen. Out of 10 lethal mutants (X-002-27, X-009-25, X-023-02, X-176-32, X-183-05, X-216-14, X-283-06, X-326-35, X-339-19 and X-370-17), I was able to rescue 7 of them with duplications (X-002-27, X-176-32, X-183-05, X-216-14, X-326-35, X-339-19 and X-370-17). 4 of the mutants (X-002-27, X-176-32, X-339-19 and X-370-17) were all rescued by the same duplication *Dp(1;Y)dx*$^{+}$*5* (a duplication of chromosomal region 4C11-6D8), X-216-14 was rescued by *Dp(1;f)R* (1A3-3A1), X-183-05 was rescued by *Dp(1;Y)W39* (16F1-18A7) and X-326-35 was rescued by *Dp(1;f)y*$^{+}$ (11D-12B7).

Flies from each of the mutants identified in the screen were then crossed to each other, if there were no transheterozygote progeny, then the parents shared a lethal mutation. From the progeny of these crosses, female flies transheterozygous for both parent chromosomes were selected and their fertility was tested. If these transheterozygote females were sterile, then both parent chromosomes shared a sterile mutation. From the complementation testing, I identified two groups of non-

complementing mutants on the X chromosome. The two non-complementing groups were X-002-27 / X-339-19 and X-107-36 / X-040-13.

X-002-27 / X-339-19 forms a lethal non-complementing group. Consistently, the lethal mutation in both X-002-27 and X-339-19 were rescued by the same duplicated region, *Dp(1;Y)dx*$^{+}$*5* (chromosomal region 4C11-6D8 on the X chromosome).

X-040-13 / X-107-36 forms a sterile non-complementing group. Examination of the ovaries of the transheterozygote offspring revealed no karyosome morphology defects. The sterile mutation was eventually mapped to the gene *Phl* (*pole hole*) (Fiona Cullen, personal communication). *Phl* has a role in pattern formation in *Drosophila* embryos (Ambrosio et al., 1989; Perrimon et al., 1984; Perrimon et al., 1985). The lack of karyosome morphology defects in the transheterozygotes and the shared mutation in *Phl* led to the conclusion that it was the defect in pattern formation in the embryos that was causing the sterility in the transheterozygotes and that the karyosome morphology defects were being caused by mutations different from each other and from *Phl*.

I was unable to carry out a full complementation test of all the mutants located on the X chromosome, as three of the X chromosome mutants (X-009-25, X-023-02 and X-283-06) could not be rescued by any of the duplication stocks. It is therefore possible that there are still some non-complementing mutant pairs to be found on the X chromosome.

4.1b: Meiotic recombination of X-339-19 revealed that the lethal mutation is linked to karyosome defects

For the lethal non-complementing mutants on the X chromosome, X-002-27 and X-339-19, I already knew that the same duplication, *Dp(1;Y)dx*$^{+}$*5*, rescued the lethality

of both mutants, as I had used it in both mutants to generate viable males for complementation testing. Therefore, the shared lethal mutation must be located in the duplicated cytological region, 4C11-6D8. However, I did not know if the lethal mutation was also causing the karyosome defect.

I used meiotic recombination to find out if the lethal mutation and the karyosome defect mutation could be separated. Sexually reproducing organisms undergo meiotic recombination between homologous chromosomes. Meiotic recombination generates chromosomes that are a random hybrid of their parent homologues. If the lethal phenotype and karyosome defect phenotype are due to two separate mutations, then meiotic recombination can separate them. The probability that the two mutations will be separated by meiotic recombination depends on the distance between the two mutations on the chromosome. (Fig. 12)

I generated 10 recombinant stocks, 6 viable and 4 lethal, and examined the karyosomes in the recombinants that had recombined near the lethal mutation as judged by visible genetic markers. These recombinants were chosen to increase the chance of identifying a recombinant that had separated the lethal and the karyosome affecting mutations. Homozygote females of the viable stocks examined all showed wild-type karyosomes. The karyosomes of the lethal stocks were examined in germline clones generated by the FLP – DFS recombination system. All the lethal recombinants examined had karyosome morphology defects similar to those seen in the parent mutation X-339-19. (Fig. 13) This indicated that either, the lethality and the karyosome defect are due to the same mutation, or the two phenotypes are caused by mutations close enough not to be separated by this round of recombination.

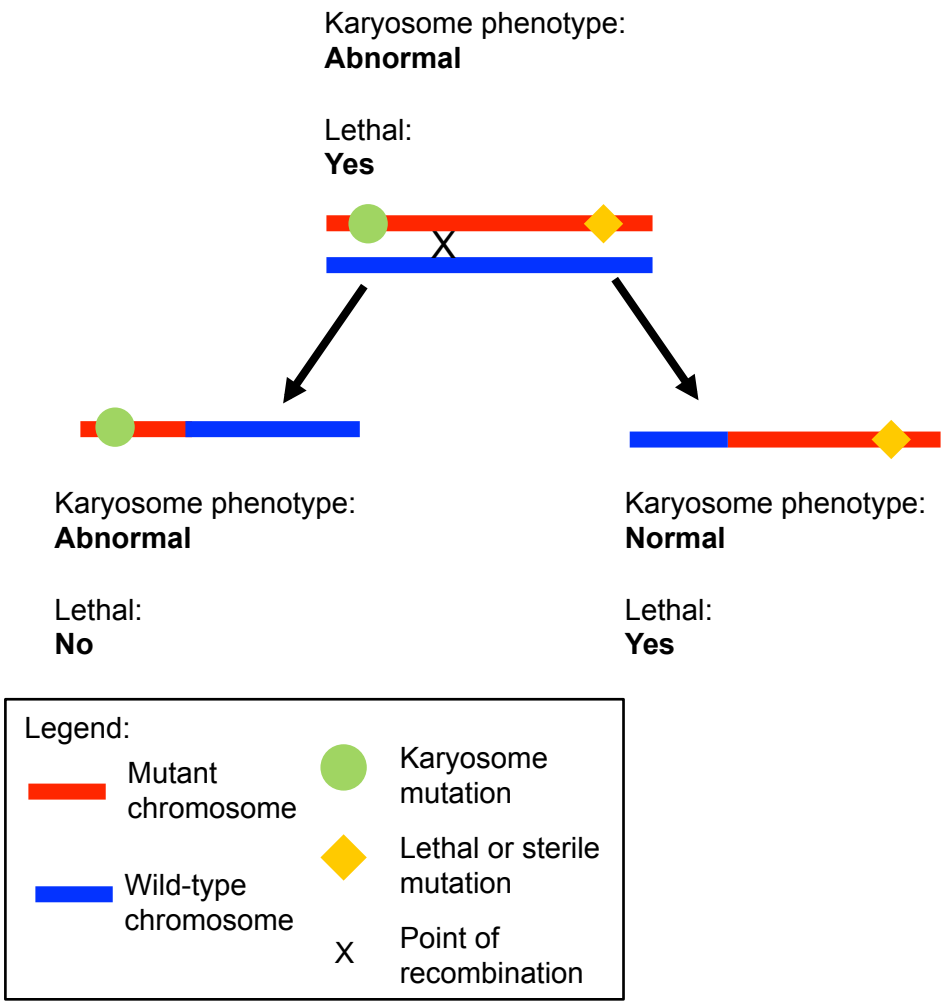

Figure 12. Attempting to separate two mutations on the X chromosome by recombination.
Recombination was used to determine whether the lethality and the karyosome morphology defects in X-339-19 were due to two different mutations. If they were due to two separate mutations, then they would be separable by recombination. This technique was also used to determine whether the sterility and the karyosome morphology defects in 2R-242-29 were due to two separate mutation.

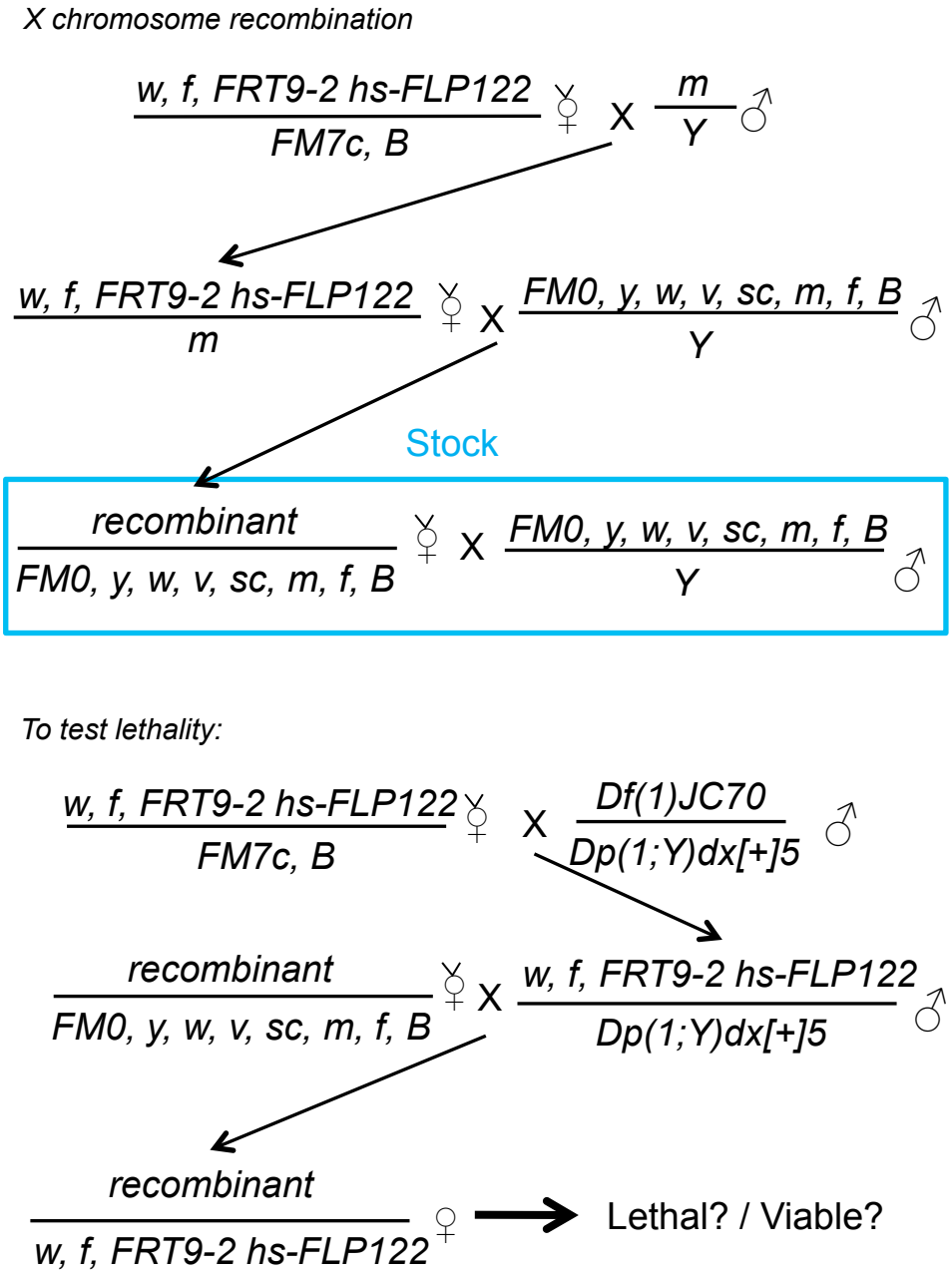

Figure 12 (cont). Attempting to separate two mutations on the X chromosome by recombination.
Recombinant here refers to the chromosome that is created from recombination between *miniature (m)* and the mutant chromosome *w, f, FRT9-2 hs-FLP122*

	Viable / Lethal	*white*	*miniature*
m (miniature)	Viable	+	-
X-339-19	Lethal	-	+
Rec(339)5	Viable	+	-
Rec(339)6	Viable	-	+
Rec(339)9	Viable	+	+
Rec(339)20	Lethal	-	+
Rec(339)21	Viable	+	+
Rec(339)23	Lethal	+	+
Rec(339)30	Viable	+	-
Rec(339)32	Lethal	-	-
Rec(339)35	Viable	+	-
Rec(339)36	Lethal	-	-

Figure 12. Attempting to separate two mutations on the X chromosome by recombination.
Genetic markers carried on the recombinants for mapping purposes are also listed (*white* and *miniature*). In this diagram, + means wild type and – indicates presence of the genetic marker.

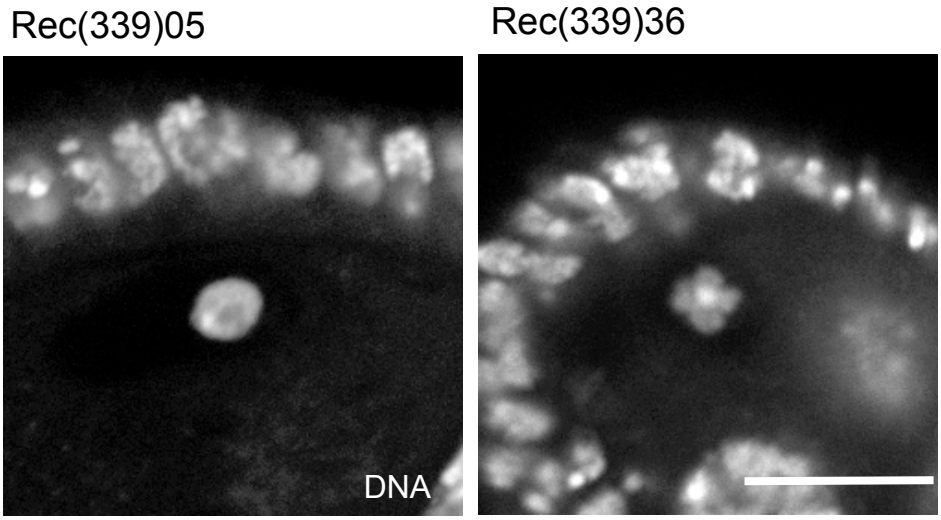

Figure 13. Karyosomes of viable and lethal X-339-19 recombinants.
Viable recombinants of X-339-19 had normal karyosomes, as can be seen in Rec(339)05. Lethal recombinants had karyosome defects, as shown in Rec(339)36. Scale bar represents 10μm.

4.1c: Deficiency mapping of the X chromosome karyosome mutants narrowed the lethal mutation to cytological region 5E1-5E4

I used a series of overlapping deficiencies to map the lethal mutation in the non-complementing group of X-002-27 and X-339-19. Deficiencies are aberrant chromosomes with large deletions. If a deficiency deletes the gene that is causing lethality or sterility in a particular mutant, then when crossed with the mutant, there will be sterility or lethality in the offspring due to non-complementation. Conversely, if the deficiency does not delete the gene causing sterility or lethality in a particular mutant, then there will be complementation in the resulting progeny and a rescue of lethality or sterility phenotypes. Using a series of overlapping deficiencies, it is possible to narrow down the region where a particular lethal or sterile mutation is located.

A series of deficiencies around the duplicated region, *Dp(1;Y)dx*$^{+}$*5* (4C11-6D8), were used to narrow down the region containing the lethal mutation. Using this method, I narrowed down the region containing the lethal mutation for X-002-27 and X-339-19 to cytological region 5E1-5E4 which encompasses 10 genes. (Fig. 14)

4.2: Deficiency mapping of the sterile X chromosome single allele mutants identified the region causing sterility in X-250-01

I also used a series of overlapping deficiencies to map the mutations in my X chromosome single allele mutants. I focused first on the sterile mutants because, as stated in section 4.1, the lethal mutants lack viable males to perform crosses with.

I crossed a collection of deficiencies with defined breakpoints that altogether spanned 60% of the X chromosome. One of the deficiencies, *Df(X)ED6521* (1E3-1F4), did not complement the sterility of mutant X-250-01. However, the karyosome

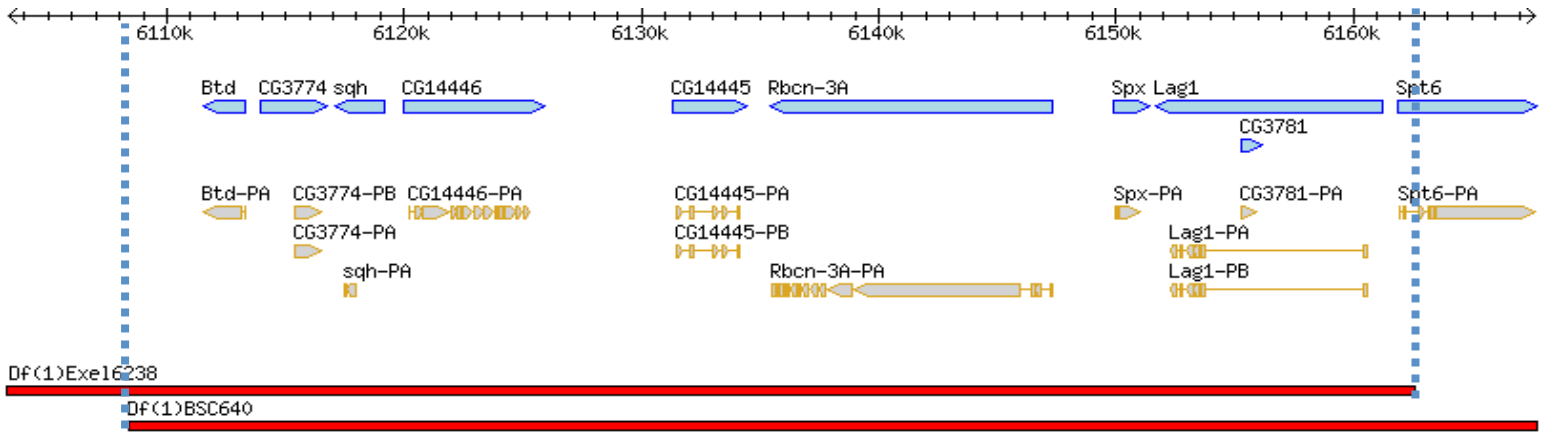

Figure 14. Shared lethality causing cytological region 5E1-5E4 in X-002-27 and X-339-19 as defined by deficiency mapping.
Deleted genes are displayed in blue and associated coding sequences in gold/grey. Mapping deficiencies are at the bottom in red. Vertical blue dashed lines indicate the extent of the mapped region. Original image was created using the Gbrowse function in flybase.

morphology of the transheterozygotes was normal, leading to the conclusion that in this case, there were two separate mutations, the first causing female sterility, which was the mutation uncovered by the deficiency, and the other responsible for the karyosome defect.

4.3: Genetic analysis of the 2R karyosome mutants

As a first step in identifying the mutated genes that were causing the karyosome morphology defects, I performed genetic analysis on the 20 2R chromosome mutants that I identified in the screen.

4.3a: Complementation testing revealed an 11 allele non-complementation group on the 2R chromosome

I carried out complementation testing on the 20 karyosome affecting mutants that I had identified on the 2R chromosome. On the 2R chromosome, there was one non-complementing group consisting of eleven mutants (2R-017-39, 2R-126-18, 2R-156-29, 2R-196-33, 2R-217-15, 2R-231-14, 2R-242-29, 2R-322-03, 2R-328-38, 2R-352-24, and 2R-361-19).

The 2R chromosome non-complementation group was a sterile non-complementing group. Examination of the transheterozygote offspring revealed karyosome defects in the oocytes.

4.3b: Recombination mapping of 2R-322-03 and 2R-242-29 revealed that a sterile mutation is located at cytological region 40-50

I identified 11 mutants on the 2R chromosome that shared a sterile mutation. To narrow down the location of the sterile mutation, recombination mapping was carried out on 2 alleles. I chose 2R-242-29, as the healthiest allele (based on the proportion of homozygotes in the stock), and 2R-322-03, as the allele that had shown the strongest karyosome phenotype during the karyosome screen.

The mutant 2R chromosomes that I used in the recombination mapping had genetic markers, visible mutations used to demarcate chromosomal regions, at cytological regions 52D (*curved*), 58F (*plexus*) and 60B (*speck*) (the centromere on the 2nd chromosome is located between cytological regions 40 and 41 and the right arm of the chromosome terminates at region 60F). These genetic markers were examined in a pool of recombinant flies to determine the region of the chromosome associated with the sterile mutation.

For the 2R-242-29 recombination mapping, there were recombinants like Rec(242)10 that had lost all three genetic markers but had inherited the sterile mutation, and Rec(242)6 that had all three genetic markers, but had lost the sterile mutation. This indicated that the sterile mutation was not located in region defined by the genetic markers, i.e. 52D-60B. Therefore, the sterile mutation must be located elsewhere on the mutant chromosome. The regions where it might be located were between the FRT site (located at cytological regions 42B) and *curved* at 52D, or, less likely due to size, between *speck* at 60B and the end of the chromosome arm at 60F. (Fig. 15)

I examined the karyosomes of females homozygous for either the Rec(242)10 chromosome or the Rec(242)6 chromosome. The sterile Rec(242)10 homozygote females displayed karyosome abnormalities similar to those seen in the

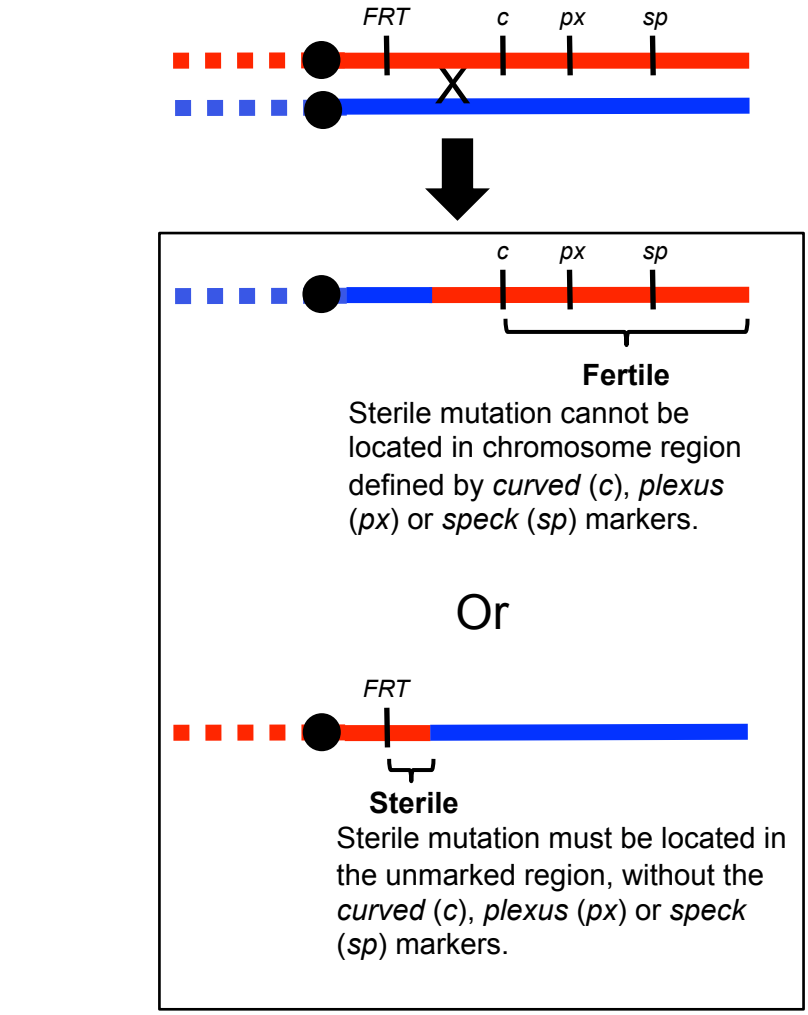

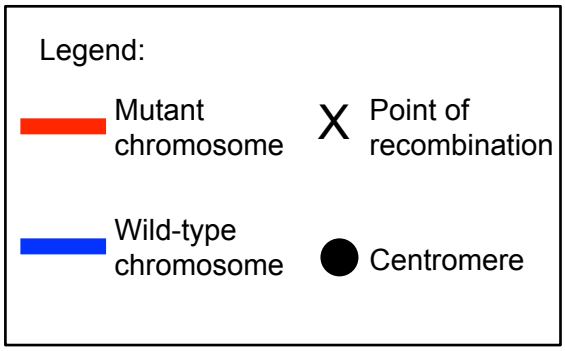

Figure 15. Meiotic recombination mapping of the sterile mutation in 2R-242-29 using genetic markers.
Recombination mapping of 2R-242-29 revealed that the sterile mutation was not located within the region defined by the *curved* (*c*), *plexus* (*px*) or *speck* (*sp*) markers. See section 4.3b for details.

2R chromosome recombination

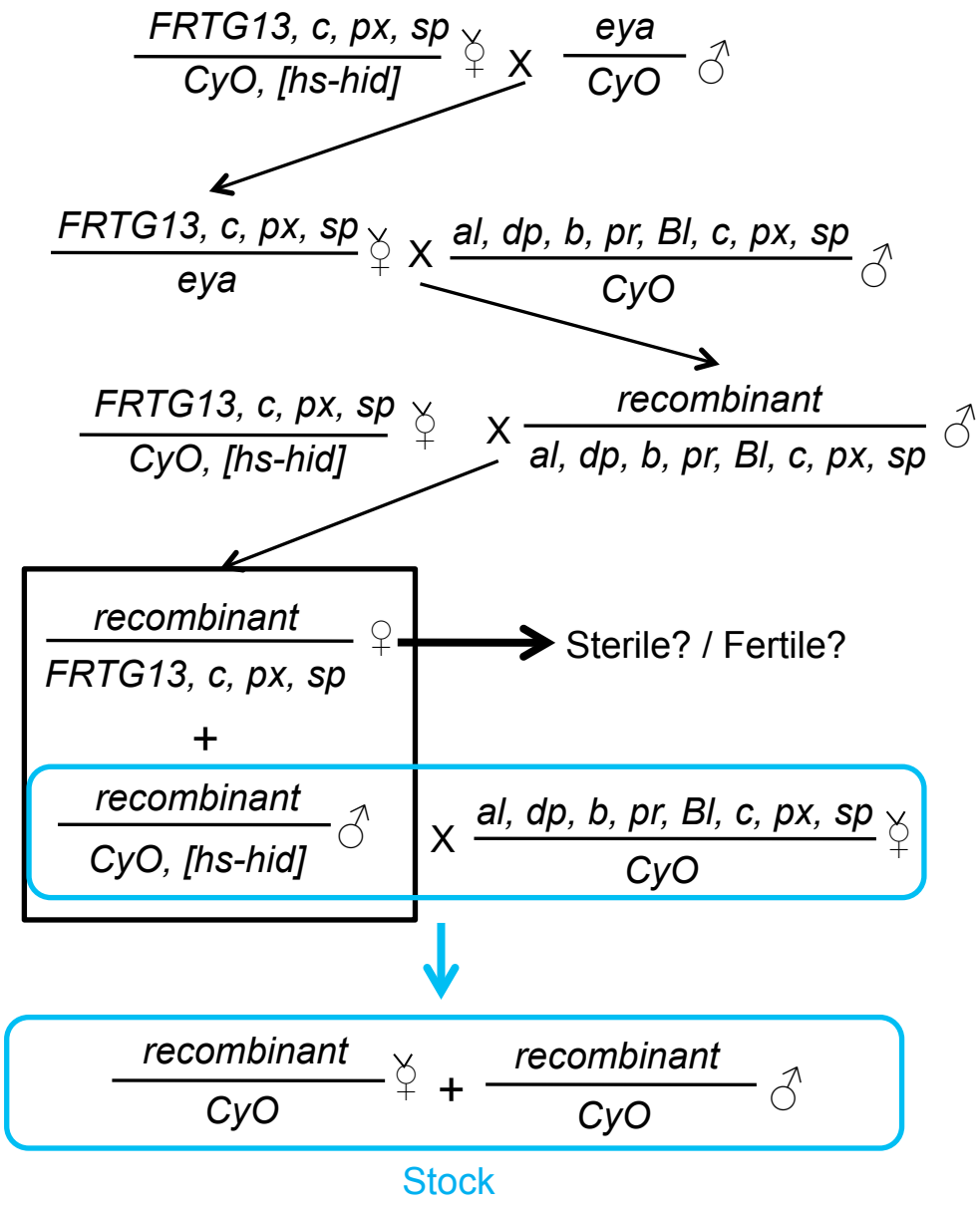

Figure 15 (cont). Meiotic recombination mapping of the sterile mutation in 2R-242-29 using genetic markers.
Recombinant here refers to the chromosome that is created from recombination between *eyes absent (eya)* and the mutant chromosome *FRTG13, c, px, sp.*

original 2R-242-29 mutant. However, the fertile Rec(242)6 homozygote females had wild-type karyosomes. This indicates that the karyosome phenotype is either the same mutation as the one causing sterility in 2R-242-29, or that the sterile and karyosome affecting mutations are too close for recombination to separate. (Fig. 16)

To confirm if the sterile mutation in Rec(242)10 was the same as that in the non-complementation group, I crossed Rec(242)10 with 2R-361-19, one of the 11 non-complementing alleles. The resulting transheterozygote offspring were sterile, indicating that Rec(242)10 shared a sterile mutation with 2R-361-19.

I carried out similar recombination mapping on the phenotypically stronger allele 2R-322-03, with the added goal of removing a separate lethal mutation also present on the chromosome. Out of the 100 recombinants generated, only one, Rec(322)83 was both sterile and viable. However, when crossed with the other 2R non-complementing alleles (2R-017-39, 2R-352-24, 2R-361-19), the resulting transheterozygote offspring were (poorly) fertile, indicating that Rec(322)83 had not inherited the shared sterile mutation of the non-complementation group.

The sterility of the Rec(322)83 homozygotes indicates that 2R-322-03 has at least 3 separate mutations, a lethal mutation removed by recombination, and two unrelated sterile mutations, one of which is shared by the non-complementing group. Further analysis of 2R-322-03 might prove problematic on account of the complications caused by trying to differentiate and separate these three mutations.

4.3c: Deficiency mapping of the 2R non-complementation mutants revealed that a sterile mutation is located at cytological region 48C

I used a series of overlapping deficiencies to map the sterile mutation shared by the 11 allele non-complementation group identified on the 2R chromosome. The deficiencies together uncovered the region between the FRT site (cytological

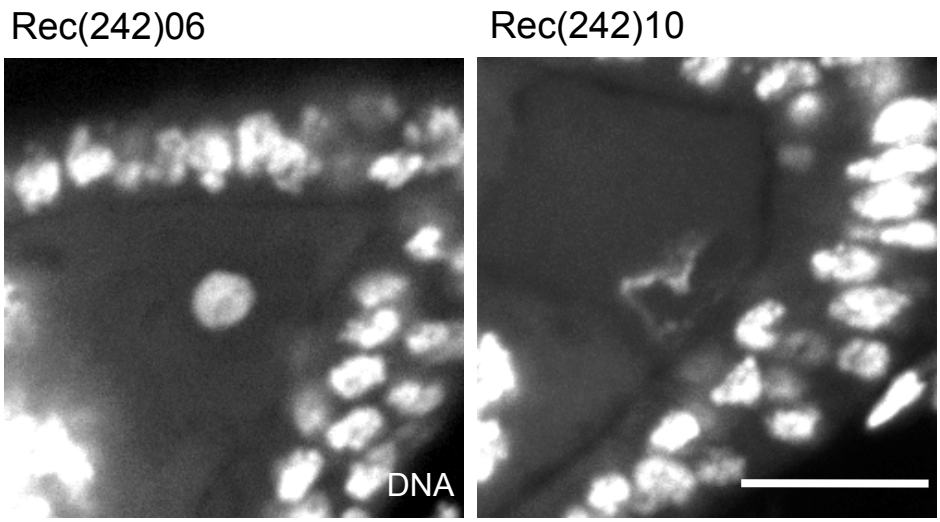

Figure 16. Karyosomes of Rec(242)06, a fertile recombinant, and Rec(242)10, a sterile recombinant.
Rec(242)06, a fertile recombinant of 2R-242-29, had normal karyosomes. Rec(242)10, a sterile recombinant, had abnormal karyosomes, some of which were attached to the oocyte nucleus periphery. Scale bar represents 10μm.

regions 42B) and the genetic marker *curved* (cytological region 52D). Using this method, the region containing the sterile mutation was narrowed down to cytological region 48C, encompassing 15 genes. (Fig. 17)

4.4: Deficiency mapping of the 2R chromosome single allele mutants narrowed down sterility causing region in 2R-129-09 to *Df(2R)ED2436, Df(2R)ED2426* and *Df(2R)Exel9015*

I used a collection of deficiencies to map the single allele 2R karyosome mutants. The deficiencies chosen were those with defined breakpoints, and together they uncovered roughly 35% of the 2R chromosome. One of the mutants, 2R-129-09, displayed sterility in combination with three overlapping deficiencies, *Df(2R)ED2436*, *Df(2R)ED2426* and *Df(2R)Exel9015*. The overlapping region of these three deficiencies contained two genes, *Dup* and *SRPK*. (Fig. 18)

4.4a: Sequencing revealed the mutation in 2R-129-09 to be in SRPK

I sequenced the coding region of the two genes identified in the deficiency mapping of 2R-129-09, *Dup* and *SRPK*. The sequencing was performed in males homozygous for 2R-129-09 and was compared to the same sequences derived from males homozygous for *FRTG13 c px sp*, the chromosome mutagenized in the Nusslein-Volhard lab to generate the 2R mutant collection (Luschnig et al., 2004). Sequencing revealed only one mutation in the entire sequenced region, a C>T single nucleotide substitution at position 1589 in the coding region of the *SRPK* gene. This substitution resulted in the introduction of a premature stop codon in *SRPK* that deleted the C-terminal 735 nucleotides of the *SRPK* coding mRNA. (Fig. 19)

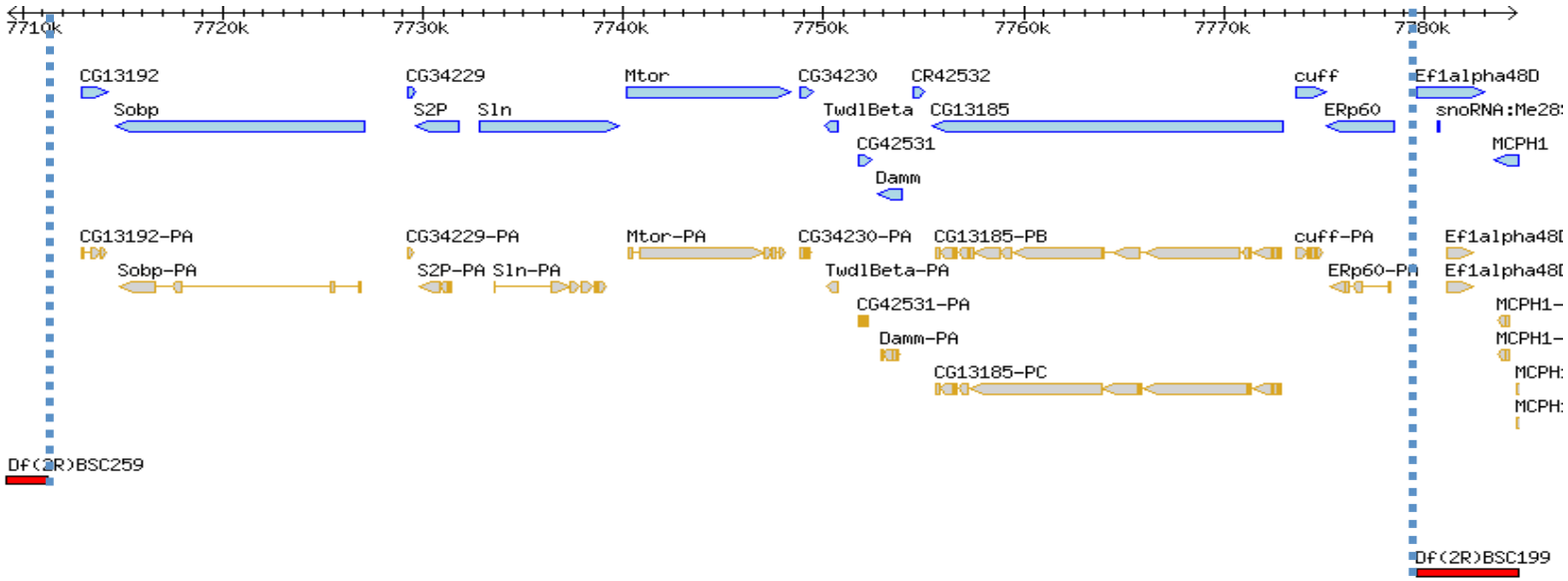

Figure 17. Shared sterility causing genomic region 48C for 2R 11 allele non complementation group as defined by deficiency mapping.
Genes are displayed in blue and associated coding sequences in gold/grey. Mapping deficiencies are at the bottom in red. Blue dashed lines indicate the extent of the mapped region. Original image was created using the Gbrowse function in flybase.

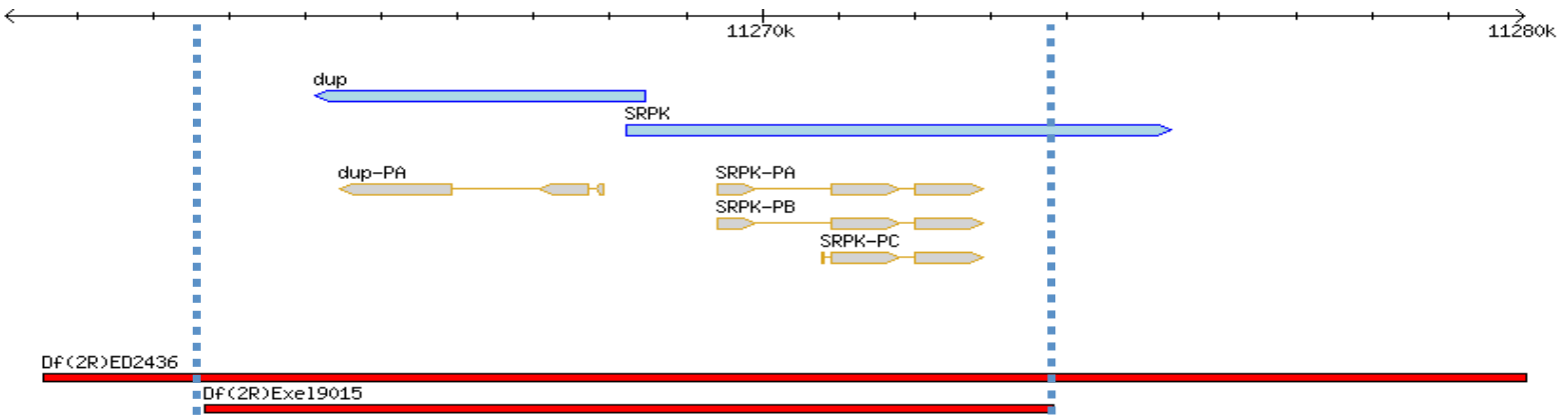

Figure 18. Sterility causing region in 2R-129-09 as defined by *Df(2R)ED2436, Df(2R)ED2426* and *Df(2R)Exel9015*. Deleted genes are displayed in blue and associated coding sequences in gold/grey. Mapping deficiencies are at the bottom in red. *Df(2R)ED2426* is not shown as it spans the entire region. Vertical blue dashed lines indicate the extent of the mapped region. Original image was created using the Gbrowse function in flybase.

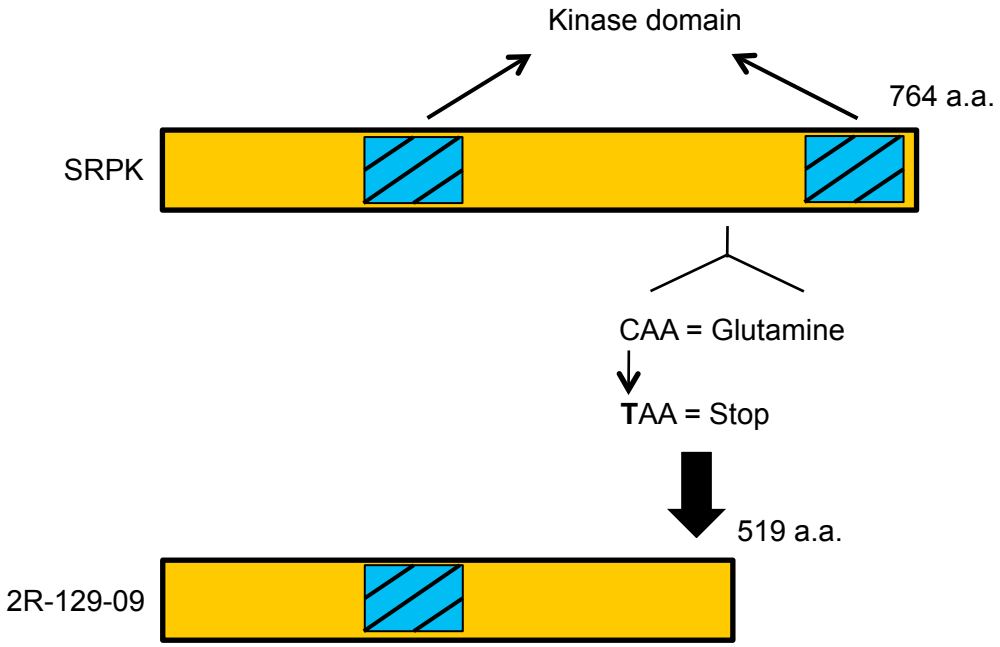

Figure 19. In the mutant 2R-129-09, a mutation in SRPK, leads to the truncation of the protein.
The kinase domain of SRPK is divided into two halves and separated by a spacer region. The mutation in 2R-129-09 introduces a premature stop codon into the spacer region and truncates half of the kinase domain.

SRPK is one of three SR protein phosphorylating kinases identified in a survey of the *Drosophila* genome for homologues of pre-messenger mRNA processing factors found in other organisms (Mount and Salz, 2000). Specifically, it is predicted to be the *Drosophila* orthologue of human SRPK2, a protein responsible for regulating the activity and cellular localization of SR proteins (Barbosa et al., 2007; Koizumi et al., 1999; Tenenbaum and Aguirre-Ghiso, 2005). SR proteins contain a serine/arginine rich RS domain, where the phosphorylation by SRPK takes place (Gui et al., 1994). SR proteins have a wide array of functions, including imparting specificity to the alternative splicing machinery and mRNA export from the nucleus (Long and Caceres, 2009).

SRPK, like its human orthologue SRPK2, has an C-terminal kinase domain that is separated into two halves by the presence of a large spacer sequence (Wang et al., 1998). The premature stop codon in 2R-129-09 falls within this large spacer sequence in SRPK, and truncates the second half of the kinase domain.

A maternal screen for genes regulating oocyte polarity in *Drosophila* had already identified SRPK as being important for the proper dorsal development of *Drosophila* eggs (Barbosa et al., 2007). However, the alleles identified in the oocyte polarity screen were examined for karyosome morphology, but no abnormal karyosomes were reported. Instead, the SRPK mutants identified in that screen displayed abnormal positioning of the *Drosophila* oocyte within the nurse cell cluster as opposed to posterior to the nurse cells as in wild type *Drosophila* eggs.

4.5: Discussion

I performed complementation testing on the mutants I identified in the karyosome screen on the X and 2nd chromosome to identify allelic mutants. Complementation testing revealed one lethal non-complementing group on the X chromosome, and 2

sterile non-complementing groups, one on the X chromosome and another on the 2nd. On the X chromosome, the lethal non-complementing group contained 2 mutants (X-002-27, X-339-19) and the sterile non-complementing group likewise contained 2 mutants (X-107-36, X-040-13). On the 2nd chromosome, the sterile non-complementing group contained 11 mutants (2R-017-39, 2R-126-18, 2R-156-29, 2R-196-33, 2R-217-15, 2R-231-14, 2R-242-29, 2R-322-03, 2R-328-38, 2R-352-24, and 2R-361-19).

Genetic mapping of these three non-complementation groups using recombination and deficiency mapping revealed the region in which the shared mutations were located. For the lethal non-complementing group on the X chromosome (X-002-27, X-339-19), the shared lethal mutation is located in 5E1-5E4, a region that contains 10 genes. The shared sterile mutation of the non-complementing group on the 2nd chromosome (2R-017-39, 2R-126-18, 2R-156-29, 2R-196-33, 2R-217-15, 2R-231-14, 2R-242-29, 2R-322-03, 2R-328-38, 2R-352-24, and 2R-361-19) is located in 48C, a region that contains 15 genes.

The shared mutation of the X chromosome sterile non-complementing group (X-107-36, X-040-13) was mapped to the gene *Phl* (*pole hole*) (Fiona Cullen, unpublished data). *Phl* is required for pattern formation in *Drosophila* embryos, but apparently does not affect karyosome formation, as the sterile transheterozygotes of these two mutants (X-107-36, X-040-13) had normal karyosomes.

I also performed deficiency mapping on the single allele X and 2nd chromosome mutants. On the 2R chromosome, I was able to map the sterility in 2R-129-09 to two genes, *Dup* and *SRPK*. Subsequent sequencing of both genes revealed that the mutation introduced a stop codon into the spacer region between the two kinase domains of *SRPK* (SR Protein Kinase).

4.5a: SRPK, roles and regulation.

The mutation that I identified in 2R-129-09 introduced a premature stop codon into the spacer region of the *Drosophila* gene SRPK that resulted in the deletion of the N-terminal 735 nucleotides of the *SRPK* coding mRNA, including half of the kinase domain. This truncation presumably leads to a kinase null phenotype, though an in-vitro kinase assay will be required to verify any loss of kinase activity.

SRPK is the kinase responsible for phosphorylating the serine and arginine rich RS domains found in SR proteins. SR proteins regulate both constitutive and alternative splicing and play a role in mRNA export from the nucleus (Long and Caceres, 2009). Phosphorylation of SR proteins enhances their interaction with other RS domain containing splicing factors (Xiao and Manley, 1997) and enhances their splicing activity in vitro, while dephosphorylation is required to catalyze splicing once the spliceosome has been assembled (Cao et al., 1997).

Phosphorylation (and dephosphorylation) is also important for the transit of the shuttling SR proteins from the nuclear interior to the cytoplasm and vice versa, and thus indirectly controls the export of associated mRNA transcripts (Lin et al., 2005). In an SRPK kinase null mutant, any or all of these activities might be affected, leading to a global decrease in splicing and transcript export. However, to understand how this affects the karyosome, it will be necessary to identify the specific mRNA transcript being affected that has a role in karyosome formation and maintenance.

Besides SR proteins, RS domains have been found in other proteins, including Lamin B Receptor (LBR). LBR is an integral nuclear transmembrane protein with a highly charged N-terminal segment consisting of two globular domains. The C-terminal half of the protein is hydrophobic and contains 8 transmembrane sequences (Human LBR: (Ye and Worman, 1994) *Drosophila* LBR: (Wagner et al.,

2004)). Besides binding to B type lamins as its name implies (Simos and Georgatos, 1992), LBR is also capable of binding to chromatin, specifically HP1 associated heterochromatin (Polioudaki et al., 2001; Ye et al., 1997). It has been shown that SRPK1 is able to phosphorylate the RS domains of LBR in-vitro (Papoutsopoulou et al., 1999) and that phosphorylation of LBR by *Xenopus* SRPK1 is responsible for increasing the affinity of LBR for chromatin (Takano et al., 2004).

Paradoxically, in my mutant 2R-129-09, where the kinase activity of SRPK was presumably abrogated by the truncation of the kinase domain, the phenotype that I observed was that of continued chromatin adherence to the nuclear membrane. If SRPK phosphorylation is required for the binding of LBR to chromatin, then the phenotype for 2R-129-09, where this phosphorylation is abolished, should be one of chromatin release from the inner nuclear membrane, and not continued binding.

However, as stated in section 4.4, SRPK is but one of three RS domain phosphorylating proteins identified in *Drosophila*. More specifically, SRPK is the *Drosophila* homologue of SRPK2, which might have a different function from the *Drosophila* orthologue of SRPK1 during female meiosis. At present, more work is required to determine whether this mutation in *Drosophila* SRPK is affecting karyosome morphology due to misregulation of the SR proteins and alternative splicing, or if phosphorylation by SRPK is required to release chromatin from proteins located at the inner nuclear membrane.

Chapter 5:

A genetic modifier screen to identify NHK-1 interacting proteins

Chapter 5: A genetic modifier screen to identify NHK-1 interacting proteins

Nucleosomal Histone Kinase 1 (NHK-1) was a protein previously identified in our lab as being important for proper karyosome formation via its phosphorylation target Barrier-to-Autointegration Factor (BAF) (Cullen et al., 2005; Lancaster et al., 2007). To identify other proteins that interact directly or indirectly with NHK-1, I carried out a genetic modifier screen using a collection of 44 deficiencies with defined breakpoints (Ryder et al., 2007; Ryder et al., 2004). By this screen, I hoped to identify proteins that are important for the regulation and function of NHK-1.

5.1: The genetic modifier screen: Using haplo-insufficiency to identify genes that interact with a semi-lethal allele of NHK-1

Genetic modifier screens identify genes that interact with a specific mutation and either increase or decrease the severity of its phenotype. To identify genes on the 2nd chromosome that interact with *NHK-1*, I used a semi-lethal allele of *NHK-1* called *NHK-1^{trip}* to screen the 2nd chromosome deficiencies fly stocks.

Drosophila melanogaster has four chromosomes but only the 2nd chromosome deficiency fly stocks were tested. The first chromosome deficiency fly stocks were not tested due to the complications involved in maintaining viability in deficiency males (as stated in section 4.1a). The third chromosome deficiency stocks were not tested because the gene encoding NHK-1 is located on the third chromosome. Since this screen examines the effect of the deficiencies in a homozygous *NHK-1^{trip}* background, it would have required recombination between *NHK-1* and the third chromosome deficiencies to produce a chromosome with both.

To carry out such recombination for every deficiency located on the third chromosome would have been inefficient given the time constraints. Finally, the small size of the fourth chromosome meant that similar to the third chromosome, it would have been inefficient to screen the 4th chromosome deficiencies.

As stated in section 4.1c, flies with deficiencies have large chromosomal deletions, with each deleting multiple genes. By placing these deficiencies in an *NHK-1^{trip}* homozygous background, I can identify which deficiencies, and ultimately which deleted genes result in an enhancement or repression of the *NHK-1^{trip}* semi-lethal phenotype.

The crossing scheme used generated a population of flies with different genotypes in a single vial. The two genotypes that I used to isolate genetic modifiers of NHK-1 were the flies heterozygous for the deficiency in an *NHK-1^{trip}* homozygous background, and otherwise wild type flies in an *NHK-1^{trip}* homozygous background. To aid in identification, flies that were heterozygous for the deficiency had orange eyes, and flies homozygous for *NHK-1^{trip}* had curly wings. (Fig. 20)

In a homozygous *NHK-1^{trip}* background, the ratio of flies with the deficiency to flies without the deficiency will indicate if a particular deficiency is enhancing or suppressing the semi-lethal phenotype of *NHK-1^{trip}*. If the deficiency had no effect on fly viability of the *NHK-1^{trip}* homozygotes, then I would expect to see a 1:1 ratio of these two populations of flies. To account for fluctuations in fly population numbers, I decided to focus only on those deficiencies that produced losses or gains in fly viability of 2 fold or more in a *NHK-1^{trip}* homozygous background.

As a control, I determined if the deficiencies, independent of *NHK-1^{trip}*, were affecting the viability of the flies. To do this, I compared the number of flies with the deficiency in a non-homozygous *NHK-1^{trip}* background to the number of flies which did not have the deficiency in the same non-homozygous *NHK-1^{trip}* background. If the deficiency was not having an effect on fly viability independent of *NHK-1^{trip}*, then

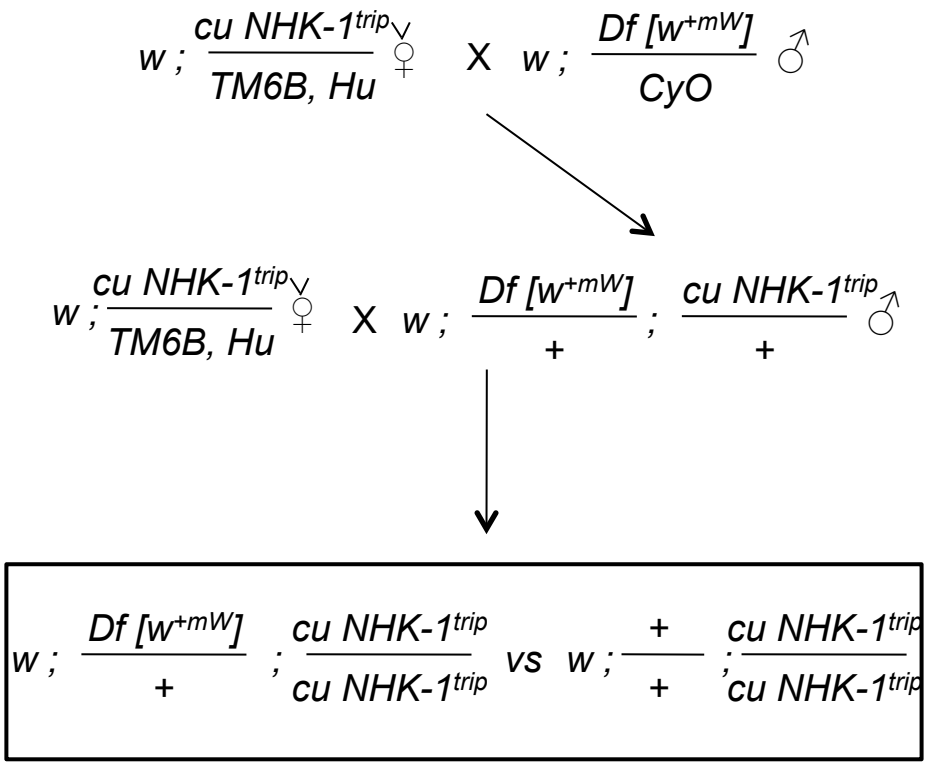

Figure 20. Two step crossing scheme for genetic modifier screen using the DrosDel deficiency collection.
DrosDel deficiencies are marked with the dominant w^{+mW} eye color marker.

I would expect the ratio of 1:1 of flies with the deficiency to flies without the deficiency.

5.2: *Df(2R)ED4065, Df(2L)ED94, Df(2L)ED19* and *Df(2R)ED1742* all enhanced the semi-lethal phenotype of *NHK-1^{trip}*

I carried out the genetic modifier screen with the collection of 2nd chromosome deficiencies. The crosses were carried out twice, the first time on all 44 deficiency fly stocks and the second on only those stocks that enhanced or suppressed the semi-lethal phenotype of *NHK-1^{trip}* in the first round of crosses.

The following 4 deficiencies produced an enhancement of the semi-lethal phenotype of the *NHK-1^{trip}* allele in both rounds of crosses:*, Df(2L)ED19, Df(2L)ED94, Df(2R)ED1742* and *Df(2R)ED4065*.

Taking in combination both rounds of crosses, *Df(2L)ED19* caused a more than 2 fold loss of viability, *Df(2L)ED94* caused nearly a 3 fold loss of viability, *Df(2R)ED1742* caused a 12 fold loss of viability and *Df(2R)ED4065* caused more than a 3 fold loss of viability. I concentrated my efforts on *Df(2R)ED1742*, the deficiency that had the strongest effect on *NHK-1^{trip}*. (Fig. 21)

5.3: The overlapping deficiency *Df(2R)ED1735* enhances the semi-lethal phenotype of *NHK-1^{trip}* similar to *Df(2R)ED1742*

The cytological region deleted in *Df(2R)ED1742* spans from 44B8-44E3 on the 2nd chromosome. Overlapping this region were two deficiencies, *Df(2R)ED1735*, and *Df(2R)ED1770*.

Df(2R)ED1735 was one of the 44 deficiency stocks used in this genetic modifier screen and had been identified in the first round of crosses to enhance the

	NHK-1^{trip} homozygous background		Non *NHK-1*^{trip} homozygous background	
	+ Df	- Df	+Df	-Df
Df(2L)ED19	16	41	136	228
Df(2L)ED94	12	32	175	223
Df(2R)ED1735	2	15	46	59
Df(2R)ED1742	4	12	142	143
Df(2R)ED4065	7	27	183	277
Df(2R)Exel6056	11	8	107	102
Df(2R)Exel6057	23	16	135	105
Df(2R)Exel6058	23	14	131	123
Df(2R)Exel7095	23	21	174	181
Df(2R)Exel7096	8	15	222	231
Df(2R)Exel8047	27	28	206	225
Df(2R)BSC266	1	27	163	132

Figure 21. Results of the *NHK-1* genetic modifier screen using semi-lethal allele of *NHK-1*, *NHK-1*^{trip}.
Df(2R)ED1742 where the *NHK-1*^{trip} interacting genetic region was originally identified and the deficiencies that overlap this region, *Df (2R)ED1735 and Df(2R)BSC266,* are indicated with red text.

semi-lethal phenotype of *NHK-1*^{trip}. It caused an 8 fold loss of viability in a homozygous *NHK-1*^{trip} background. This 8 fold loss of viability for *Df(2R)ED1735* is comparable to the 12 fold loss of viability seen in *Df(2R)ED1742*. However, in the second round of crosses, *Df(2R)ED1735* did not cause any appreciable (2 fold or more) enhancement of the semi-lethal phenotype in a homozygous *NHK-1*^{trip} background.

Knowing that the deleted cytological region of *Df(2R)ED1735* overlapped that of *Df(2R)ED1742*, and that this overlapping region uncovered more than half of the deleted cytological region of *Df(2R)ED1742*, I repeated the genetic modifier crosses for both *Df(2R)ED1735* and *Df(2R)ED1742* (as a control).

Both *Df(2R)ED1735* and *Df(2R)ED1742* enhanced the semi-lethal phenotype in a *NHK-1*^{trip} homozygous background. *Df(2R)ED1735* showed a 7 fold loss of viability in a homozygous *NHK-1*^{trip} background and Df(2R)ED1742 showed a 3 fold loss of viability. This shared enhancement of the semi-lethal phenotype of *NHK-1*^{trip} indicates that the gene interacting with *NHK-1* is located in the overlap cytological region of 44B8-44D4.

5.4: The deficiency *Df(2R)BSC266* that overlaps both *Df(2R)ED1742* and *Df(2R)ED1735* also enhances the semi-lethal phenotype of *NHK-1*^{trip}

I used other deficiencies to further narrow down the region enhancing the semi-lethal phenotype of *NHK-1*^{trip}. The following deficiencies uncovered the overlapping region of *Df(2R)ED1742* and *Df(2R)ED1735*: *Df(2R)Exel6056, Df(2R)Exel6057, Df(2R)Exel6058, Df(2R)Exel7095, Df(2R)Exel7096*, *Df(2R)Exel8047* and *Df(2R)BSC266* (Parks et al., 2004; Thibault et al., 2004).

As *Df(2R)Exel6056, Df(2R)Exel6057, Df(2R)Exel6058* all have the w^+ gene on their deficiency chromosomes, I was able to identify progeny with the deficiency

in a similar fashion to *Df(2R)ED1742* and *Df(2R)ED1735* (as laid out in section 5.1, progeny with the deficiency chromosome would have orange eyes). I carried out the genetic modifier screen as laid out in section 5.1 for these deficiencies with *Df(2R)ED1742* as a positive control. While *Df(2R)ED1742* showed a 15 fold loss of viability in a *NHK-1*^{trip} homozygous background consistent with previous results, none of these deficiencies caused a similar loss of viability.

Unlike *Df(2R)ED1742*, the remaining deficiencies, *Df(2R)Exel7095, Df(2R)Exel7096, Df(2R)Exel8047* and *Df(2R)BSC266*, did not have any visible markers on their deficiency chromosome. Therefore, I used a different three step crossing scheme to test these deficiencies. (Fig. 22)

The crossing scheme is set up such that the only possible genotypes that are homozygous for *NHK-1*^{trip} will be flies that are heterozygous for either the deficiency or *noc*^{Sco}. *noc*^{Sco} is a dominant mutation and the presence of its phenotype (missing dorsal bristles) in a homozygous *NHK-1*^{trip} background will mean the absence of the deficiency, and vice versa (Ashburner et al., 1983; Ashburner and Harrington, 1984; McGill et al., 1988).

I carried out this genetic modifier cross on the remaining deficiencies with *Df(2R)ED1742* as a positive control. Only the deficiency *Df(2R)BSC266* demonstrated a loss of viability phenotype similar to that seen in *Df(2R)ED1742* (27 fold loss of viability in *Df(2R)BSC266* and 15 fold loss of viability in *Df(2R)ED1742*). This shared enhancement of the semi-lethal phenotype of *NHK-1*^{trip} indicates that the gene interacting with *NHK-1* is located in the overlap cytological region of 44B8-44D1, a region containing 41 genes. (Fig. 23)

This region, 44B8-44D1, is completely uncovered by three deficiencies *Df(2R)Exel6057, Df(2R)Exel6058 and Df(2R)Exel7096*. As stated earlier in this section, these three deficiencies have already been tested for interaction with the *NHK-1*^{trip}, and, paradoxically, none of them displayed a loss of viability phenotype

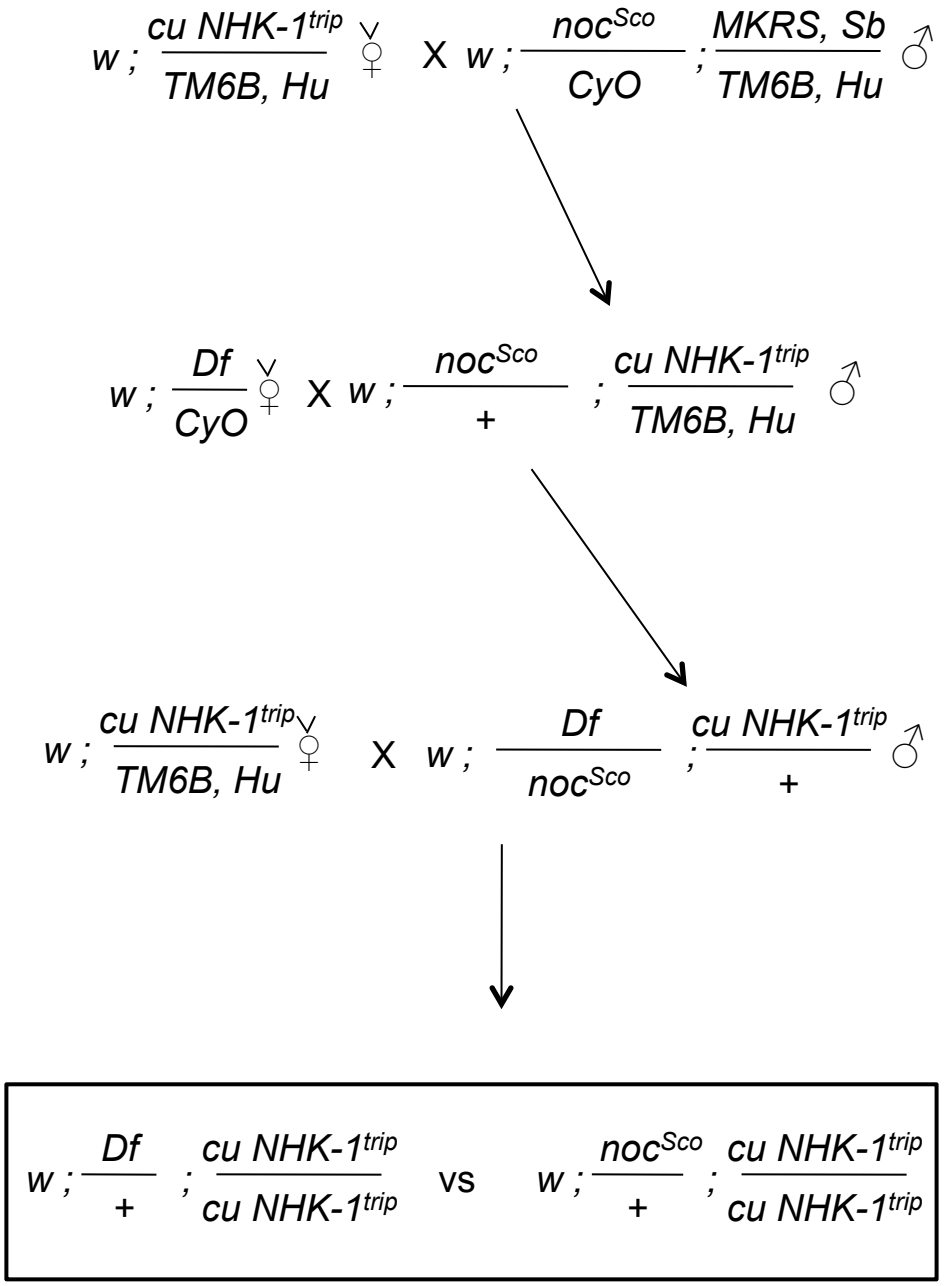

Figure 22. Three step crossing scheme for genetic modifier screen using deficiencies without dominant w^{+mW} eye color marker.
noc^{Sco}, a dominant bristle affecting marker was used to identify the deficiency carrying flies.

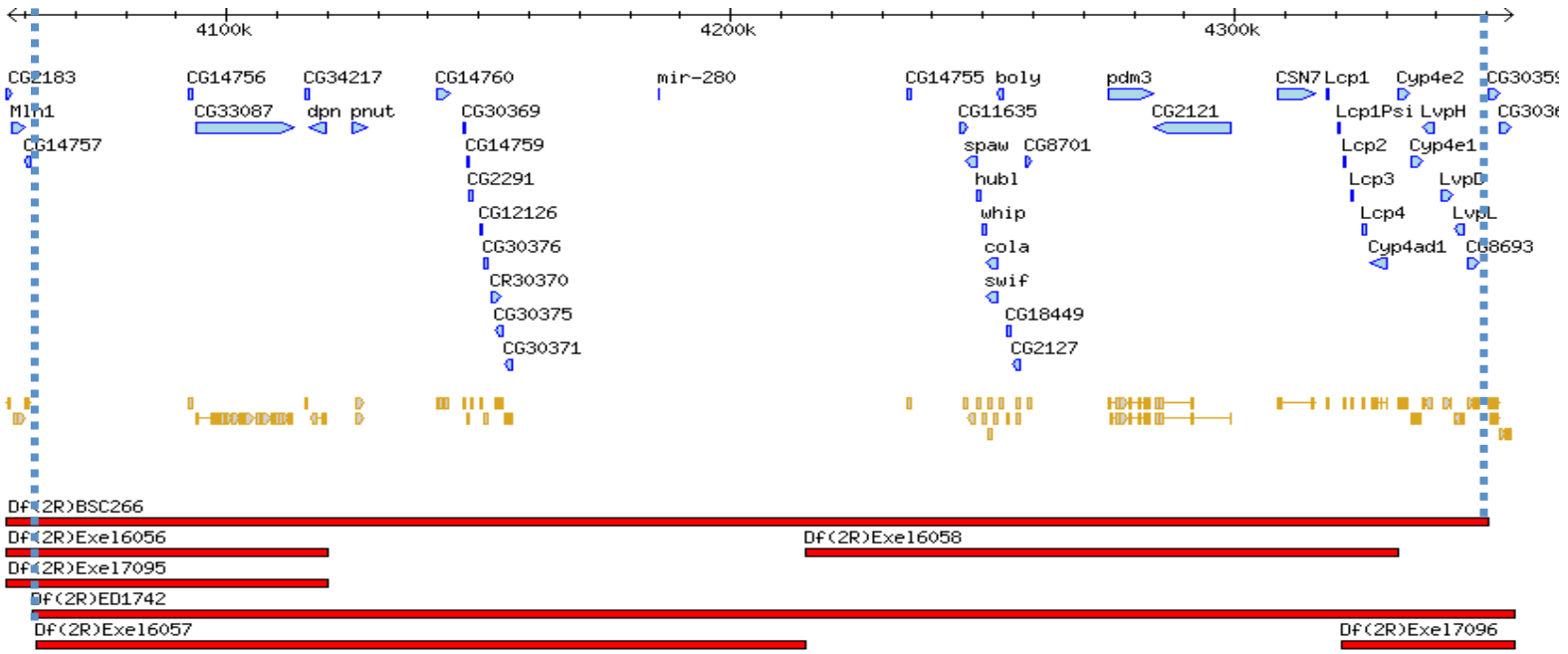

Figure 23. Region containing genetic modifier of *NHK-1* as defined by genetic modifier screen.
Deleted genes are displayed in blue and associated coding sequences in gold/grey. Deficiencies used in the genetic modifier screen are at the bottom in red. Vertical blue dashed lines indicate the extent of the region identified in the genetic modifier screen. Original image was created using the Gbrowse function in flybase.

comparable to *Df(2R)ED1742* in a homozygous *NHK-1^{trip}* background. However, as with the overlapping deficiency *Df(2R)ED1735*, which, as stated in section 5.3, did not show a loss of viability phenotype comparable to *Df(2R)ED1742* in the second round of crosses, these results might be due to random fluctuations in fly population. Further testing will be required to determine which of these deficiencies, if any, uncovers the region containing the gene that interacts with *NHK-1*.

5.5: Discussion

Nucleosomal Histone Kinase 1 (NHK-1) was previously identified in the lab as a protein that was essential to the proper formation of the karyosome. To identify genes that interact with *NHK-1*, I conducted a deficiency modifier screen on a collection of 44 deficiencies with molecularly defined breakpoints, using a semi-lethal mutant of NHK-1, *NHK-1^{trip}*.

The screen identified 4 deficiencies, *Df(2L)ED19, Df(2L)ED94, Df(2R)ED1742* and *Df(2R)ED4065,* that enhanced the semi-lethal phenotype of *NHK-1^{trip}.* In a *NHK-1^{trip}* homozygous background, *Df(2L)ED19, Df(2L)ED94* and *Df(2R)ED4065* all caused between 2 and 4 fold losses in fly viability, while *Df(2R)ED1742* caused a 12 fold loss of viability. Since it demonstrated the strongest interaction with *NHK-1^{trip}*, I chose to study *Df(2R)ED1742* further.

Using two deficiencies that overlapped *Df(2R)ED1742*, I attempted to narrow down the deleted region causing the loss of viability in conjunction with *NHK-1^{trip}*. One of the deficiencies, *Df(2R)ED1735,* caused a loss of viability in a homozygous *NHK-1^{trip}* background similar to that of *Df(2R)ED1742*, indicating that the gene interacting with *NHK-1* is probably located in the overlap region: 44B8-44D4. Out of the 7 deficiencies that overlap this cytological region, in a *NHK-1^{trip}* homozygous background, only the deficiency *Df(2R)BSC266* caused a loss of viability similar to

Df(2R)ED1742, further narrowing down the region containing the interacting gene to 44B8-44D1. Puzzlingly, this region is uncovered by three of the overlapping deficiencies, but none of these deficiencies showed any interaction with *NHK-1*^{trip}.

5.5a: Haplo-insufficiency testing in a homozygous background

Traditionally, deficiency modifier screens involve using dominant mutations to identify genetic modifiers of a certain gene. The benefit of this is that only one cross is required to generate flies heterozygous for both the deficiency and the dominant mutation. However, the accompanying drawback is that this strategy doesn't work with recessive mutations.

To address this shortcoming, I have developed a two step crossing scheme that generates flies that are homozygous for the mutation (in this case *NHK-1*^{trip}) and either heterozygous for the deficiency or otherwise wild type. Though slower than the traditional one step method, this crossing scheme is both broader and more sensitive, as it allows for the screening of recessive mutants.

The development that made the two step crossing scheme feasible was the creation of the DrosDel collection of deficiencies fly stocks (Ryder et al., 2007; Ryder et al., 2004). DrosDel deficiency stocks have the dominant w^{+mW} eye color gene on their deficiency chromosomes, which allows for efficient identification of the deficiency bearing progeny in the F2 generation. Without this dominant marker, an extra crossing step would be required to introduce appropriate markers to identify the deficiency chromosome as was the case for *Df(2R)Exel7095, Df(2R)Exel7096, Df(2R)Exel8047* and *Df(2R)BSC266*.

5.5b: Rough-eyes and dead flies, two different approaches to genetic modifier screens

In *Drosophila*, the eye is the most popular organ in which to conduct modifier screens for two reasons (1) the ~800 ommatidia (cells that comprise the eye) makes for both easy and nuanced scoring and (2) the eye is not required for viability or fertility (St Johnston, 2002). Genetic modifiers of essential genes cannot be studied in the whole organism because mutations in essential genes can cause lethality. However, these modifiers can be identified in the eye if the mutated essential genes are expressed as a transgenic construct with the enhancer region of *sev* (*Sevenless*), a gene encoding a receptor tyrosine kinase (RTK) that determines cell fate in the eye (Simon, 1994). If this eye-specific expression of a mutated gene causes the rough-eye phenotype, then enhancers or suppressors of this phenotype can be screened for (St Johnston, 2002).

The suitability of the *Drosophila* eye as a system for enhancer/suppressor genetic modifier screens does beg the question, why didn't I screen for genetic interactors of *NHK-1* in the *Drosophila* eye? The obvious answer is that a transgenic *NHK-1*^{trip} construct, with the enhancer region of *sev* driving the expression of *NHK-1*^{trip} in the eye, would not necessarily have caused the rough-eye phenotype required for this kind of screening. Instead, using the semi-lethality of *NHK-1*^{trip} as a testable phenotype, I was able to identify deficiencies that interacted with *NHK-1*^{trip} in the context of the entire organism.

The main advantage of this screening methodology was the easy scoring of the suppression / enhancement of the *NHK-1*^{trip} mutation, which basically involved counting and comparing the relative populations of flies with different markers. This screening methodology also has the added advantage in that it can be used to screen other semi-lethal mutations and thus has applications beyond the scope of

NHK-1. More work will be required to establish the true efficacy of this novel technique.

Chapter 6:

Conclusion

Chapter 6: Conclusion

In the introduction, I set out two objectives, (1) identify mutants and ultimately proteins that affect the formation and maintenance of the karyosome and (2) locate genes that interact with *NHK-1*, that encode proteins that are essential for karyosome formation. To that end, I carried out two separate but related projects, a cytological screen for mutants that affected the formation and maintenance of the karyosome and a deficiency modifier screen for genetic interactors of $NHK\text{-}1^{trip}$, a semi-lethal allele of NHK-1.

As both were novel experiments in approach and aim, much of the methodology had to be devised specifically for each screen, and success was not simply predicated upon faithfully reproducing the work of others. However, in spite of all this, both screens were successful, and produced results that represent a foundation for future experiments. In this chapter, I will discuss the significance of the results and the avenues that they open for further work.

6.1: Conclusions and future work

It has been proposed that proper formation of the karyosome is important for the assembly of the female meiotic bipolar spindle, however despite this, little is actually known about the proteins and pathways involved in the formation of the karyosome. The discovery that NHK-1 plays a direct role in karyosome formation marked the beginning of a concerted effort in our lab to unravel the proteins and pathways involved in the formation of this previously enigmatic structure.

Therefore, my screen is important because it represents the first ever deliberate search for mutants, and ultimately genes and proteins that directly affect

the formation of the karyosome. In the process of this screen, through trial and error, I was able to create a set of protocols for screening and evaluating karyosome morphology in a collection of mutants which can be used in future screens. I successfully identified 46 mutants on both the 1st and 2nd chromosome that affected the formation of the karyosome and am currently performing genetic analysis to isolate the genes responsible for the karyosome abnormalities in these mutants.

From the results of this screen, several avenues for future work are apparent:

(1)Though sequencing revealed that in 2R-129-09, there was a mutation in the gene *SRPK*, the mutated genes causing the karyosome defects in the remaining 45 mutants identified in the screen still have yet to be identified. Good candidates for further analysis are the two non-complementing groups of mutants that were identified on the 1st and 2nd chromosomes. Deficiency mapping has been successful in narrowing down the cytological region containing the lethal mutation on the 1st chromosome and the sterile mutation on the 2nd chromosome to 10 and 15 genes respectively. Sequencing of these regions will identify the actual mutated genes in both of these non-complementing groups.

(2) The 3rd and 4th chromosomes remain to be screened for karyosome defective mutants, though the 3rd chromosome and 4th chromosome mutants still need to be generated. Selection criteria for new mutants should include “eggs laid showed proper dorsal development” to exclude mutants where the meiotic recombination checkpoint is activated.

(3) The mutants identified to have weak dorsal patterning could be analyzed to identify mutants that activate the MRC. The (Barbosa et al., 2007) screen specifically did not study this category of mutants as the phenotype was too weak, so there might still be proteins involved in the MRC there to identify.

(4) Even though the SRPK mutant (2R-129-09) had a strong, if not penetrant, karyosome phenotype, how this comes about is still not known. There are two obvious possibilities to explain this. The first is that SRPK is important for karyosome formation via its regulation of the SR proteins which are involved in alternative splicing. The second is that SRPK regulates karyosome formation by phosphorylating Lamin B Receptor (LBR), which binds to chromatin at the nuclear periphery. To determine which, if either, of these possibilities is true, a phosphomimetic form of either the SR proteins or LBR could be expressed, in place of the wild type proteins, within the oocytes of 2R-129-09 females with germline clone ovaries. If either the phosphomimetic SR proteins or LBR rescues the karyosome morphology defect of 2R-129-09, then the protein that is actually causing the karyosome morphology defect downstream of SRPK will have been identified.

Following on from previous work done in the lab, I also carried out a genetic modifier screen searching for interactors of *NHK-1*, a protein that has previously been shown to have a direct effect on the formation of the karyosome. This screen involved observing the effect of deficiencies in a homozygous mutant background, a hitherto untested methodology for conducting genetic modifier screens. Using this methodology I was able to successfully isolate 4 deficiencies containing genes that interacted with *NHK-1*. Further analysis of the strongest interacting deficiency, *Df(2R)ED1742*, using overlapping deficiencies narrowed down the region of interaction to 41 genes. From the results of the deficiency modifier screen the possibilities for future work are as follows:

(1) The interacting gene located in Df(2R)ED1742 still needs to be located. Though the cytological region containing the interacting gene has been narrowed down to 41 genes, 4 deficiencies that overlap that region have shown no genetic interaction with *NHK-1*. Re-testing of the overlapping deficiencies should reveal which, if any, of them contain the gene that is interacting with *NHK-1*.

(2) The deficiencies used in this genetic modifier screen did not cover the entirety of the 2nd chromosome, thus it will be useful to screen the deficiencies that uncover the rest of the 2nd chromosome for genes that interact with *NHK-1*.

(3) Having verified that this screening methodology is valid, I suggest that it can be used to screen for interactors of other genes with recessive semi-lethal alleles. I have already applied this methodology to screen for interactors with *msps* (*Mini-Spindles*) though in this case I wasn't able to identify any interactors with *msps* on the second chromosome.

Chapter 7:

Literature cited

Chapter 7: Literature cited

Agudo, M., Abad, J. P., Molina, I., Losada, A., Ripoll, P., and Villasante, A. (2000). A dicentric chromosome of Drosophila melanogaster showing alternate centromere inactivation. Chromosoma *109*, 190-196.

Aihara, H., Nakagawa, T., Yasui, K., Ohta, T., Hirose, S., Dhomae, N., Takio, K., Kaneko, M., Takeshima, Y., Muramatsu, M., and Ito, T. (2004). Nucleosomal histone kinase-1 phosphorylates H2A Thr 119 during mitosis in the early Drosophila embryo. Genes Dev *18*, 877-888.

Allan, J., Hartman, P. G., Crane-Robinson, C., and Aviles, F. X. (1980). The structure of histone H1 and its location in chromatin. Nature *288*, 675-679.

Ambrosio, L., Mahowald, A. P., and Perrimon, N. (1989). l(1)pole hole is required maternally for pattern formation in the terminal regions of the embryo. Development *106*, 145-158.

Ashburner, M. (1989). Drosophila : a laboratory handbook, (Cold Spring Harbor, N.Y.: Cold Spring Harbor Laboratory Press).

Ashburner, M., Detwiler, C., Tsubota, S., and Woodruff, R. C. (1983). The genetics of a small autosomal region of Drosophila melanogaster containing the structural gene for alcohol dehydrogenase. VI. Induced revertants of scutoid. Genetics *104*, 405-431.

Ashburner, M., and Harrington, G. (1984). A cytological analysis of the Scutoid mutation of Drosophila melanogaster, and its induced revertants. Chromosoma *89*, 329-337.

Barboro, P., D'Arrigo, C., Diaspro, A., Mormino, M., Alberti, I., Parodi, S., Patrone, E., and Balbi, C. (2002). Unraveling the organization of the internal nuclear matrix: RNA-dependent anchoring of NuMA to a lamin scaffold. Exp Cell Res *279*, 202-218.

Barbosa, V., Kimm, N., and Lehmann, R. (2007). A maternal screen for genes regulating Drosophila oocyte polarity uncovers new steps in meiotic progression. Genetics *176*, 1967-1977.

Bassett, A., Cooper, S., Wu, C., and Travers, A. (2009). The folding and unfolding of eukaryotic chromatin. Curr Opin Genet Dev *19*, 159-165.

Bellotto, M., Bopp, D., Senti, K. A., Burke, R., Deak, P., Maroy, P., Dickson, B., Basler, K., and Hafen, E. (2002). Maternal-effect loci involved in Drosophila oogenesis and embryogenesis: P element-induced mutations on the third chromosome. Int J Dev Biol *46*, 149-157.

Belmont, A. S. (2006). Mitotic chromosome structure and condensation. Curr Opin Cell Biol *18*, 632-638.

Bischoff, F. R., Klebe, C., Kretschmer, J., Wittinghofer, A., and Ponstingl, H. (1994). RanGAP1 induces GTPase activity of nuclear Ras-related Ran. Proc Natl Acad Sci U S A *91*, 2587-2591.

Bischoff, F. R., and Ponstingl, H. (1991). Catalysis of guanine nucleotide exchange on Ran by the mitotic regulator RCC1. Nature *354*, 80-82.

Black, B. E., Brock, M. A., Bedard, S., Woods, V. L., Jr., and Cleveland, D. W. (2007a). An epigenetic mark generated by the incorporation of CENP-A into centromeric nucleosomes. Proc Natl Acad Sci U S A *104*, 5008-5013.

Black, B. E., Foltz, D. R., Chakravarthy, S., Luger, K., Woods, V. L., Jr., and Cleveland, D. W. (2004). Structural determinants for generating centromeric chromatin. Nature *430*, 578-582.

Black, B. E., Jansen, L. E., Maddox, P. S., Foltz, D. R., Desai, A. B., Shah, J. V., and Cleveland, D. W. (2007b). Centromere identity maintained by nucleosomes assembled with histone H3 containing the CENP-A targeting domain. Mol Cell *25*, 309-322.

Blower, M. D., and Karpen, G. H. (2001). The role of Drosophila CID in kinetochore formation, cell-cycle progression and heterochromatin interactions. Nat Cell Biol *3*, 730-739.

Blower, M. D., Sullivan, B. A., and Karpen, G. H. (2002). Conserved organization of centromeric chromatin in flies and humans. Dev Cell *2*, 319-330.

Bolzer, A., Kreth, G., Solovei, I., Koehler, D., Saracoglu, K., Fauth, C., Muller, S., Eils, R., Cremer, C., Speicher, M. R., and Cremer, T. (2005). Three-dimensional maps of all chromosomes in human male fibroblast nuclei and prometaphase rosettes. PLoS Biol *3*, e157.

Bridger, J. M., Boyle, S., Kill, I. R., and Bickmore, W. A. (2000). Re-modelling of nuclear architecture in quiescent and senescent human fibroblasts. Curr Biol *10*, 149-152.

Camahort, R., Li, B., Florens, L., Swanson, S. K., Washburn, M. P., and Gerton, J. L. (2007). Scm3 is essential to recruit the histone h3 variant cse4 to centromeres and to maintain a functional kinetochore. Mol Cell *26*, 853-865.

Cao, W., Jamison, S. F., and Garcia-Blanco, M. A. (1997). Both phosphorylation and dephosphorylation of ASF/SF2 are required for pre-mRNA splicing in vitro. RNA *3*, 1456-1467.

Casolari, J. M., Brown, C. R., Komili, S., West, J., Hieronymus, H., and Silver, P. A. (2004). Genome-wide localization of the nuclear transport machinery couples transcriptional status and nuclear organization. Cell *117*, 427-439.

Cassimeris, L. (2006). Mitosis: riding the protofilament curl. Curr Biol *16*, R214-216.

Chang, C. J., Goulding, S., Earnshaw, W. C., and Carmena, M. (2003). RNAi analysis reveals an unexpected role for topoisomerase II in chromosome arm congression to a metaphase plate. J Cell Sci *116*, 4715-4726.

Cheeseman, I. M., Anderson, S., Jwa, M., Green, E. M., Kang, J., Yates, J. R., 3rd, Chan, C. S., Drubin, D. G., and Barnes, G. (2002). Phospho-regulation of kinetochore-microtubule attachments by the Aurora kinase Ipl1p. Cell *111*, 163-172.

Cheeseman, I. M., Chappie, J. S., Wilson-Kubalek, E. M., and Desai, A. (2006). The conserved KMN network constitutes the core microtubule-binding site of the kinetochore. Cell *127*, 983-997.

Chou, T. B., and Perrimon, N. (1992). Use of a yeast site-specific recombinase to produce female germline chimeras in Drosophila. Genetics *131*, 643-653.

Clarke, L., and Carbon, J. (1980). Isolation of a yeast centromere and construction of functional small circular chromosomes. Nature *287*, 504-509.

Conde e Silva, N., Black, B. E., Sivolob, A., Filipski, J., Cleveland, D. W., and Prunell, A. (2007). CENP-A-containing nucleosomes: easier disassembly versus exclusive centromeric localization. J Mol Biol *370*, 555-573.

Cooke, C. A., Schaar, B., Yen, T. J., and Earnshaw, W. C. (1997). Localization of CENP-E in the fibrous corona and outer plate of mammalian kinetochores from prometaphase through anaphase. Chromosoma *106*, 446-455.

Cremer, M., Kupper, K., Wagler, B., Wizelman, L., von Hase, J., Weiland, Y., Kreja, L., Diebold, J., Speicher, M. R., and Cremer, T. (2003). Inheritance of gene density-related higher order chromatin arrangements in normal and tumor cell nuclei. J Cell Biol *162*, 809-820.

Cremer, M., von Hase, J., Volm, T., Brero, A., Kreth, G., Walter, J., Fischer, C., Solovei, I., Cremer, C., and Cremer, T. (2001). Non-random radial higher-order chromatin arrangements in nuclei of diploid human cells. Chromosome Res *9*, 541-567.

Croft, J. A., Bridger, J. M., Boyle, S., Perry, P., Teague, P., and Bickmore, W. A. (1999). Differences in the localization and morphology of chromosomes in the human nucleus. J Cell Biol *145*, 1119-1131.

Cromie, G. A., and Smith, G. R. (2007). Branching out: meiotic recombination and its regulation. Trends Cell Biol *17*, 448-455.

Cullen, C. F., Brittle, A. L., Ito, T., and Ohkura, H. (2005). The conserved kinase NHK-1 is essential for mitotic progression and unifying acentrosomal meiotic spindles in Drosophila melanogaster. J Cell Biol *171*, 593-602.

Cullen, C. F., and Ohkura, H. (2001). Msps protein is localized to acentrosomal poles to ensure bipolarity of Drosophila meiotic spindles. Nat Cell Biol *3*, 637-642.

Dalal, Y., Furuyama, T., Vermaak, D., and Henikoff, S. (2007a). Structure, dynamics, and evolution of centromeric nucleosomes. Proc Natl Acad Sci U S A *104*, 15974-15981.

Dalal, Y., Wang, H., Lindsay, S., and Henikoff, S. (2007b). Tetrameric structure of centromeric nucleosomes in interphase Drosophila cells. PLoS Biol *5*, e218.

Davenport, J., Harris, L. D., and Goorha, R. (2006). Spindle checkpoint function requires Mad2-dependent Cdc20 binding to the Mad3 homology domain of BubR1. Exp Cell Res *312*, 1831-1842.

Davies, H. G. (1968). Electron-microscope observations on the organization of heterochromatin in certain cells. J Cell Sci *3*, 129-150.

de Cuevas, M., and Spradling, A. C. (1998). Morphogenesis of the Drosophila fusome and its implications for oocyte specification. Development *125*, 2781-2789.

Debey, P., Szollosi, M. S., Szollosi, D., Vautier, D., Girousse, A., and Besombes, D. (1993). Competent mouse oocytes isolated from antral follicles exhibit different chromatin organization and follow different maturation dynamics. Mol Reprod Dev *36*, 59-74.

Dernburg, A. F., Sedat, J. W., and Hawley, R. S. (1996). Direct evidence of a role for heterochromatin in meiotic chromosome segregation. Cell *86*, 135-146.

Dillon, N. (2004). Heterochromatin structure and function. Biol Cell *96*, 631-637.

Dillon, N., and Festenstein, R. (2002). Unravelling heterochromatin: competition between positive and negative factors regulates accessibility. Trends Genet *18*, 252-258.

Doubilet, S., and McKim, K. S. (2007). Spindle assembly in the oocytes of mouse and Drosophila--similar solutions to a problem. Chromosome Res *15*, 681-696.

Dunleavy, E. M., Roche, D., Tagami, H., Lacoste, N., Ray-Gallet, D., Nakamura, Y., Daigo, Y., Nakatani, Y., and Almouzni-Pettinotti, G. (2009). HJURP is a cell-cycle-dependent maintenance and deposition factor of CENP-A at centromeres. Cell *137*, 485-497.

Earnshaw, W. C., Halligan, B., Cooke, C. A., Heck, M. M., and Liu, L. F. (1985). Topoisomerase II is a structural component of mitotic chromosome scaffolds. J Cell Biol *100*, 1706-1715.

Earnshaw, W. C., and Migeon, B. R. (1985). Three related centromere proteins are absent from the inactive centromere of a stable isodicentric chromosome. Chromosoma *92*, 290-296.

Eichenlaub-Ritter, U. (1996). Parental age-related aneuploidy in human germ cells and offspring: a story of past and present. Environ Mol Mutagen *28*, 211-236.

Fang, G. (2002). Checkpoint protein BubR1 acts synergistically with Mad2 to inhibit anaphase-promoting complex. Mol Biol Cell *13*, 755-766.

Fedorova, S. A., Nokkala, S., and Omel'ianchuk, L. V. (2001). [Genetic screening of meiotic mutations in mosaic clones of the Drosophila melanogaster female germline]. Genetika *37*, 1621-1631.

Fitzgerald-Hayes, M., Buhler, J. M., Cooper, T. G., and Carbon, J. (1982a). Isolation and subcloning analysis of functional centromere DNA (CEN11) from Saccharomyces cerevisiae chromosome XI. Mol Cell Biol *2*, 82-87.

Fitzgerald-Hayes, M., Clarke, L., and Carbon, J. (1982b). Nucleotide sequence comparisons and functional analysis of yeast centromere DNAs. Cell *29*, 235-244.

Foltz, D. R., Jansen, L. E., Bailey, A. O., Yates, J. R., 3rd, Bassett, E. A., Wood, S., Black, B. E., and Cleveland, D. W. (2009). Centromere-specific assembly of CENP-a nucleosomes is mediated by HJURP. Cell *137*, 472-484.

Foster, H. A., and Bridger, J. M. (2005). The genome and the nucleus: a marriage made by evolution. Genome organisation and nuclear architecture. Chromosoma *114*, 212-229.

Furukawa, K. (1999). LAP2 binding protein 1 (L2BP1/BAF) is a candidate mediator of LAP2-chromatin interaction. J Cell Sci *112 (Pt 15)*, 2485-2492.

Gaitanos, T. N., Santamaria, A., Jeyaprakash, A. A., Wang, B., Conti, E., and Nigg, E. A. (2009). Stable kinetochore-microtubule interactions depend on the Ska complex and its new component Ska3/C13Orf3. EMBO J *28*, 1442-1452.

Garagna, S., Merico, V., Sebastiano, V., Monti, M., Orlandini, G., Gatti, R., Scandroglio, R., Redi, C. A., and Zuccotti, M. (2004). Three-dimensional localization and dynamics of centromeres in mouse oocytes during folliculogenesis. J Mol Histol *35*, 631-638.

Gasser, S. M., Laroche, T., Falquet, J., Boy de la Tour, E., and Laemmli, U. K. (1986). Metaphase chromosome structure. Involvement of topoisomerase II. J Mol Biol *188*, 613-629.

Ghabrial, A., Ray, R. P., and Schupbach, T. (1998). okra and spindle-B encode components of the RAD52 DNA repair pathway and affect meiosis and patterning in Drosophila oogenesis. Genes Dev *12*, 2711-2723.

Ghabrial, A., and Schupbach, T. (1999). Activation of a meiotic checkpoint regulates translation of Gurken during Drosophila oogenesis. Nat Cell Biol *1*, 354-357.

Gonzalez-Reyes, A., Elliott, H., and St Johnston, D. (1997). Oocyte determination and the origin of polarity in Drosophila: the role of the spindle genes. Development *124*, 4927-4937.

Gorbsky, G. J. (1994). Cell cycle progression and chromosome segregation in mammalian cells cultured in the presence of the topoisomerase II inhibitors ICRF-187 [(+)-1,2-bis(3,5-dioxopiperazinyl-1-yl)propane; ADR-529] and ICRF-159 (Razoxane). Cancer Res *54*, 1042-1048.

Gorlich, D., Kostka, S., Kraft, R., Dingwall, C., Laskey, R. A., Hartmann, E., and Prehn, S. (1995). Two different subunits of importin cooperate to recognize nuclear localization signals and bind them to the nuclear envelope. Curr Biol *5*, 383-392.

Gorlich, D., Pante, N., Kutay, U., Aebi, U., and Bischoff, F. R. (1996). Identification of different roles for RanGDP and RanGTP in nuclear protein import. EMBO J *15*, 5584-5594.

Gruber, S., Haering, C. H., and Nasmyth, K. (2003). Chromosomal cohesin forms a ring. Cell *112*, 765-777.

Gruss, O. J., Carazo-Salas, R. E., Schatz, C. A., Guarguaglini, G., Kast, J., Wilm, M., Le Bot, N., Vernos, I., Karsenti, E., and Mattaj, I. W. (2001). Ran induces spindle

assembly by reversing the inhibitory effect of importin alpha on TPX2 activity. Cell *104*, 83-93.

Gruss, O. J., and Vernos, I. (2004). The mechanism of spindle assembly: functions of Ran and its target TPX2. J Cell Biol *166*, 949-955.

Gui, J. F., Lane, W. S., and Fu, X. D. (1994). A serine kinase regulates intracellular localization of splicing factors in the cell cycle. Nature *369*, 678-682.

Happel, N., and Doenecke, D. (2009). Histone H1 and its isoforms: contribution to chromatin structure and function. Gene *431*, 1-12.

Hassold, T., Hall, H., and Hunt, P. (2007). The origin of human aneuploidy: where we have been, where we are going. Hum Mol Genet *16 Spec No. 2*, R203-208.

Hassold, T., and Hunt, P. (2001). To err (meiotically) is human: the genesis of human aneuploidy. Nat Rev Genet *2*, 280-291.

Hatsumi, M., and Endow, S. A. (1992). Mutants of the microtubule motor protein, nonclaret disjunctional, affect spindle structure and chromosome movement in meiosis and mitosis. J Cell Sci *101 (Pt 3)*, 547-559.

Hauf, S., Waizenegger, I. C., and Peters, J. M. (2001). Cohesin cleavage by separase required for anaphase and cytokinesis in human cells. Science *293*, 1320-1323.

Hayashi, T., Fujita, Y., Iwasaki, O., Adachi, Y., Takahashi, K., and Yanagida, M. (2004). Mis16 and Mis18 are required for CENP-A loading and histone deacetylation at centromeres. Cell *118*, 715-729.

Hayden, J. H., Bowser, S. S., and Rieder, C. L. (1990). Kinetochores capture astral microtubules during chromosome attachment to the mitotic spindle: direct visualization in live newt lung cells. J Cell Biol *111*, 1039-1045.

He, D. C., Martin, T., and Penman, S. (1991). Localization of heterogeneous nuclear ribonucleoprotein in the interphase nuclear matrix core filaments and on perichromosomal filaments at mitosis. Proc Natl Acad Sci U S A *88*, 7469-7473.

He, D. C., Nickerson, J. A., and Penman, S. (1990). Core filaments of the nuclear matrix. J Cell Biol *110*, 569-580.

Hemmerich, P., Weidtkamp-Peters, S., Hoischen, C., Schmiedeberg, L., Erliandri, I., and Diekmann, S. (2008). Dynamics of inner kinetochore assembly and maintenance in living cells. J Cell Biol *180*, 1101-1114.

Heng, H. H., Goetze, S., Ye, C. J., Liu, G., Stevens, J. B., Bremer, S. W., Wykes, S. M., Bode, J., and Krawetz, S. A. (2004). Chromatin loops are selectively anchored using scaffold/matrix-attachment regions. J Cell Sci *117*, 999-1008.

Hirano, T., Kobayashi, R., and Hirano, M. (1997). Condensins, chromosome condensation protein complexes containing XCAP-C, XCAP-E and a Xenopus homolog of the Drosophila Barren protein. Cell *89*, 511-521.

Hirano, T., and Mitchison, T. J. (1993). Topoisomerase II does not play a scaffolding role in the organization of mitotic chromosomes assembled in Xenopus egg extracts. J Cell Biol *120*, 601-612.

Hirota, T., Gerlich, D., Koch, B., Ellenberg, J., and Peters, J. M. (2004). Distinct functions of condensin I and II in mitotic chromosome assembly. J Cell Sci *117*, 6435-6445.

Hizume, K., Yoshimura, S. H., and Takeyasu, K. (2005). Linker histone H1 per se can induce three-dimensional folding of chromatin fiber. Biochemistry *44*, 12978-12989.

Hoffmann, G. R. (1980). Genetic effects of dimethyl sulfate, diethyl sulfate, and related compounds. Mutat Res *75*, 63-129.

Horowitz-Scherer, R. A., and Woodcock, C. L. (2006). Organization of interphase chromatin. Chromosoma *115*, 1-14.

Howell, B. J., McEwen, B. F., Canman, J. C., Hoffman, D. B., Farrar, E. M., Rieder, C. L., and Salmon, E. D. (2001). Cytoplasmic dynein/dynactin drives kinetochore protein transport to the spindle poles and has a role in mitotic spindle checkpoint inactivation. J Cell Biol *155*, 1159-1172.

Hozak, P., Sasseville, A. M., Raymond, Y., and Cook, P. R. (1995). Lamin proteins form an internal nucleoskeleton as well as a peripheral lamina in human cells. J Cell Sci *108 (Pt 2)*, 635-644.

Hudson, D. F., Vagnarelli, P., Gassmann, R., and Earnshaw, W. C. (2003). Condensin is required for nonhistone protein assembly and structural integrity of vertebrate mitotic chromosomes. Dev Cell *5*, 323-336.

Ivanovska, I., Khandan, T., Ito, T., and Orr-Weaver, T. L. (2005). A histone code in meiosis: the histone kinase, NHK-1, is required for proper chromosomal architecture in Drosophila oocytes. Genes Dev *19*, 2571-2582.

Jang, J. K., Rahman, T., and McKim, K. S. (2005). The kinesinlike protein Subito contributes to central spindle assembly and organization of the meiotic spindle in Drosophila oocytes. Mol Biol Cell *16*, 4684-4694.

Karsenti, E., Newport, J., Hubble, R., and Kirschner, M. (1984). Interconversion of metaphase and interphase microtubule arrays, as studied by the injection of centrosomes and nuclei into Xenopus eggs. J Cell Biol *98*, 1730-1745.

Keith, K. C., Baker, R. E., Chen, Y., Harris, K., Stoler, S., and Fitzgerald-Hayes, M. (1999). Analysis of primary structural determinants that distinguish the centromere-specific function of histone variant Cse4p from histone H3. Mol Cell Biol *19*, 6130-6139.

King, R. C. (1970). Ovarian development in Drosophila melanogaster, (New York,: Academic Press).

Kireeva, N., Lakonishok, M., Kireev, I., Hirano, T., and Belmont, A. S. (2004). Visualization of early chromosome condensation: a hierarchical folding, axial glue model of chromosome structure. J Cell Biol *166*, 775-785.

Koizumi, J., Okamoto, Y., Onogi, H., Mayeda, A., Krainer, A. R., and Hagiwara, M. (1999). The subcellular localization of SF2/ASF is regulated by direct interaction with SR protein kinases (SRPKs). J Biol Chem *274*, 11125-11131.

Kornberg, R. D., and Lorch, Y. (1999). Twenty-five years of the nucleosome, fundamental particle of the eukaryote chromosome. Cell *98*, 285-294.

Lan, W., Zhang, X., Kline-Smith, S. L., Rosasco, S. E., Barrett-Wilt, G. A., Shabanowitz, J., Hunt, D. F., Walczak, C. E., and Stukenberg, P. T. (2004). Aurora B phosphorylates centromeric MCAK and regulates its localization and microtubule depolymerization activity. Curr Biol *14*, 273-286.

Lancaster, O. M., Cullen, C. F., and Ohkura, H. (2007). NHK-1 phosphorylates BAF to allow karyosome formation in the Drosophila oocyte nucleus. J Cell Biol *179*, 817-824.

Lasko, P. F., and Ashburner, M. (1988). The product of the Drosophila gene vasa is very similar to eukaryotic initiation factor-4A. Nature *335*, 611-617.

Li, H. Y., and Zheng, Y. (2004). Phosphorylation of RCC1 in mitosis is essential for producing a high RanGTP concentration on chromosomes and for spindle assembly in mammalian cells. Genes Dev *18*, 512-527.

Lin, H., and Spradling, A. C. (1995). Fusome asymmetry and oocyte determination in Drosophila. Dev Genet *16*, 6-12.

Lin, S., Xiao, R., Sun, P., Xu, X., and Fu, X. D. (2005). Dephosphorylation-dependent sorting of SR splicing factors during mRNP maturation. Mol Cell *20*, 413-425.

Liu, D., Vader, G., Vromans, M. J., Lampson, M. A., and Lens, S. M. (2009). Sensing chromosome bi-orientation by spatial separation of aurora B kinase from kinetochore substrates. Science *323*, 1350-1353.

Liu, J. L., Buszczak, M., and Gall, J. G. (2006). Nuclear bodies in the Drosophila germinal vesicle. Chromosome Res *14*, 465-475.

Lo, A. W., Magliano, D. J., Sibson, M. C., Kalitsis, P., Craig, J. M., and Choo, K. H. (2001). A novel chromatin immunoprecipitation and array (CIA) analysis identifies a 460-kb CENP-A-binding neocentromere DNA. Genome Res *11*, 448-457.

Long, J. C., and Caceres, J. F. (2009). The SR protein family of splicing factors: master regulators of gene expression. Biochem J *417*, 15-27.

Longo, F., Garagna, S., Merico, V., Orlandini, G., Gatti, R., Scandroglio, R., Redi, C. A., and Zuccotti, M. (2003). Nuclear localization of NORs and centromeres in mouse oocytes during folliculogenesis. Mol Reprod Dev *66*, 279-290.

Luschnig, S., Moussian, B., Krauss, J., Desjeux, I., Perkovic, J., and Nusslein-Volhard, C. (2004). An F1 genetic screen for maternal-effect mutations affecting embryonic pattern formation in Drosophila melanogaster. Genetics *167*, 325-342.

Lydall, D., Nikolsky, Y., Bishop, D. K., and Weinert, T. (1996). A meiotic recombination checkpoint controlled by mitotic checkpoint genes. Nature *383*, 840-843.

Ma, H., Siegel, A. J., and Berezney, R. (1999). Association of chromosome territories with the nuclear matrix. Disruption of human chromosome territories correlates with the release of a subset of nuclear matrix proteins. J Cell Biol *146*, 531-542.

MacQueen, A. J., Colaiacovo, M. P., McDonald, K., and Villeneuve, A. M. (2002). Synapsis-dependent and -independent mechanisms stabilize homolog pairing during meiotic prophase in C. elegans. Genes Dev *16*, 2428-2442.

Mahowald, A. P. (1972). Ultrastructural observations on oogenesis in Drosophila. J Morphol *137*, 29-48.

Malik, H. S., and Henikoff, S. (2001). Adaptive evolution of Cid, a centromere-specific histone in Drosophila. Genetics *157*, 1293-1298.

Mao, Y., Desai, A., and Cleveland, D. W. (2005). Microtubule capture by CENP-E silences BubR1-dependent mitotic checkpoint signaling. J Cell Biol *170*, 873-880.

Mattaj, I. W., and Englmeier, L. (1998). Nucleocytoplasmic transport: the soluble phase. Annu Rev Biochem *67*, 265-306.

Mattson, B. A., and Albertini, D. F. (1990). Oogenesis: chromatin and microtubule dynamics during meiotic prophase. Mol Reprod Dev *25*, 374-383.

McEwen, B. F., Hsieh, C. E., Mattheyses, A. L., and Rieder, C. L. (1998). A new look at kinetochore structure in vertebrate somatic cells using high-pressure freezing and freeze substitution. Chromosoma *107*, 366-375.

McGill, S., Chia, W., Karp, R., and Ashburner, M. (1988). The molecular analyses of an antimorphic mutation of Drosophila melanogaster, Scutoid. Genetics *119*, 647-661.

McKee, B. D. (2004). Homologous pairing and chromosome dynamics in meiosis and mitosis. Biochim Biophys Acta *1677*, 165-180.

McKee, B. D., Lumsden, S. E., and Das, S. (1993). The distribution of male meiotic pairing sites on chromosome 2 of Drosophila melanogaster: meiotic pairing and segregation of 2-Y transpositions. Chromosoma *102*, 180-194.

McKim, K. S., Green-Marroquin, B. L., Sekelsky, J. J., Chin, G., Steinberg, C., Khodosh, R., and Hawley, R. S. (1998). Meiotic synapsis in the absence of recombination. Science *279*, 876-878.

McKim, K. S., Jang, J. K., and Manheim, E. A. (2002). Meiotic recombination and chromosome segregation in Drosophila females. Annu Rev Genet *36*, 205-232.

Meaburn, K. J., and Misteli, T. (2007). Cell biology: chromosome territories. Nature *445*, 379-781.

Miranda, J. J., De Wulf, P., Sorger, P. K., and Harrison, S. C. (2005). The yeast DASH complex forms closed rings on microtubules. Nat Struct Mol Biol *12*, 138-143.

Mitchison, T., Evans, L., Schulze, E., and Kirschner, M. (1986). Sites of microtubule assembly and disassembly in the mitotic spindle. Cell *45*, 515-527.

Mizuguchi, G., Xiao, H., Wisniewski, J., Smith, M. M., and Wu, C. (2007). Nonhistone Scm3 and histones CenH3-H4 assemble the core of centromere-specific nucleosomes. Cell *129*, 1153-1164.

Monje-Casas, F., Prabhu, V. R., Lee, B. H., Boselli, M., and Amon, A. (2007). Kinetochore orientation during meiosis is controlled by Aurora B and the monopolin complex. Cell *128*, 477-490.

Moreno-Moreno, O., Torras-Llort, M., and Azorin, F. (2006). Proteolysis restricts localization of CID, the centromere-specific histone H3 variant of Drosophila, to centromeres. Nucleic Acids Res *34*, 6247-6255.

Mount, S. M., and Salz, H. K. (2000). Pre-messenger RNA processing factors in the Drosophila genome. J Cell Biol *150*, F37-44.

Musacchio, A., and Salmon, E. D. (2007). The spindle-assembly checkpoint in space and time. Nat Rev Mol Cell Biol *8*, 379-393.

Nag, D. K., Scherthan, H., Rockmill, B., Bhargava, J., and Roeder, G. S. (1995). Heteroduplex DNA formation and homolog pairing in yeast meiotic mutants. Genetics *141*, 75-86.

Nemergut, M. E., Mizzen, C. A., Stukenberg, T., Allis, C. D., and Macara, I. G. (2001). Chromatin docking and exchange activity enhancement of RCC1 by histones H2A and H2B. Science *292*, 1540-1543.

Neri, L. M., Raymond, Y., Giordano, A., Capitani, S., and Martelli, A. M. (1999). Lamin A is part of the internal nucleoskeleton of human erythroleukemia cells. J Cell Physiol *178*, 284-295.

Neuman-Silberberg, F. S., and Schupbach, T. (1993). The Drosophila dorsoventral patterning gene gurken produces a dorsally localized RNA and encodes a TGF alpha-like protein. Cell *75*, 165-174.

Nichols, R. J., Wiebe, M. S., and Traktman, P. (2006). The vaccinia-related kinases phosphorylate the N' terminus of BAF, regulating its interaction with DNA and its retention in the nucleus. Mol Biol Cell *17*, 2451-2464.

Nonaka, N., Kitajima, T., Yokobayashi, S., Xiao, G., Yamamoto, M., Grewal, S. I., and Watanabe, Y. (2002). Recruitment of cohesin to heterochromatic regions by Swi6/HP1 in fission yeast. Nat Cell Biol *4*, 89-93.

Osipova, T. N., Karpova, E. V., and Vorob'ev, V. I. (1990). Chromatin higher-order structure: two-start double superhelix formed by zig-zag shaped nucleosome chain with folded linker DNA. J Biomol Struct Dyn *8*, 11-22.

Page, S. L., and Hawley, R. S. (2001). c(3)G encodes a Drosophila synaptonemal complex protein. Genes Dev *15*, 3130-3143.

Page, S. L., and Hawley, R. S. (2004). The genetics and molecular biology of the synaptonemal complex. Annu Rev Cell Dev Biol *20*, 525-558.

Page, S. L., Nielsen, R. J., Teeter, K., Lake, C. M., Ong, S., Wright, K. R., Dean, K. L., Agne, D., Gilliland, W. D., and Hawley, R. S. (2007). A germline clone screen for meiotic mutants in Drosophila melanogaster. Fly (Austin) *1*, 172-181.

Palmer, D. K., O'Day, K., Wener, M. H., Andrews, B. S., and Margolis, R. L. (1987). A 17-kD centromere protein (CENP-A) copurifies with nucleosome core particles and with histones. J Cell Biol *104*, 805-815.

Papoutsopoulou, S., Nikolakaki, E., and Giannakouros, T. (1999). SRPK1 and LBR protein kinases show identical substrate specificities. Biochem Biophys Res Commun *255*, 602-607.

Parfenov, V., Potchukalina, G., Dudina, L., Kostyuchek, D., and Gruzova, M. (1989). Human antral follicles: oocyte nucleus and the karyosphere formation (electron microscopic and autoradiographic data). Gamete Res *22*, 219-231.

Parks, A. L., Cook, K. R., Belvin, M., Dompe, N. A., Fawcett, R., Huppert, K., Tan, L. R., Winter, C. G., Bogart, K. P., Deal, J. E.*, et al.* (2004). Systematic generation of high-resolution deletion coverage of the Drosophila melanogaster genome. Nat Genet *36*, 288-292.

Paulson, J. R., and Laemmli, U. K. (1977). The structure of histone-depleted metaphase chromosomes. Cell *12*, 817-828.

Perrimon, N., Engstrom, L., and Mahowald, A. P. (1984). Developmental genetics of the 2E-F region of the Drosophila X chromosome: a region rich in "developmentally important" genes. Genetics *108*, 559-572.

Perrimon, N., Engstrom, L., and Mahowald, A. P. (1985). A pupal lethal mutation with a paternally influenced maternal effect on embryonic development in Drosophila melanogaster. Dev Biol *110*, 480-491.

Perrimon, N., Engstrom, L., and Mahowald, A. P. (1989). Zygotic lethals with specific maternal effect phenotypes in Drosophila melanogaster. I. Loci on the X chromosome. Genetics *121*, 333-352.

Petronczki, M., Siomos, M. F., and Nasmyth, K. (2003). Un menage a quatre: the molecular biology of chromosome segregation in meiosis. Cell *112*, 423-440.

Pidoux, A. L., Choi, E. S., Abbott, J. K., Liu, X., Kagansky, A., Castillo, A. G., Hamilton, G. L., Richardson, W., Rappsilber, J., He, X., and Allshire, R. C. (2009). Fission yeast Scm3: A CENP-A receptor required for integrity of subkinetochore chromatin. Mol Cell *33*, 299-311.

Polioudaki, H., Kourmouli, N., Drosou, V., Bakou, A., Theodoropoulos, P. A., Singh, P. B., Giannakouros, T., and Georgatos, S. D. (2001). Histones H3/H4 form a tight complex with the inner nuclear membrane protein LBR and heterochromatin protein 1. EMBO Rep *2*, 920-925.

Ramakrishnan, V. (1997). Histone structure and the organization of the nucleosome. Annu Rev Biophys Biomol Struct *26*, 83-112.

Rexach, M., and Blobel, G. (1995). Protein import into nuclei: association and dissociation reactions involving transport substrate, transport factors, and nucleoporins. Cell *83*, 683-692.

Robinson, P. J., Fairall, L., Huynh, V. A., and Rhodes, D. (2006). EM measurements define the dimensions of the "30-nm" chromatin fiber: evidence for a compact, interdigitated structure. Proc Natl Acad Sci U S A *103*, 6506-6511.

Robinson, P. J., and Rhodes, D. (2006). Structure of the '30 nm' chromatin fibre: a key role for the linker histone. Curr Opin Struct Biol *16*, 336-343.

Rydberg, B., Holley, W. R., Mian, I. S., and Chatterjee, A. (1998). Chromatin conformation in living cells: support for a zig-zag model of the 30 nm chromatin fiber. J Mol Biol *284*, 71-84.

Ryder, E., Ashburner, M., Bautista-Llacer, R., Drummond, J., Webster, J., Johnson, G., Morley, T., Chan, Y. S., Blows, F., Coulson, D.*, et al.* (2007). The DrosDel deletion collection: a Drosophila genomewide chromosomal deficiency resource. Genetics *177*, 615-629.

Ryder, E., Blows, F., Ashburner, M., Bautista-Llacer, R., Coulson, D., Drummond, J., Webster, J., Gubb, D., Gunton, N., Johnson, G.*, et al.* (2004). The DrosDel collection: a set of P-element insertions for generating custom chromosomal aberrations in Drosophila melanogaster. Genetics *167*, 797-813.

Saitoh, N., Goldberg, I. G., Wood, E. R., and Earnshaw, W. C. (1994). ScII: an abundant chromosome scaffold protein is a member of a family of putative ATPases with an unusual predicted tertiary structure. J Cell Biol *127*, 303-318.

Sakaguchi, A., and Kikuchi, A. (2004). Functional compatibility between isoform alpha and beta of type II DNA topoisomerase. J Cell Sci *117*, 1047-1054.

Sambrook, J., Maniatis, T., and Fritsch, E. F. (1989). Molecular cloning : a laboratory manual, 2nd edn (Cold Spring Harbor, N.Y.: Cold Spring Harbor Laboratory Press).

Santaguida, S., and Musacchio, A. (2009). The life and miracles of kinetochores. EMBO J *28*, 2511-2531.

Savvidou, E., Cobbe, N., Steffensen, S., Cotterill, S., and Heck, M. M. (2005). Drosophila CAP-D2 is required for condensin complex stability and resolution of sister chromatids. J Cell Sci *118*, 2529-2543.

Sawin, K. E., LeGuellec, K., Philippe, M., and Mitchison, T. J. (1992). Mitotic spindle organization by a plus-end-directed microtubule motor. Nature *359*, 540-543.

Segura-Totten, M., and Wilson, K. L. (2004). BAF: roles in chromatin, nuclear structure and retrovirus integration. Trends Cell Biol *14*, 261-266.

Shumaker, D. K., Lee, K. K., Tanhehco, Y. C., Craigie, R., and Wilson, K. L. (2001). LAP2 binds to BAF.DNA complexes: requirement for the LEM domain and modulation by variable regions. EMBO J *20*, 1754-1764.

Simon, M. A. (1994). Signal transduction during the development of the Drosophila R7 photoreceptor. Dev Biol *166*, 431-442.

Simos, G., and Georgatos, S. D. (1992). The inner nuclear membrane protein p58 associates in vivo with a p58 kinase and the nuclear lamins. EMBO J *11*, 4027-4036.

Simpson, R. T. (1978). Structure of the chromatosome, a chromatin particle containing 160 base pairs of DNA and all the histones. Biochemistry *17*, 5524-5531.

St Johnston, D. (2002). The art and design of genetic screens: Drosophila melanogaster. Nat Rev Genet *3*, 176-188.

Staynov, D. Z. (2008). The controversial 30 nm chromatin fibre. Bioessays *30*, 1003-1009.

Staynov, D. Z., and Proykova, Y. G. (1998). Quantitative analysis of DNase I digestion patterns of oligo- and polynucleosomes. J Mol Biol *279*, 59-71.

Stoler, S., Rogers, K., Weitze, S., Morey, L., Fitzgerald-Hayes, M., and Baker, R. E. (2007). Scm3, an essential Saccharomyces cerevisiae centromere protein required for G2/M progression and Cse4 localization. Proc Natl Acad Sci U S A *104*, 10571-10576.

Strunnikov, A. V., Hogan, E., and Koshland, D. (1995). SMC2, a Saccharomyces cerevisiae gene essential for chromosome segregation and condensation, defines a subgroup within the SMC family. Genes Dev *9*, 587-599.

Styhler, S., Nakamura, A., Swan, A., Suter, B., and Lasko, P. (1998). vasa is required for GURKEN accumulation in the oocyte, and is involved in oocyte differentiation and germline cyst development. Development *125*, 1569-1578.

Sun, H., Treco, D., Schultes, N. P., and Szostak, J. W. (1989). Double-strand breaks at an initiation site for meiotic gene conversion. Nature *338*, 87-90.

Sun, H. B., Shen, J., and Yokota, H. (2000). Size-dependent positioning of human chromosomes in interphase nuclei. Biophys J *79*, 184-190.

Szostak, J. W., Orr-Weaver, T. L., Rothstein, R. J., and Stahl, F. W. (1983). The double-strand-break repair model for recombination. Cell *33*, 25-35.

Takano, M., Koyama, Y., Ito, H., Hoshino, S., Onogi, H., Hagiwara, M., Furukawa, K., and Horigome, T. (2004). Regulation of binding of lamin B receptor to chromatin by SR protein kinase and cdc2 kinase in Xenopus egg extracts. J Biol Chem *279*, 13265-13271.

Talbert, P. B., Bryson, T. D., and Henikoff, S. (2004). Adaptive evolution of centromere proteins in plants and animals. J Biol *3*, 18.

Tanaka, T. U., Rachidi, N., Janke, C., Pereira, G., Galova, M., Schiebel, E., Stark, M. J., and Nasmyth, K. (2002). Evidence that the Ipl1-Sli15 (Aurora kinase-INCENP) complex promotes chromosome bi-orientation by altering kinetochore-spindle pole connections. Cell *108*, 317-329.

Tenenbaum, S. A., and Aguirre-Ghiso, J. (2005). Dephosphorylation shows SR proteins the way out. Mol Cell *20*, 499-501.

Thibault, S. T., Singer, M. A., Miyazaki, W. Y., Milash, B., Dompe, N. A., Singh, C. M., Buchholz, R., Demsky, M., Fawcett, R., Francis-Lang, H. L.*, et al.* (2004). A complementary transposon tool kit for Drosophila melanogaster using P and piggyBac. Nat Genet *36*, 283-287.

Thomas, J. O. (1999). Histone H1: location and role. Curr Opin Cell Biol *11*, 312-317.

Tinker, R., Silver, D., and Montell, D. J. (1998). Requirement for the vasa RNA helicase in gurken mRNA localization. Dev Biol *199*, 1-10.

Tomancak, P., Guichet, A., Zavorszky, P., and Ephrussi, A. (1998). Oocyte polarity depends on regulation of gurken by Vasa. Development *125*, 1723-1732.

Torras-Llort, M., Moreno-Moreno, O., and Azorin, F. (2009). Focus on the centre: the role of chromatin on the regulation of centromere identity and function. EMBO J *28*, 2337-2348.

Tremethick, D. J. (2007). Higher-order structures of chromatin: the elusive 30 nm fiber. Cell *128*, 651-654.

Vagnarelli, P., and Earnshaw, W. C. (2004). Chromosomal passengers: the four-dimensional regulation of mitotic events. Chromosoma *113*, 211-222.

Vagnarelli, P., Hudson, D. F., Ribeiro, S. A., Trinkle-Mulcahy, L., Spence, J. M., Lai, F., Farr, C. J., Lamond, A. I., and Earnshaw, W. C. (2006). Condensin and Repo-Man-PP1 co-operate in the regulation of chromosome architecture during mitosis. Nat Cell Biol *8*, 1133-1142.

Van Hooser, A. A., Ouspenski, II, Gregson, H. C., Starr, D. A., Yen, T. J., Goldberg, M. L., Yokomori, K., Earnshaw, W. C., Sullivan, K. F., and Brinkley, B. R. (2001). Specification of kinetochore-forming chromatin by the histone H3 variant CENP-A. J Cell Sci *114*, 3529-3542.

Vermaak, D., Hayden, H. S., and Henikoff, S. (2002). Centromere targeting element within the histone fold domain of Cid. Mol Cell Biol *22*, 7553-7561.

Vogt, N., Koch, I., Schwarz, H., Schnorrer, F., and Nusslein-Volhard, C. (2006). The gammaTuRC components Grip75 and Grip128 have an essential microtubule-anchoring function in the Drosophila germline. Development *133*, 3963-3972.

von Wettstein, D. (1984). The synaptonemal complex and genetic segregation. Symp Soc Exp Biol *38*, 195-231.

Wagner, N., Weber, D., Seitz, S., and Krohne, G. (2004). The lamin B receptor of Drosophila melanogaster. J Cell Sci *117*, 2015-2028.

Waizenegger, I., Gimenez-Abian, J. F., Wernic, D., and Peters, J. M. (2002). Regulation of human separase by securin binding and autocleavage. Curr Biol *12*, 1368-1378.

Wang, H. Y., Lin, W., Dyck, J. A., Yeakley, J. M., Songyang, Z., Cantley, L. C., and Fu, X. D. (1998). SRPK2: a differentially expressed SR protein-specific kinase involved in mediating the interaction and localization of pre-mRNA splicing factors in mammalian cells. J Cell Biol *140*, 737-750.

Watanabe, Y. (2005). Sister chromatid cohesion along arms and at centromeres. Trends in Genetics *21*, 405-412.

Watanabe, Y., and Kitajima, T. S. (2005). Shugoshin protects cohesin complexes at centromeres. Philos Trans R Soc Lond B Biol Sci *360*, 515-521, discussion 521.

Waters, J. C., Skibbens, R. V., and Salmon, E. D. (1996). Oscillating mitotic newt lung cell kinetochores are, on average, under tension and rarely push. J Cell Sci *109 (Pt 12)*, 2823-2831.

Westermann, S., Wang, H. W., Avila-Sakar, A., Drubin, D. G., Nogales, E., and Barnes, G. (2006). The Dam1 kinetochore ring complex moves processively on depolymerizing microtubule ends. Nature *440*, 565-569.

Williams, B. C., Murphy, T. D., Goldberg, M. L., and Karpen, G. H. (1998). Neocentromere activity of structurally acentric mini-chromosomes in Drosophila. Nat Genet *18*, 30-37.

Williams, J. S., Hayashi, T., Yanagida, M., and Russell, P. (2009). Fission yeast Scm3 mediates stable assembly of Cnp1/CENP-A into centromeric chromatin. Mol Cell *33*, 287-298.

Xiao, S. H., and Manley, J. L. (1997). Phosphorylation of the ASF/SF2 RS domain affects both protein-protein and protein-RNA interactions and is necessary for splicing. Genes Dev *11*, 334-344.

Yao, X., Anderson, K. L., and Cleveland, D. W. (1997). The microtubule-dependent motor centromere-associated protein E (CENP-E) is an integral component of kinetochore corona fibers that link centromeres to spindle microtubules. J Cell Biol *139*, 435-447.

Ye, Q., Callebaut, I., Pezhman, A., Courvalin, J. C., and Worman, H. J. (1997). Domain-specific interactions of human HP1-type chromodomain proteins and inner nuclear membrane protein LBR. J Biol Chem *272*, 14983-14989.

Ye, Q., and Worman, H. J. (1994). Primary structure analysis and lamin B and DNA binding of human LBR, an integral protein of the nuclear envelope inner membrane. J Biol Chem *269*, 11306-11311.

Ye, Q., and Worman, H. J. (1996). Interaction between an integral protein of the nuclear envelope inner membrane and human chromodomain proteins homologous to Drosophila HP1. J Biol Chem *271*, 14653-14656.

Yoda, K., Ando, S., Morishita, S., Houmura, K., Hashimoto, K., Takeyasu, K., and Okazaki, T. (2000). Human centromere protein A (CENP-A) can replace histone H3 in nucleosome reconstitution in vitro. Proc Natl Acad Sci U S A *97*, 7266-7271.

Zuccotti, M., Giorgi Rossi, P., Martinez, A., Garagna, S., Forabosco, A., and Redi, C. A. (1998). Meiotic and developmental competence of mouse antral oocytes. Biol Reprod *58*, 700-704.

Zuccotti, M., Piccinelli, A., Giorgi Rossi, P., Garagna, S., and Redi, C. A. (1995). Chromatin organization during mouse oocyte growth. Mol Reprod Dev *41*, 479-485.

Zuccotti, M., Ponce, R. H., Boiani, M., Guizzardi, S., Govoni, P., Scandroglio, R., Garagna, S., and Redi, C. A. (2002). The analysis of chromatin organisation allows selection of mouse antral oocytes competent for development to blastocyst. Zygote *10*, 73-78.

Zur, A., and Brandeis, M. (2001). Securin degradation is mediated by fzy and fzr, and is required for complete chromatid separation but not for cytokinesis. EMBO J *20*, 792-801.